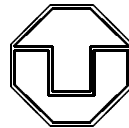


Quantum Radiation in Leaky Cavities

Diplomarbeit
zur Erlangung des wissenschaftlichen Grades
Diplom-Physiker

vorgelegt von

Gernot Schaller
geboren in Wismar



Institut für Theoretische Physik
Fachrichtung Physik
Fakultät Mathematik und Naturwissenschaften
der Technischen Universität Dresden

2001

eingereicht am 27. September 2001

Gutachter: Prof. Dr. Gerhard Soff

Priv.-Doz. Dr. Günter Plunien

Abstract

This thesis presents several approaches to the dynamical Casimir effect within resonantly vibrating cavities with losses at finite temperature. After an introduction to the topic and the currently known results the canonical formalism is applied to the example of a massless scalar field. A model for a cavity with leaks is introduced and its eigenmodes are calculated. Within the framework of the rotating wave approximation an effective Hamiltonian is derived. The effect of non-stationary boundary conditions on the particle number is calculated by means of response theory, a master equation approach, and a non-perturbative approach. All results are being compared and the generalization to the electromagnetic field is outlined.

Kurzfassung

Diese Diplomarbeit präsentiert mehrere Ansätze zum dynamischen Casimir-Effekt in resonant vibrierenden Kavitäten mit Verlusten und bei endlicher Temperatur. Nach einer Einführung in das Thema und in die bisher bekannten Resultate wird der kanonische Formalismus auf das Beispiel eines masselosen skalaren Feldes angewandt. Für Kavitäten mit Verlusten wird ein Modell eingeführt und dessen Eigenmoden werden berechnet. Im Rahmen der "rotating wave approximation" wird ein effektiver Hamilton-Operator abgeleitet. Der Effekt nichtstationärer Randbedingungen auf die Teilchenzahl wird mittels Antwort-Theorie, eines Mastergleichungsansatzes und mit einem nichtperturbativen Ansatz berechnet. Alle Resultate werden miteinander verglichen und die Verallgemeinerung zum elektromagnetischen Feld wird skizziert.

Contents

1	Introduction	7
1.1	Motivation	7
1.2	Overview	9
1.3	Notations	10
2	General Formalism	13
2.1	Lagrangian	13
2.2	Hamiltonian	14
2.3	Canonical Quantization	15
2.4	A Model Cavity	17
2.5	Eigenmodes	19
2.6	Effective Time Evolution	25
2.6.1	Rotating Wave Approximation (RWA)	25
2.6.2	Effective Squeezing Hamiltonian	28
2.6.3	Effective Velocity Hamiltonian	30
2.6.4	Detuned Resonance	32
3	Response Theory	35
3.1	Expectation Values	35
3.2	The Quadratic Response	38
3.3	Squeezing	39
3.4	An Example: Particle Creation	40
3.4.1	The Fundamental Resonance Mode	40
3.4.2	Coupling Modes	43

4	Master Equation Approach	45
4.1	Introductory Remarks	45
4.2	The Zwanzig Master Equation	46
4.3	Approximations	48
4.3.1	Born Approximation	48
4.3.2	Markov Approximation	48
4.3.3	Approximate Master Equation	49
4.4	Solution Of The Master Equation	51
4.5	An Example: Particle Creation	52
5	A Non-Perturbative Approach	55
5.1	General Procedure	55
5.2	Generalized Expectation Values	57
5.3	An Example: Particle Creation	58
5.4	Comparison With Known Results	62
5.5	Multi-Mode Squeezing	66
6	Discussion	69
6.1	Estimates	69
6.2	Conclusions	72
6.3	Outlook	73
7	Appendix	75
7.1	Eigenfunctions	75
7.2	Traces Of Ladder Operators	76
7.3	Properties Of Time Ordering	77
7.4	Integrals	79
7.5	Time Evolution Matrix	80
7.6	Employed Symbols	82
8	Acknowledgements	85
	Bibliography	87

Chapter 1

Introduction

1.1 Motivation

The existence of virtual quantum fluctuations is one of the basic consequences of quantum field theory. These virtual fluctuations can have real consequences. For example dynamical external disturbances can lead to a creation of particles out of the vacuum! This phenomenon is referred to as quantum radiation, since a classical analog does not exist. If the external disturbances are represented by time-dependent boundary conditions imposed on the quantum fields, e.g. moving mirrors, the scenario is also known as the dynamical Casimir effect.

The foundations of the dynamical Casimir effect have been laid with its static counterpart as early as 1948 by Casimir in his famous paper *On The Attraction Between Two Perfectly Conducting Plates* [1]. There a purely quantum-theoretical effect – the attractive Casimir force between two parallel perfectly reflecting and neutral mirrors placed in the vacuum – was predicted. This static Casimir force has been verified experimentally with high precision [2, 3] for several geometries. Since then the Casimir effect has attracted the interest of many authors, for a brief overview see e.g. [4, 5] and references therein.

However, the dynamical Casimir effect – where one or both of the mirrors are moving thus inducing the creation of particles – has not yet been observed rigorously in an according experiment. This effect – also known under the name *non-stationary Casimir effect* (NSCE) – predicts (closely related) interesting phenomena like a modification of the known static Casimir force (see e.g. [6, 7, 8, 9, 10, 11]) and the creation of particles (e.g. photons in the case of the electromagnetic field) out of the vacuum induced by moving mirrors. This thesis is devoted to the latter effect. The observation of quantum radiation would provide a substantial test

of quantum field theory and thus be of special relevance. It was proposed by Schwinger [12] that the phenomenon of sonoluminescence might be based on the NSCE. However, it remains doubtful whether the required extreme conditions are realized in the corresponding scenario. The complete understanding of the dynamical Casimir effect is still a challenging theoretical problem.

In 1970 Moore [13] succeeded in presenting the first calculation of quantum radiation exploiting the conformal invariance of scalar fields in 1+1 space-time dimensions. Based on this method Fulling and Davies [14] calculated the radiation emitted by a moving mirror in 1+1 dimensions. These considerations were improved by a long line of authors, see e.g. [15, 16, 17, 19, 20]. Some authors (see e.g. [21, 22, 23]) considered the effects of losses in 1+1 dimensions. Many publications were also devoted to the calculation of particle creation effects in resonantly vibrating cavities, since this configuration was found to lead to significant effects [15, 7]. However, it must be mentioned that all those calculations exploited the special structure of 1+1 space-time dimensions via applying approaches based on the conformal mapping methods developed in [13, 14]. They are therefore a priori restricted to 1+1 dimensions. Since the character of quantum radiation in 3+1 dimensions differs drastically from the two-dimensional situation, the method of conformal mapping can not be obviously generalized to higher space-time dimensions. A different – and also consistent – approach was presented by Ford and Vilenkin [24] in 1981, where the radiation of a single moving mirror was considered. The quantization of the field has always been a challenging problem [25, 26, 27], but the complete theory including non-ideal dynamical boundary conditions is not completely solved at the moment. The Hamiltonian approach, whose advantages were demonstrated in e.g. [28, 29, 30] can also be generalized to an arbitrary number of dimensions. But even within this approach the results differ a lot, since the spectrum of cavity eigenmodes is not equidistant anymore in higher than two-dimensional space-times. Since the velocity of the boundaries will under laboratory conditions always be much smaller than the speed of light, the quantum effect of particle creation was found to be small except in the case of parametric resonance (see e.g. [6, 31, 32]) in analogy to the two-dimensional results. In this case a boundary of the cavity is oscillating at twice an eigenfrequency. This leads to a squeezing of the vacuum state thereby inducing the creation of particles out of the vacuum.

Accordingly, several authors (see e.g. [18, 33, 34, 35, 36, 37]) considered 3+1 dimensional dynamical cavity models with ideal mirrors. Since the cavities are assumed to be initially empty, these publications neglect the effects of finite temperatures. However, as was shown in [38, 39, 40] these temperature effects may even dominate the pure vacuum effect by several

orders of magnitude at room temperature and therefore their neglect is not justified.

In the resonance case in 3+1 dimensions an exponential growth of the particle number versus the perturbation time was predicted, see e.g. [18, 33, 34, 38, 39, 40]. In view of this prediction an experimental observation of quantum radiation within the scenario of parametric resonance seems to be rather simple, provided the cavity is oscillating for a sufficiently long time. However, in all the aforementioned considerations ideal boundary conditions were used, i.e. the mirrors bounding the cavities were assumed to be perfectly reflecting. This unphysical presumption is not an adequate description of real systems. It is therefore essential to include the effects of losses and finite temperature in a realistic experiment. In addition, for the case of parametric resonance also the impact of a detuned oscillation frequency will have to be examined, since this seems to pose a challenging experimental problem [41, 42, 43, 44].

In order to include the effects of losses in 3+1 dimensions an approach based on an ad hoc master equation ansatz has been applied in [43, 44]. However, this ansatz is suitable for the corresponding stationary system (i.e. without a moving boundary) and not necessarily for a vibrating one. (Possible limitations to this master equation ansatz were already expected in these publications and the need for a master equation derived starting from first principles was also expressed.) In addition, temperature effects were not taken into account rigorously.

The canonical approach [38, 39] enables a convenient calculation of temperature effects. However, this method still lacks a generalization for systems with leaks. The quantum electrodynamics of single transparent mirrors has already been considered [45], a realistic 3+1 dimensional vibrating cavity however, has not been examined so far. The present thesis aims at providing a remedy in this field by applying the canonical approach to such a cavity, taking into account simultaneously the effects of finite temperature and losses.

1.2 Overview

This thesis is organized as follows.

In chapter 2 the general canonical formalism is presented and the quantization scheme is outlined. A model cavity is considered and a solution of its eigenfrequency spectrum is found perturbatively where the transmittance of the dispersive mirror serves as a perturbation parameter. For the case of parametric resonance an effective time evolution operator is derived using the rotating wave approximation (RWA).

In chapter 3 the number of created particle due to the dynamical Casimir effect will be calculated perturbatively using the framework of response theory.

Chapter 4 is devoted to the derivation of a master equation describing the model system with losses. In addition, this master equation is solved for an effective statistical operator accounting for the relevant observables. This statistical operator enables the calculation of expectation values and thus the comparison with the results of the previous chapter.

A complete treatment of time-evolution governed by an arbitrary quadratic Hamiltonian in form of a non-perturbative method is presented in chapter 5. The perturbatively obtained particle creation results of the previous sections are found to be consistent within the corresponding limit.

Finally, chapter 6 gives a summary and discussion of the results of this thesis.

An overview of the employed conventions will be given in the following section and a list of all used symbols can be found on page 82.

1.3 Notations

In this thesis the following conventions will be employed.

- Throughout this thesis natural units given by

$$\hbar = c = \varepsilon_0 = \mu_0 = 1 \quad (1.1)$$

will be used.

- Since all calculations are performed in a flat spacetime the conventional choice of the metric is given by

$$g_{\mu\nu} = \begin{pmatrix} +1 & 0 & 0 & 0 \\ 0 & -1 & 0 & 0 \\ 0 & 0 & -1 & 0 \\ 0 & 0 & 0 & -1 \end{pmatrix}. \quad (1.2)$$

- All Lorentz vectors and tensors are labeled with lowercase Greek indices running from zero (time component) to three (spatial components) whereas lowercase Latin indices only stand for the spatial components (running from one to three). For these indices the commonly practiced Einstein sum convention is employed whenever possible.
- If no special range of an integral or sum is specified then the integration or summation will have to be extended to the largest possible range.

- The commutator of two operators \hat{A} and \hat{B} is defined by

$$\left[\hat{A}, \hat{B} \right] = \hat{A}\hat{B} - \hat{B}\hat{A}, \quad (1.3)$$

whereas the anti-commutator is given by

$$\left\{ \hat{A}, \hat{B} \right\} = \hat{A}\hat{B} + \hat{B}\hat{A}. \quad (1.4)$$

- The time-ordered product of two time-dependent bosonic operators $\hat{A}_1(t_1)$ and $\hat{A}_2(t_2)$ is defined as

$$\hat{\mathcal{T}} \left[\hat{A}_1(t_1) \hat{A}_2(t_2) \right] = \hat{A}_1(t_1) \hat{A}_2(t_2) \Theta(t_1 - t_2) + \hat{A}_2(t_2) \hat{A}_1(t_1) \Theta(t_2 - t_1), \quad (1.5)$$

where $\Theta(x)$ stands for the Heaviside Step function. Anti-chronological ordering is defined via

$$\hat{\mathcal{T}}^\dagger \left[\hat{A}_1(t_1) \hat{A}_2(t_2) \right] = \hat{A}_1(t_1) \hat{A}_2(t_2) \Theta(t_2 - t_1) + \hat{A}_2(t_2) \hat{A}_1(t_1) \Theta(t_1 - t_2). \quad (1.6)$$

These formulas can easily be generalized to an arbitrary number of time-ordered operators, see also appendix 7.3.

- For reasons of brevity the time-dependence of the initial (i.e. before any disturbance) creation and annihilation operators is omitted

$$\hat{a}_\mu(0) = \hat{a}_\mu, \quad \hat{a}_\mu^\dagger(0) = \hat{a}_\mu^\dagger. \quad (1.7)$$

- In addition, the shorthand notation for the hyperbolic sine and cosine functions

$$\mathcal{S}(t) = \sinh(2\xi t), \quad \mathcal{C}(t) = \cosh(2\xi t), \quad (1.8)$$

with ξ being the squeezing parameter will be used whenever possible.

Chapter 2

General Formalism

2.1 Lagrangian

For reasons of simplicity a massless, noninteracting, and neutral (i.e. real) scalar field $\Phi(\mathbf{r}, t)$ coupled to an external potential $V(\mathbf{r}; t)$ is considered inside a domain $G(t)$ with Dirichlet boundary conditions. These boundary conditions are incorporated by the external potential. Accordingly, the theory is characterized by the corresponding Lagrangian density

$$\mathcal{L} = \frac{1}{2}(\partial_\mu \Phi)(\partial^\mu \Phi) - V(\mathbf{r}; t)\Phi^2. \quad (2.1)$$

It is advantageous to introduce a set of eigenfunctions $\{f_\mu\}$ determined by the eigenvalue equation

$$\{2V - \nabla^2\} f_\mu(\mathbf{r}; t) = \Omega_\mu^2(t) f_\mu(\mathbf{r}; t), \quad (2.2)$$

where the potential $V(\mathbf{r}; t)$ also imposes the (time-dependent) Dirichlet boundary conditions

$$\forall \mu : f_\mu(\mathbf{r}; t)|_{\partial G(t)} = 0. \quad (2.3)$$

The time-dependence of the eigenfunctions and eigenfrequencies is introduced by the time-dependence of the domain $G(t)$, i.e. the moving boundary of the cavity. Above eigenvalue equation does not completely determine the set $\{f_\mu\}$ – in addition the set of functions is complete

$$\sum_\mu f_\mu^*(\mathbf{r}; t) f_\mu(\mathbf{r}'; t) = \delta^3(\mathbf{r} - \mathbf{r}') \quad (2.4)$$

and orthonormal

$$\int d^3r f_\mu^*(\mathbf{r}, t) f_\nu(\mathbf{r}, t) = \delta_{\mu\nu}. \quad (2.5)$$

For the description of neutral scalar fields it suffices to consider real-valued eigenfunctions, i.e. the field Φ can be expanded

$$\Phi(\mathbf{r}, t) = \sum_{\mu} Q_{\mu}(t) f_{\mu}(\mathbf{r}; t), \quad (2.6)$$

where the time-dependent coefficients $Q_{\mu}(t)$ are uniquely determined. By inserting this expansion into the Lagrange function L and defining the coupling matrix

$$M_{\mu\nu}(t) = \int d^3r \frac{\partial f_{\mu}(\mathbf{r}; t)}{\partial t} f_{\nu}(\mathbf{r}; t) \quad (2.7)$$

the Lagrange function yields (see also [38]) the form

$$\begin{aligned} L &= \int d^3r \mathcal{L} \\ &= \frac{1}{2} \sum_{\mu} \dot{Q}_{\mu}^2 - \frac{1}{2} \sum_{\mu} \Omega_{\mu}^2(t) Q_{\mu}^2 + \sum_{\mu, \nu} Q_{\mu} M_{\mu\nu}(t) \dot{Q}_{\nu} + \frac{1}{2} \sum_{\mu, \nu, \kappa} Q_{\mu} M_{\mu\kappa}(t) M_{\nu\kappa}(t) Q_{\nu}. \end{aligned} \quad (2.8)$$

Note that due to the ortho-normality of the set $\{f_{\mu}\}$ and the Dirichlet boundary conditions the coupling matrix $M_{\mu\nu}(t)$ turns out to be antisymmetric

$$M_{\mu\nu} + M_{\nu\mu} = \int_{G(t)} dG \frac{\partial}{\partial t} [f_{\mu}(\mathbf{r}; t) f_{\nu}(\mathbf{r}; t)] = \frac{d\delta_{\mu\nu}}{dt} - \int_{\partial G(t)} d\dot{G} f_{\mu}(\mathbf{r}; t) f_{\nu}(\mathbf{r}; t) = 0, \quad (2.9)$$

see also [34, 38]. The matrix $M_{\mu\nu}(t)$ accounts for the strength of coupling between two different modes μ and ν .

2.2 Hamiltonian

For the calculation of time-evolution operators a Hamiltonian representation is advantageous. The Hamiltonian can be obtained from the Lagrangian by virtue of a Legendre transform

$$H = \sum_{\mu} P_{\mu} \dot{Q}_{\mu} - L, \quad (2.10)$$

where with the Lagrangian of section 2.1 the canonical conjugated momenta determines to

$$P_{\mu} = \frac{\partial L}{\partial \dot{Q}_{\mu}} = \dot{Q}_{\mu} + \sum_{\nu} Q_{\nu} M_{\nu\mu}(t). \quad (2.11)$$

Accordingly, the Hamilton function (cf. [28, 38]) reads

$$H = \frac{1}{2} \sum_{\mu} P_{\mu}^2 + \frac{1}{2} \sum_{\mu} \Omega_{\mu}^2 Q_{\mu}^2 + \sum_{\mu\nu} P_{\mu} M_{\mu\nu} Q_{\nu}. \quad (2.12)$$

Aiming at performing the calculations in the interaction picture it is advantageous to split this Hamiltonian into three parts $H = H_0 + H_I^S + H_I^V$ where the unperturbed Hamiltonian H_0

$$H_0 = \frac{1}{2} \sum_{\mu} P_{\mu}^2 + \frac{1}{2} \sum_{\mu} (\Omega_{\mu}^0)^2 Q_{\mu}^2 \quad (2.13)$$

corresponds to a set of harmonic oscillators having the frequency Ω_{μ}^0 . The interaction Hamiltonian splits up into two parts, of which

$$H_I^S = \frac{1}{2} \sum_{\mu} \Delta\Omega_{\mu}^2(t) Q_{\mu}^2, \quad (2.14)$$

will further-on be called squeezing interaction Hamiltonian. The term

$$\Delta\Omega_{\mu}^2(t) = \Omega_{\mu}^2(t) - (\Omega_{\mu}^0)^2 \quad (2.15)$$

denotes the difference of the (squared) time-dependent eigenfrequencies $\Omega_{\mu}^2(t)$ from the unperturbed ones $(\Omega_{\mu}^0)^2$. The other part – the velocity interaction Hamiltonian – is given by

$$H_I^V = \sum_{\mu,\nu} P_{\mu} M_{\mu\nu}(t) Q_{\nu}. \quad (2.16)$$

This distinction (see also e.g. [38, 39]) is – independent of the particular geometry under consideration [36] – well motivated, since H_I^S is determined by the time-dependent eigenfrequency deviation $\Delta\Omega_{\mu}^2(t)$ and H_I^V is induced by the non-vanishing coupling matrix $M_{\mu\nu}(t)$ which is due to the time-dependent eigenfunctions. In the case of a stationary system (where eigenfunctions and eigenfrequencies do not depend on time) both $\Delta\Omega_{\mu}^2(t)$ and $M_{\mu\nu}(t)$ will vanish. In the interaction picture this case corresponds to the unperturbed system.

2.3 Canonical Quantization

The scheme of Canonical Quantization can be executed via introducing the field momentum

$$\Pi(\mathbf{r}, t) = \frac{\partial \mathcal{L}}{\partial \dot{\Phi}(\mathbf{r}, t)} = \dot{\Phi}(\mathbf{r}, t) = \sum_{\mu} P_{\mu}(t) f_{\mu}(\mathbf{r}, t), \quad (2.17)$$

which can also be expanded into the complete set $\{f_\mu\}$ with time-dependent coefficients $P_\mu(t)$. The quantization is now performed by switching from classical fields to field operators and demanding the equal time commutation relations

$$\begin{aligned} [\hat{\Phi}(\mathbf{r}, t), \hat{\Pi}(\mathbf{r}', t)] &= i\delta(\mathbf{r} - \mathbf{r}'), \\ [\hat{\Phi}(\mathbf{r}, t), \hat{\Phi}(\mathbf{r}', t)] &= 0, \quad [\hat{\Pi}(\mathbf{r}, t), \hat{\Pi}(\mathbf{r}', t)] = 0. \end{aligned} \quad (2.18)$$

These commutation relations are valid inside the domain $G(t)$. Accordingly, the coefficients in the field expansions also become operators $Q_\mu \rightarrow \hat{Q}_\mu$ and $P_\mu \rightarrow \hat{P}_\mu$, which have to obey

$$\begin{aligned} [\hat{Q}_\mu(t), \hat{P}_\nu(t)] &= i\delta_{\mu\nu}, \\ [\hat{Q}_\mu(t), \hat{Q}_\nu(t)] &= 0, \quad [\hat{P}_\mu(t), \hat{P}_\nu(t)] = 0. \end{aligned} \quad (2.19)$$

However, to consider systems with many particles it is convenient to introduce the annihilation and creation operators, respectively

$$\hat{a}_\mu(t) = \frac{1}{\sqrt{2\Omega_\mu^0}} \left(\Omega_\mu^0 \hat{Q}_\mu(t) + i\hat{P}_\mu(t) \right), \quad \hat{a}_\mu^\dagger(t) = \frac{1}{\sqrt{2\Omega_\mu^0}} \left(\Omega_\mu^0 \hat{Q}_\mu(t) - i\hat{P}_\mu(t) \right). \quad (2.20)$$

These operators have to obey the usual bosonic equal time commutation relations

$$\begin{aligned} [\hat{a}_\mu(t), \hat{a}_\nu^\dagger(t)] &= \delta_{\mu\nu}, \\ [\hat{a}_\mu(t), \hat{a}_\nu(t)] &= 0, \quad [\hat{a}_\mu^\dagger(t), \hat{a}_\nu^\dagger(t)] = 0. \end{aligned} \quad (2.21)$$

The diagonal unperturbed Hamiltonian yields – with the chosen normalization – the form

$$\hat{H}_0 = \sum_\mu \Omega_\mu^0 \left(\hat{a}_\mu^\dagger(t) \hat{a}_\mu(t) + \frac{1}{2} \right). \quad (2.22)$$

In the interaction picture the dynamics of the ladder operators is governed by

$$\frac{d\hat{a}_\mu(t)}{dt} = i [\hat{H}_0, \hat{a}_\mu(t)] = -i\Omega_\mu^0 \hat{a}_\mu(t). \quad (2.23)$$

This differential equation leads to an oscillating time-dependence

$$\hat{a}_\mu(t) = \hat{a}_\mu e^{-i\Omega_\mu^0 t} \quad (2.24)$$

of the ladder operators. Accordingly, in the interaction picture the particle number operator is explicitly time-independent

$$\hat{N}_\mu = \hat{a}_\mu^\dagger(t) \hat{a}_\mu(t) = \hat{a}_\mu^\dagger \hat{a}_\mu \quad (2.25)$$

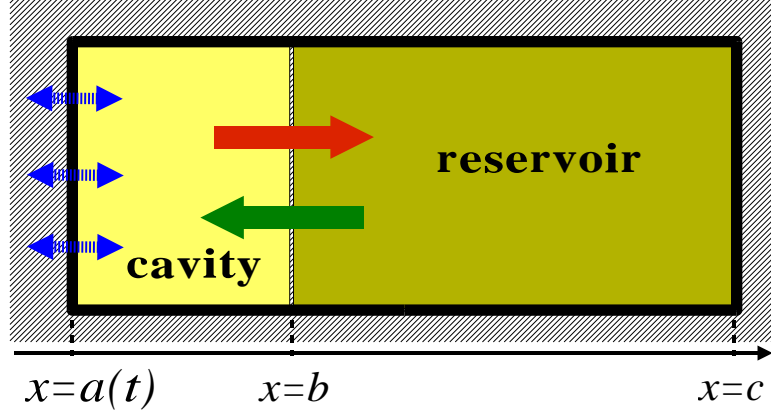


Figure 2.1: Model of a leaky cavity. A large ideal cavity is split up by a dispersive mirror into a leaky cavity and a reservoir. The left (perfectly reflecting) wall of the cavity is moving.

for all modes μ . With these ladder operators, the squeezing and velocity Hamiltonians $\hat{H}_I^S(t)$ and $\hat{H}_I^V(t)$ in the interaction picture are given by

$$\begin{aligned}\hat{H}_I^S(t) &= \sum_{\mu} \frac{1}{4} \frac{\Delta\Omega_{\mu}^2(t)}{\Omega_{\mu}^0} [(\hat{a}_{\mu})^2(t) + (\hat{a}_{\mu}^{\dagger})^2(t) + \hat{a}_{\mu}(t)\hat{a}_{\mu}^{\dagger}(t) + \hat{a}_{\mu}^{\dagger}(t)\hat{a}_{\mu}(t)] , \\ \hat{H}_I^V(t) &= \sum_{\mu,\nu} \frac{i}{2} \sqrt{\frac{\Omega_{\mu}^0}{\Omega_{\nu}^0}} M_{\mu\nu}(t) [\hat{a}_{\mu}^{\dagger}(t)\hat{a}_{\nu}^{\dagger}(t) + \hat{a}_{\mu}^{\dagger}(t)\hat{a}_{\nu}(t) - \hat{a}_{\mu}(t)\hat{a}_{\nu}^{\dagger}(t) - \hat{a}_{\mu}(t)\hat{a}_{\nu}(t)] .\end{aligned}\quad (2.26)$$

2.4 A Model Cavity

A first step towards leaky systems is to examine the influence of transparent mirrors on quantum electrodynamics as was done in [45, 46]. Mirrors with a finite transmittance can for example be modeled by some external potential $V(x; t)$ by which the field Φ is influenced. The construction of a leaky system is then completed by employing transparent mirrors to form a cavity. In order to obtain bound states it will be necessary to enclose the leaky system by a larger ideal cavity. The simplest model for a leaky cavity surrounded by an ideal one is obtained by inserting a transparent mirror into an ideal cavity, see also figure 2.1. To allow for dynamical external conditions the left wall of the cavity is moving with a prescribed trajectory $a(t)$ in time. The corresponding static system in 1+1 dimensions has already been treated in [48, 26]. However, the dynamical system considered here has interesting properties. For ideal cavities the non-

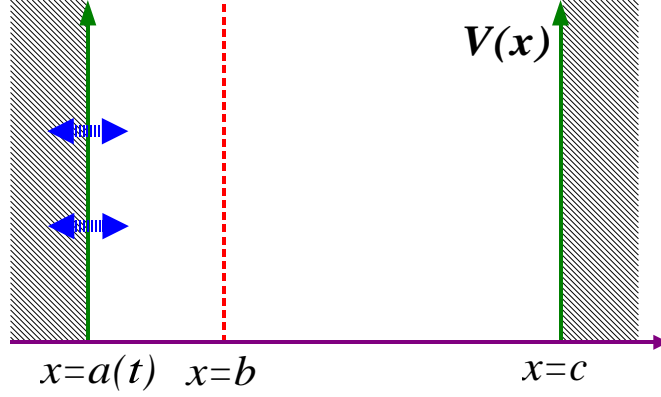


Figure 2.2: Diagram of the x -dependence of $V(x)$. The Dirichlet boundary conditions are simulated by infinitely high potential walls whereas the dispersive mirror at $x = b$ is approximated by a δ -function potential.

stationary boundary conditions are known to lead to a squeezing of the vacuum state which causes the creation of particles inside the cavity, see e.g. [38, 39]. In the system considered here the boundary conditions only vary in the left non-ideal cavity. In a general case for an arbitrarily shaped cavity the only condition on the potential $V(x)$ would be that it should be infinitely large outside the cavity domain $G(t)$ to prevent any particle losses. Following the idea in [45, 48] one can model a transparent mirror by a δ -type potential whereas the perfectly reflecting mirrors can be incorporated by infinitely large potential walls

$$V(x; t) = \begin{cases} \gamma \delta(x - b) & \text{if } a(t) < x < c \\ \infty & \text{otherwise} \end{cases}, \quad (2.27)$$

where $\delta(x)$ denotes the Dirac δ -distribution. An illustration of this potential is given in figure 2.2. The parameter γ enters the reflection and transmission amplitudes of the internal dispersive mirror at a given frequency ω via [45, 46]

$$\mathcal{R} = -\frac{i\gamma}{\omega + i\gamma}, \quad \mathcal{T} = \frac{\omega}{\omega + i\gamma}, \quad (2.28)$$

where $|\mathcal{R}|^2 + |\mathcal{T}|^2 = 1$ holds. Thus any desired transmittance of the dispersive mirror can be adjusted. The method is not confined to this very simple model: Any functional dependence inside the domain $G(t)$ modeling a dispersive mirror would hold. The ansatz used here is a simplified version of an experimentally significant scenario where the electromagnetic field is examined in an ideal cavity with a thin dielectric slab with thickness d – having a very large

dielectric constant – inserted. The potential could then be incorporated by a space-dependent permittivity [48]

$$\varepsilon(x) = 1 + \alpha \delta(x), \quad (2.29)$$

where α has the dimension of a length and relates with the dielectric constant ε_s of the slab via

$$\varepsilon_s = 1 + \frac{\alpha}{d}. \quad (2.30)$$

2.5 Eigenmodes

For a complete knowledge of the Hamiltonian in section 2.2 the set of eigenfunctions $\{f_\mu\}$ determined by the eigenvalue equation $\{2V - \nabla^2\} f_\mu(\mathbf{r}; t) = \Omega_\mu^2(t) f_\mu(\mathbf{r}; t)$ needs to be known. Note that the potential from section 2.4 also imposes the Dirichlet boundary conditions $f_\mu(\mathbf{r}; t)|_{\partial G(t)} = 0$. Any time dependence of eigenfunctions and eigenfrequencies is therefore only introduced via the time-dependent boundary parameters. This differential equation can be solved with the separation ansatz [38]

$$f_\mu(\mathbf{r}) = f_\mu^\parallel(\mathbf{r}_\parallel) f_\mu^\perp(\mathbf{r}_\perp), \quad (2.31)$$

where f_μ^\parallel depends only on the coordinate parallel to the wall velocity and f_μ^\perp is dependent on the perpendicular coordinates. For the special case of the rectangular model system this means

$$f_\mu^\parallel(\mathbf{r}_\parallel) = f_\mu^x(x), \quad f_\mu^\perp(\mathbf{r}_\perp) = f_\mu^y(y) f_\mu^z(z). \quad (2.32)$$

Separating the frequency contributions

$$\Omega_\mu^2 = (\Omega_\mu^\parallel)^2 + (\Omega_\mu^\perp)^2 = (\Omega_\mu^x)^2 + (\Omega_\mu^y)^2 + (\Omega_\mu^z)^2, \quad (2.33)$$

leads to the well-known trivial y and z solutions of a particle within a box potential

$$\begin{aligned} f_\mu^y(y) &= \sqrt{\frac{2}{\Delta y}} \sin \left[\frac{n_y \pi}{\Delta y} y \right], & \Omega_\mu^y &= \frac{n_y \pi}{\Delta y}, \\ f_\mu^z(z) &= \sqrt{\frac{2}{\Delta z}} \sin \left[\frac{n_z \pi}{\Delta z} z \right], & \Omega_\mu^z &= \frac{n_z \pi}{\Delta z}, \end{aligned} \quad (2.34)$$

where Δy and Δz denote the dimensions of the cavity in the perpendicular directions. The quantum numbers n_y and n_z can assume all positive integer values $n_y, n_z \in \mathbb{N}_+$. The remaining differential equation for $f_\mu^x(x)$ reads

$$\{2\gamma\delta(x-b) - \partial_x^2\} f_\mu^x(x) = (\Omega_\mu^x)^2 f_\mu^x(x), \quad (2.35)$$

where the Dirichlet boundary conditions

$$f_\mu^x|_{x=a(t)} = f_\mu^x|_{x=c} = 0 \quad (2.36)$$

have to be imposed. These boundary conditions are already satisfied by the solution ansatz [48, 26]

$$f_\mu^x(x) = \begin{cases} L_\mu \sin[\Omega_\mu^x(x-a)] & \text{if } a < x < b \\ R_\mu \sin[\Omega_\mu^x(c-x)] & \text{if } b < x < c \\ 0 & \text{elsewhere} \end{cases}, \quad (2.37)$$

where L_μ and R_μ denote constant coefficients for the left and right side, respectively. By integration $\int_{b-0}^{b+0} dx$ one can find [48, 45] the connection condition

$$\frac{\partial f_\mu^x}{\partial x}(x \downarrow b) - \frac{\partial f_\mu^x}{\partial x}(x \uparrow b) = 2\gamma f_\mu^x(b). \quad (2.38)$$

In addition the solution has to be continuous which implies

$$f_\mu^x(x \downarrow b) - f_\mu^x(x \uparrow b) = 0. \quad (2.39)$$

These conditions do not only link the coefficients L_μ and R_μ but can also be combined to an equation to determine Ω_μ^x

$$-\frac{2\gamma}{\Omega_\mu^x} = \cot[\Omega_\mu^x(b-a)] + \cot[\Omega_\mu^x(c-b)]. \quad (2.40)$$

For given cavity parameters $\{a, b, c, \gamma\}$ a numerical solution of this equation can always be obtained. However, via introducing the dimensionless perturbation parameter

$$\eta_\mu = \frac{\Omega_\mu^x}{\gamma}, \quad (2.41)$$

it is also possible to obtain an approximate analytical solution. Note that this parameter is small $\eta_\mu \ll 1$ in the limit of the internal mirror being nearly perfectly reflecting. Since the trigonometric cot functions are very sensitive to small variations of the frequency Ω_μ^x , one can equivalently solve the equation

$$\frac{-2}{\eta_\mu} = \cot[\Omega_\mu^x(b-a)] + \cot[\Omega_\mu^x(c-b)] \quad (2.42)$$

by a series expansion in η_μ . If $2/\eta_\mu$ goes to ∞ the equation can only be fulfilled if one or even both of the cot functions diverge. (Whether one or both are contributing is determined by the ratio $(b-a)/(c-b)$ and its inverse which are both assumed to be non-integer numbers in

the following perturbative calculations meaning that only one of the addends is dominating.) Expanding one of the addends around the poles at $x = n\pi$

$$\cot(x) = \frac{1}{x - n\pi} - \frac{1}{3}(x - n\pi) - \frac{1}{45}(x - n\pi)^3 + \mathcal{O}((x - n\pi)^5) \quad (2.43)$$

and the other one around the same frequency value yields a polynomial that can be solved for the frequency Ω_μ^x as a series expansion in $\eta_\mu \ll 1$. Depending on which addend is expanded around its pole one obtains two sets of approximate eigenfrequencies

$$\begin{aligned} \Omega_{n_x, l}^x &= \frac{n_x \pi}{b - a} - \frac{1}{2(b - a)} \eta_{n_x, l} + \frac{1}{4(b - a)} \cot\left(n_x \pi \frac{c - b}{b - a}\right) \eta_{n_x, l}^2 + \mathcal{O}(\eta_{n_x, l}^3), \\ \Omega_{n_x, r}^x &= \frac{n_x \pi}{c - b} - \frac{1}{2(c - b)} \eta_{n_x, r} + \frac{1}{4(c - b)} \cot\left(n_x \pi \frac{b - a}{c - b}\right) \eta_{n_x, r}^2 + \mathcal{O}(\eta_{n_x, r}^3), \end{aligned} \quad (2.44)$$

where $\mu = (n_x, l/r)$ with l -left for $\cot[\omega(b - a)]$ and r -right for $\cot[\omega(c - b)]$ is found to be a multi-index. Inserting the parameter η_μ yields a polynomial that can be solved for Ω_μ^x . As is demonstrated in figure 2.3, the quality of the linear (in η) approximation suffices already for moderate values of $\gamma \geq 50$. The insertion of the eigenfrequencies in the ansatz (2.37) leads to two classes of eigenfunctions, see also figure 2.4. The remaining global factor L_μ is determined by demanding the set $\{f_\mu\}$ to be normalized. In the limit of small η_μ one can therefore distinguish between two classes of solutions: right- and left-dominated eigenfrequencies also implying the existence of right- and left-dominated eigenmodes. These shall be denoted by the flags r and l , respectively, in the following. According to figure 2.4 the eigenfunctions are mainly concentrated in the respective part of the cavity. Thus the eigenfunctions are labeled by multi-indices: 3 quantum numbers $n_x, n_y, n_z \in \mathbb{N}_+$ and a flag r/l denoting the class (right- or left-dominated, respectively) of the eigenfunction, i.e. a certain mode can be labeled by $\mu = (n_x, n_y, n_z, r/l)$.

A perturbative expression for the eigenfunctions up to $\mathcal{O}(\eta_\mu)$ is given in appendix 7.1.

The time-dependence of eigenfrequencies and eigenfunctions due to dynamical external conditions can now be incorporated via the time-dependent boundary parameter $a(t)$.

If the velocity of the boundary $\dot{a}(t)$ is small – meaning $\dot{a}(t) = \mathcal{O}(\epsilon)$ with some $\epsilon \ll 1$ – then the coupling matrix $M_{\mu\nu}$ can be factorized into an approximately constant factor $m_{\mu\nu}$ – representing the geometry of the system under consideration – and the velocity of the boundary

$$M_{\mu\nu}(t) = m_{\mu\nu} \dot{a}(t) + \mathcal{O}(\epsilon^2) \quad \text{with} \quad m_{\mu\nu} = \int d^3r \frac{\partial f_\mu}{\partial a} f_\nu. \quad (2.45)$$

Since the time-dependence of the right-dominated modes is less complicated than that of the left-dominated ones, it may sometimes be advantageous to exploit the antisymmetry of $m_{\mu\nu}$.

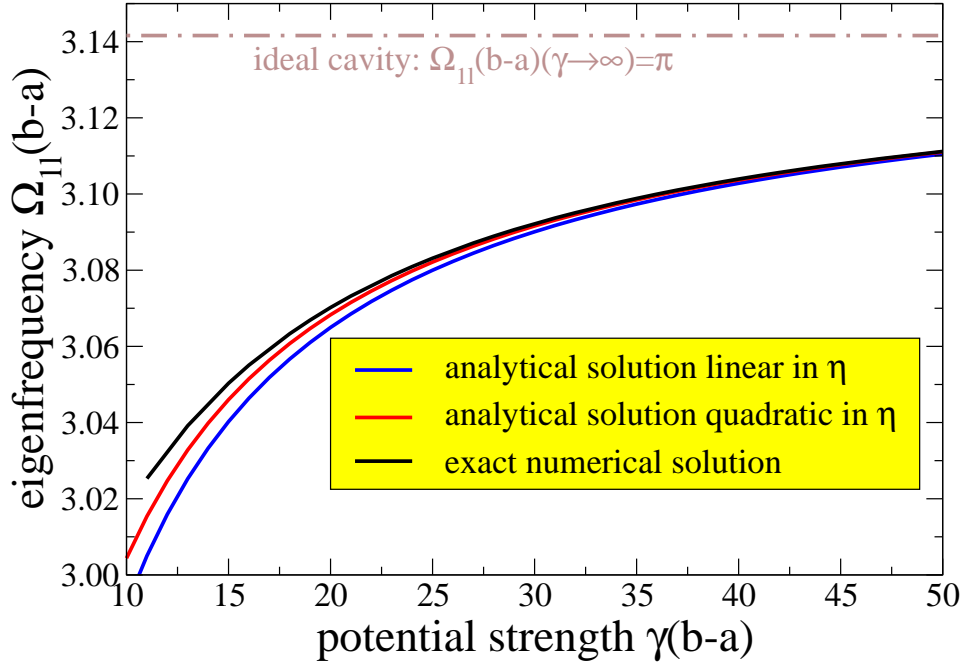


Figure 2.3: Comparison of the dimensionless exact numerical and approximate analytical eigenfrequencies (2.44) $\Omega_{1l}^x(b-a)$. The linear approximation is already sufficient at moderate values of $\gamma(b-a) \geq 50$. In these calculations a ratio of $(c-b)/(b-a) = 10/3$ has been assumed.

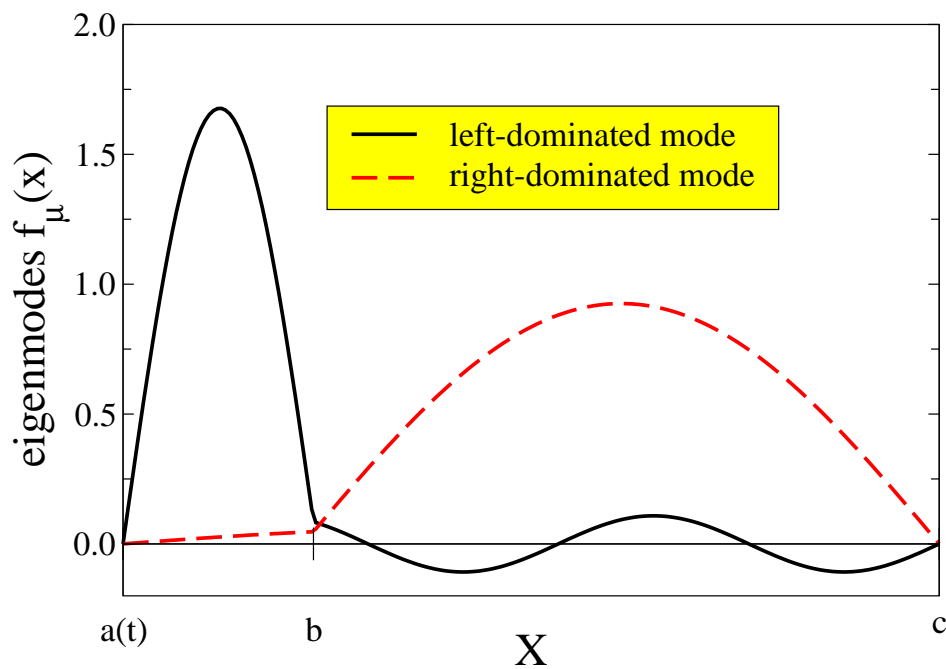


Figure 2.4: Illustration of the x dependence of the lowest ($n_x = 1$) left- and right-dominated eigenmodes $f_\mu^x(x)$ for $\eta_{1r/1l} = 0.1$. The modes are mainly concentrated in the corresponding part of the complete system thus substantiating the nomenclature. At the position of the dispersive mirror b the derivatives of the functions are discontinuous.

The calculation of the geometry factor $m_{\mu\nu}$ between the two modes $\mu = (n_x, n_y, n_z, f)$ and $\mu = (n'_x, n'_y, n'_z, f')$ reduces to only one integration, since for a rectangular cavity the dy and dz integrations simply generate Kronecker symbols. Accordingly, one finds for the geometry factor

$$\begin{aligned}
m_{\mu\nu} &= \int d^3r \frac{\partial f_\mu}{\partial a} f_\nu = \delta_{n_y, n'_y} \delta_{n_z, n'_z} \int_a^c \frac{\partial f_\mu^x(x)}{\partial a} f_\nu^x(x) dx \\
&= \delta_{n_y, n'_y} \delta_{n_z, n'_z} \left[L_\nu \frac{\partial L_\mu}{\partial a} I_{\mu\nu}^1(b-a) + L_\nu \frac{\partial \Omega_\mu^x}{\partial a} I_{\mu\nu}^2(b-a) \right. \\
&\quad \left. - L_\nu \Omega_\mu^x I_{\mu\nu}^3(b-a) + R_\nu \frac{\partial R_\mu}{\partial a} I_{\mu\nu}^1(c-b) + R_\nu \frac{\partial \Omega_\mu^x}{\partial a} I_{\mu\nu}^2(c-b) \right], \tag{2.46}
\end{aligned}$$

where the integrals $I_{\mu\nu}^i(x)$ are defined via

$$\begin{aligned}
I_{\mu\nu}^1(x) &= \int_0^x \sin(\Omega_\mu^x y) \sin(\Omega_\nu^x y) dy, \\
I_{\mu\nu}^2(x) &= \int_0^x y \cos(\Omega_\mu^x y) \sin(\Omega_\nu^x y) dy, \\
I_{\mu\nu}^3(x) &= \int_0^x \cos(\Omega_\mu^x y) \sin(\Omega_\nu^x y) dy. \tag{2.47}
\end{aligned}$$

For the following calculations the coupling between different modes will be of special relevance. In these cases the occurrence of many perturbation parameters η_μ can be avoided by defining the fundamental perturbation parameter

$$\eta = \eta_{1l} = \frac{\Omega_{1l}^x}{\gamma}, \tag{2.48}$$

and expressing all others via $\eta_\mu = (\Omega_\mu^x / \Omega_{1l}^x) \eta$. The coupling of the lowest left-dominated mode $\mu = (1, 1, 1, l)$ to some right-dominated one $\nu = (n_x, n_y, n_z, r)$ will be given here explicitly

$$\begin{aligned}
m_{\mu\nu} &= -\delta_{1, n_y} \delta_{1, n_z} \int_a^c dx f_\mu^x \frac{\partial f_\nu^x}{\partial a} \\
&= \frac{\delta_{1, n_y} \delta_{1, n_z} (-1)^{n_x} n_x \sqrt{\frac{b-a}{c-b}}}{(c-b) \sin\left(n_x \pi \frac{b-a}{c-b}\right) \left[n_x^2 \left(\frac{b-a}{c-b}\right)^2 - 1\right]} \frac{\Omega_{n_x r}^x}{\Omega_{1l}^x} \eta + \mathcal{O}(\eta^2) = \mathcal{O}(\eta), \tag{2.49}
\end{aligned}$$

to demonstrate that the coupling between these modes is small. Note that this expression diverges if $(b-a)/(c-b)$ is an integral number or if $n_x = (c-b)/(b-a)$ which has been excluded from the beginning.

2.6 Effective Time Evolution

In the interaction picture the time evolution operator is given by the formal expression

$$\hat{U}(T, 0) = \hat{\mathcal{T}}_t \exp \left(-i \int_0^T \hat{H}_I(t) dt \right), \quad (2.50)$$

where $\hat{\mathcal{T}}_t$ denotes time-ordering and $\hat{H}_I(t) = \hat{H}_I^S(t) + \hat{H}_I^V(t)$ denotes the time-dependent perturbation Hamiltonian in the interaction picture. Above operator equation shall be understood as the corresponding series expansion of the exponential. In general the arbitrary time-dependence of $\hat{H}_I(t)$ makes the calculation of \hat{U} very difficult. If $\hat{H}_I T$ is small, then an expansion of the exponential yields a power series in $\hat{H}_I T$ suitable for perturbation theory. However, in view of an experimental verification of the dynamical Casimir effect \hat{U} should deviate significantly from the identity which implies that $\hat{H}_I T$ should be large. Therefore another approximation needs to be found. It has been predicted by several authors that the phenomenon of parametric resonance where the cavity wall performs harmonic oscillations at a certain frequency is the most promising scenario for an experimental observation of quantum radiation. For an ideal cavity this resonance leads to an exponential growth of the particle number and is therefore favorable for an experiment. Via time-averaging over the oscillations (see subsection 2.6.1)

$$\hat{U}(T, 0) = \sum_{n=0}^{\infty} \frac{(-i)^n}{n!} \int_0^T dt_1 \dots dt_n \hat{\mathcal{T}}_t \left[\hat{H}_I(t_1) \dots \hat{H}_I(t_n) \right], \quad (2.51)$$

an effective time evolution operator can be defined within the rotating wave approximation (RWA)

$$\hat{U}_{\text{eff}}(T, 0) \stackrel{\text{RWA}}{=} \exp \left(-i \hat{H}_{\text{eff}}^I T \right), \quad (2.52)$$

see e.g. [39, 28, 30]. Thereby the time-ordering is neglected and an effective interaction Hamiltonian can be defined via

$$\hat{H}_{\text{eff}}^I \stackrel{\text{RWA}}{=} \frac{1}{T} \int_0^T \hat{H}_I(t) dt = \frac{1}{T} \int_0^T \hat{H}_I^S(t) dt + \frac{1}{T} \int_0^T \hat{H}_I^V(t) dt. \quad (2.53)$$

The justification for this procedure will be given in the following section.

2.6.1 Rotating Wave Approximation (RWA)

The series expansion of the time-evolution operator contains time-ordered products of the time-integrated interaction Hamiltonians. In the case of parametric resonance the rotating

wave approximation allows for an approximate solution of these integrals via averaging over the fast oscillations. The time-ordered products can also be rewritten as (see also appendix 7.3)

$$\begin{aligned}
\hat{\mathcal{T}}_t \left[\hat{H}_I(t_1) \dots \hat{H}_I(t_n) \right] &= \hat{H}_I(t_1) \dots \hat{H}_I(t_n) \\
&- \sum_{P \in S_n \setminus P_e} \Theta(t_{P(1)} - t_{P(2)}) \dots \Theta(t_{P(n-1)} - t_{P(n)}) \times \\
&\sum_{\text{sets}\{k,l\}} \delta(P, \{k, l\}) \hat{H}_I(t_{P(1)}) \dots \left[\hat{H}_I(t_{P(k)}), \hat{H}_I(t_{P(l)}) \right] \times \\
&\dots \hat{H}_I(t_{P(n)}), \tag{2.54}
\end{aligned}$$

where S_n denotes the permutation group of the integer numbers $\{1, 2, \dots, n-1, n\}$ and P_e stands for the identity permutation. The function $\delta(P, \{k, l\}) \in \{0, 1\}$ regulates which terms contribute for a given permutation P , see also the appendix 7.3. This leads to two basic types of integrals in the time-evolution operator series expansion.

Effective Interaction Hamiltonian Since in the first term of (2.54) no time-ordering is present, all the dt_i -integrations factorize and one just has to consider the time-integrated interaction Hamiltonian. In the interaction picture squeezing and velocity interaction Hamiltonian contain all possible quadratic combinations of the time-dependent creation and annihilation operators. In addition there is a time-dependent factor induced by the deviation $\Delta\Omega_\mu^2(t)$ in the squeezing Hamiltonian and the coupling matrix $M_{\mu\nu}(t)$ in the velocity Hamiltonian. In the case of parametric resonance a parameter $a(t)$ accounting for the position of one boundary performs harmonic oscillations at an external vibration frequency ω

$$a(t) = a_0 + \epsilon l_0 \sin(\omega t), \tag{2.55}$$

where l_0 is some characteristic length of the system and $\epsilon \ll 1$ denotes the dimensionless vibration amplitude. Accordingly, one finds via expanding around a_0 for the time-dependent factors (2.15) and (2.45) a purely oscillating behavior

$$\begin{aligned}
\Delta\Omega_\mu^2(t) &= 2\Omega_\mu^0 \frac{\partial \Omega_\mu^0}{\partial a_0} l_0 \epsilon \sin(\omega t) + \mathcal{O}(\epsilon^2), \\
M_{\mu\nu}(t) &= m_{\mu\nu} l_0 \omega \epsilon \cos(\omega t) + \mathcal{O}(\epsilon^2). \tag{2.56}
\end{aligned}$$

Together with the trivial time-dependence of the ladder operators

$$\hat{a}_\mu(t) = \hat{a}_\mu e^{-i\Omega_\mu^0 t}, \quad \hat{a}_\mu^\dagger(t) = \hat{a}_\mu^\dagger e^{+i\Omega_\mu^0 t} \tag{2.57}$$

this leads in (2.53) to generic integrals of the form

$$\begin{aligned}\frac{1}{T} \int_0^T \hat{H}_I^S(t) dt &= \frac{1}{T} \sum_{\mu} \hat{A}_{\mu}^{\pm} \int_0^T \sin(\omega t) \exp(\pm i 2 \Omega_{\mu}^0 t) dt, \\ \frac{1}{T} \int_0^T \hat{H}_V^S(t) dt &= \frac{1}{T} \sum_{\mu\nu} \hat{B}_{\mu\nu}^{\pm} \int_0^T \cos(\omega t) \exp(\pm i (\Omega_{\mu}^0 \pm \Omega_{\nu}^0) t) dt,\end{aligned}\quad (2.58)$$

where all operators as well as the time-independent parameters of the external disturbance have been absorbed in \hat{A}_{μ}^{\pm} and $\hat{B}_{\mu\nu}^{\pm}$. Considering these integrals over many periods (in the limit $\omega T \gg 1$) one finds

$$\begin{aligned}I_1 &= \frac{1}{T} \int_0^T \sin[\omega(1+\delta)t] e^{\pm i \omega t} dt = \frac{1}{2} \frac{1 - e^{\mp i \delta \omega T}}{\delta \omega T} + \mathcal{O}\left(\frac{1}{\omega T}\right) \\ &\stackrel{\delta \rightarrow 0}{=} \pm \frac{i}{2} + \mathcal{O}\left(\frac{1}{\omega T}\right), \\ I_2 &= \frac{1}{T} \int_0^T \cos[\omega(1+\delta)t] e^{\pm i \omega t} dt = \frac{\mp i}{2} \frac{1 - e^{\mp i \delta \omega T}}{\delta \omega T} + \mathcal{O}\left(\frac{1}{\omega T}\right) \\ &\stackrel{\delta \rightarrow 0}{=} \frac{1}{2} + \mathcal{O}\left(\frac{1}{\omega T}\right).\end{aligned}\quad (2.59)$$

Obviously significant contributions can only arise if the deviation $\delta \ll 1$, see also subsection 2.6.4. Equivalently, in the squeezing Hamiltonian only those terms where the squeezing resonance condition [40, 43, 44, 32, 39]

$$\omega = 2\Omega_{\mu}^0 \quad (2.60)$$

holds for some mode μ will be kept. Assuming a nondegenerate spectrum of the eigenfrequencies of the cavity this condition projects the sum onto only one mode μ .

In the velocity interaction Hamiltonian one finds due to the quadratic combinations of different ladder operators the more sophisticated velocity resonance condition [40, 39]

$$\omega = |\Omega_{\mu}^0 \pm \Omega_{\nu}^0|, \quad (2.61)$$

which could – in contrast to the squeezing Hamiltonian – in general be fulfilled by a set of paired modes $\{\mu\nu\}$. This depends on the dimensions and the geometry of the cavity under consideration. Note that due to the antisymmetry of the coupling matrix $m_{\mu\nu}$ the two coupling modes are not allowed to be the same.

Accordingly, the first term in (2.54) yields a product of n effective interaction Hamiltonians $\hat{H}_{\text{eff}}^I T$ within the RWA.

Neglect of Time-Ordering The remaining terms in (2.54) do consist of a sum over products with commutators. A typical corresponding integral in the time evolution operator is therefore given by

$$I_3 = \frac{1}{T^2} \int_0^T dt_{P(k)} dt_{P(l)} \left[\hat{H}_I(t_{P(k)}), \hat{H}_I(t_{P(l)}) \right] \times \\ \Theta(t_{P(k-1)} - t_{P(k)}) \Theta(t_{P(k)} - t_{P(k+1)}) \Theta(t_{P(l-1)} - t_{P(l)}) \Theta(t_{P(l)} - t_{P(l+1)}) . \quad (2.62)$$

In the case of parametric resonance the Hamiltonians carry an oscillating time-dependence and constant contributions $\hat{H}_I(t) = \hat{A}^{\text{const}} + \hat{B}^{\text{osc}}(t)$, which follows directly from their Fourier expansion $\hat{H}_I(t) = \sum_n \hat{A}_n e^{in\omega t}$ if one identifies $\hat{A}^{\text{const}} = \hat{A}_0$ and $\hat{B}^{\text{osc}}(t) = \sum_{n \neq 0} \hat{A}_n e^{in\omega t}$. Therefore the commutator cannot yield anything but oscillating contributions to the integral I_3

$$\begin{aligned} \left[\hat{H}_I(t_{P(k)}), \hat{H}_I(t_{P(l)}) \right] &= \left[\hat{A}^{\text{const}}, \hat{B}^{\text{osc}}(t_{P(l)}) - \hat{B}^{\text{osc}}(t_{P(k)}) \right] \\ &\quad + \left[\hat{B}^{\text{osc}}(t_{P(k)}), \hat{B}^{\text{osc}}(t_{P(l)}) \right] \\ &= \sum_{n \neq 0} \left[\hat{A}_0, \hat{A}_n \right] \left(e^{in\omega t_{P(l)}} - e^{in\omega t_{P(k)}} \right) \\ &\quad + \sum_{n, m \neq 0} \left[\hat{A}_n, \hat{A}_m \right] \exp \left[i\omega (nt_{P(k)} + mt_{P(l)}) \right] , \end{aligned} \quad (2.63)$$

since n, m are discrete and t is a continuous variable. Accordingly, these terms are neglected within the RWA

$$I_3 = \mathcal{O} \left(\frac{1}{\omega T} \right) , \quad (2.64)$$

which is a neglect of time-ordering [39] itself.

Accordingly, the series expansion for the time-evolution operator can be re-summed in the rotating wave approximation to yield

$$\int_0^T dt_1 \dots dt_n \hat{\mathcal{T}}_t \left[\hat{H}_I(t_1) \dots \hat{H}_I(t_n) \right] \stackrel{\text{RWA}}{=} \left(\hat{H}_{\text{eff}}^I T \right)^n , \quad (2.65)$$

which leads to the effective time evolution operator (2.52).

2.6.2 Effective Squeezing Hamiltonian

For the resonance case one obtains via inserting the frequency deviation (2.56) into (2.26) for the squeezing interaction Hamiltonian

$$\begin{aligned} \hat{H}_I^S(t) &= \sum_{\mu} \frac{1}{2} \frac{\partial \Omega_{\mu}^0}{\partial a_0} \epsilon l_0 \sin(\omega t) \left[(\hat{a}_{\mu})^2(t) + (\hat{a}_{\mu}^{\dagger})^2(t) + \hat{a}_{\mu}(t) \hat{a}_{\mu}^{\dagger}(t) + \hat{a}_{\mu}^{\dagger}(t) \hat{a}_{\mu}(t) \right] \\ &\quad + \mathcal{O}(\epsilon^2) . \end{aligned} \quad (2.66)$$

According to subsection 2.6.1 one can only expect significant contributions in the time integral if the resonance condition $\omega = 2\Omega_\mu^0$ holds, where μ can in principle be any mode of the system under consideration. Therefore with the aid of (2.59) the effective squeezing Hamiltonian reads

$$\hat{H}_{\text{eff}}^S = \frac{i}{4} \frac{\partial \Omega_\mu^0}{\partial a_0} \epsilon l_0 [(\hat{a}_\mu^\dagger)^2 - (\hat{a}_\mu)^2] . \quad (2.67)$$

This is obviously a generator for a squeezing operator for the mode μ . For the model system of a rectangular cavity where $l_0 = (b - a_0)$ this means that two cases will have to be distinguished:

- $\mu = (n_x, n_y, n_z, r)$ is a right-dominated mode. In this case one finds

$$\frac{\partial \Omega_\mu^0}{\partial a_0} = \mathcal{O}(\eta^2) , \quad (2.68)$$

since the unperturbed eigenfrequencies of right-dominated modes (2.44) do not depend on a_0 up to $\mathcal{O}(\eta)$. This case leads to a corresponding suppression by a factor of at least η^2 in the effective squeezing Hamiltonian and is not considered here.

- $\mu = (n_x, n_y, n_z, l)$ is a left-dominated mode. Hence one finds with

$$\frac{\partial \Omega_\mu^0}{\partial a_0} = \frac{\Omega_\mu^0}{b - a_0} \left(\frac{\Omega_\mu^{x0}}{\Omega_\mu^0} \right)^2 + \mathcal{O}(\eta^2) \quad (2.69)$$

that this scenario is not suppressed and therefore more important for an experiment. Among all left-dominated modes the lowest one is of special relevance since in an experiment lower frequencies are favorable. In addition, this choice reduces the number of possible combinations fulfilling the velocity resonance condition simultaneously. Accordingly, here the case of fundamental resonance is considered which is incorporated by the squeezing resonance condition [39, 40, 43, 44]

$$\omega = 2\Omega_L^0 . \quad (2.70)$$

From now on the fundamental resonance mode will be denoted with the multi-index $L = (1, 1, 1, l)$.

The effective squeezing interaction Hamiltonian (cf. [28, 39]) therefore determines according to

$$\hat{H}_{\text{eff}}^S = i\xi [(\hat{a}_L^\dagger)^2 - (\hat{a}_L)^2] , \quad (2.71)$$

with the squeezing parameter ξ given by

$$\xi = \frac{1}{4} \epsilon \Omega_L^0 \left(\frac{\Omega_L^{x0}}{\Omega_L^0} \right)^2 . \quad (2.72)$$

The Hamiltonian H_{eff}^S is a generator for a squeezing operator for the mode L .

2.6.3 Effective Velocity Hamiltonian

The same procedure can be applied for the velocity interaction Hamiltonian which reads with the aid of (2.56) and (2.26) in the case of parametric resonance

$$\begin{aligned} \hat{H}_I^V(t) = & \frac{i}{2} \sum_{\mu, \nu} \sqrt{\frac{\Omega_\mu^0}{\Omega_\nu^0}} m_{\mu\nu} \epsilon \omega l_0 \cos(\omega t) [\hat{a}_\mu^\dagger(t) \hat{a}_\nu^\dagger(t) + \hat{a}_\mu^\dagger(t) \hat{a}_\nu(t) - \hat{a}_\mu(t) \hat{a}_\nu^\dagger(t) - \hat{a}_\mu(t) \hat{a}_\nu(t)] \\ & + \mathcal{O}(\epsilon^2) . \end{aligned} \quad (2.73)$$

The occurrence of inter-mode couplings now results in the more sophisticated resonance condition (see also e.g. [39, 40])

$$\omega = |\Omega_\mu^0 \pm \Omega_\nu^0| . \quad (2.74)$$

Generally, this resonance condition can be fulfilled by several pairs of right- or left-dominated modes, i.e. the (symmetrized) effective velocity Hamiltonian reduces with (2.59) to

$$\begin{aligned} \hat{H}_{\text{eff}}^V = & \frac{i}{4} \sum_{\mu\nu: \Omega_\mu^0 + \Omega_\nu^0 = \omega} \frac{1}{2} \left(\sqrt{\frac{\Omega_\mu^0}{\Omega_\nu^0}} - \sqrt{\frac{\Omega_\nu^0}{\Omega_\mu^0}} \right) m_{\mu\nu} \epsilon \omega l_0 [\hat{a}_\mu^\dagger \hat{a}_\nu^\dagger - \hat{a}_\mu \hat{a}_\nu] \\ & + \frac{i}{4} \sum_{\mu\nu: |\Omega_\mu^0 - \Omega_\nu^0| = \omega} \frac{1}{2} \left(\sqrt{\frac{\Omega_\mu^0}{\Omega_\nu^0}} + \sqrt{\frac{\Omega_\nu^0}{\Omega_\mu^0}} \right) m_{\mu\nu} \epsilon \omega l_0 [\hat{a}_\mu^\dagger \hat{a}_\nu - \hat{a}_\mu \hat{a}_\nu^\dagger] . \end{aligned} \quad (2.75)$$

The structure of creation and annihilation operators in the first sum resembles a non-diagonal multi-mode squeezing generator whereas the second sum consists of hopping operators. Accordingly, multi-mode squeezing is induced by the velocity interaction Hamiltonian, whereas the squeezing interaction Hamiltonian leads to single-mode squeezing. Two important cases (\oplus and \ominus coupling) have to be considered. For the example of the model system of a rectangular cavity proposed in section 2.4 the Hamiltonian shall be calculated explicitly. For simplicity it will be assumed here that only one pair of modes fulfills the resonance condition.

- \oplus coupling $\omega = \Omega_1^0 + \Omega_2^0$. In this case the effective velocity Hamiltonian simplifies according to

$$\hat{H}_{\text{eff}}^V = \frac{i}{8} \left(\sqrt{\frac{\Omega_1^0}{\Omega_2^0}} - \sqrt{\frac{\Omega_2^0}{\Omega_1^0}} \right) m_{12} \epsilon \omega (b - a_0) (\hat{a}_1^\dagger \hat{a}_2^\dagger - \hat{a}_1 \hat{a}_2) , \quad (2.76)$$

which is a multi-mode squeezing Hamiltonian. If one wants to fulfill squeezing and velocity resonance conditions simultaneously, i.e. $2\Omega_L^0 = \Omega_1^0 + \Omega_2^0$ the number of possible combinations – depending on the cavity dimensions – reduces significantly.

- Ω_i^0 are both right-dominated modes. This combination requires large quantum numbers of the right-dominated modes since the reservoir is assumed to be larger than the leaky cavity.
- Ω_1^0 is a left-dominated mode and Ω_2^0 a right-dominated mode, respectively. Also this combination is possible but requires $\Omega_1^0 \neq \Omega_L^0$ since this case would lead to $\Omega_L^0 = \Omega_2^0$ which was excluded in the solution of the eigenvalue equation.
- Ω_i^0 are both left-dominated modes. This case can only be fulfilled if $\Omega_i^0 = \Omega_L^0$ since Ω_L^0 is already the lowest left-dominated mode. However, due to the antisymmetry of the coupling matrix $M_{LL} = 0$ this combination vanishes and therefore does not contribute at all.
- \ominus coupling $\omega = \Omega_2^0 - \Omega_1^0$. For this case the resulting effective velocity Hamiltonian does not resemble a squeezing but a hopping operator

$$\hat{H}_{\text{eff}}^V = \frac{i}{8} \left(\sqrt{\frac{\Omega_1^0}{\Omega_2^0}} + \sqrt{\frac{\Omega_2^0}{\Omega_1^0}} \right) m_{12} \epsilon \omega (b - a_0) \left(\hat{a}_1^\dagger \hat{a}_2 - \hat{a}_1 \hat{a}_2^\dagger \right). \quad (2.77)$$

The \ominus coupling is of special interest since if one does not insist on simultaneously fulfilling the squeezing resonance condition parametric resonance could also be induced by lower external frequencies $\omega = \Omega_2^0 - \Omega_1^0 < 2\Omega_L^0$ whose generation would simplify the experiment. In the case of simultaneously fulfilling both conditions one finds several combinations.

- The frequencies Ω_i^0 are both right-dominated modes. This combination is possible but large quantum numbers are required since the reservoir is larger than the cavity.
- Both modes are left-dominated. Also this combination is possible but requires large quantum numbers. In addition, due to the non-equidistant eigenfrequencies of the cavity and the shift induced by the non-ideal walls the fulfillment of this resonance condition is hardly possible.
- Ω_2^0 is a right-dominated mode and Ω_1^0 some left-dominated mode, respectively. The lowest possible right-dominated mode would therefore be given by $\Omega_2^0 = \Omega_R^0 = 3\Omega_L^0$, i.e. with $\Omega_1^0 = \Omega_L^0$. This case will be considered in all further examples.

Note that the general procedure lined out in this thesis would most likely be applicable to any possible combination – for the non-perturbative approach this is demonstrated explicitly in section 5.5. However, in the chapters 3 and 4 only one special case of \ominus coupling will be

considered $\omega = 2\Omega_L^0 = \Omega_R^0 - \Omega_L^0$, where the multi-index R stands for the right-dominated mode fulfilling

$$\Omega_R^0 = 3\Omega_L^0. \quad (2.78)$$

In this case the effective velocity Hamiltonian (2.75) (cf. [39]) simplifies to

$$H_{\text{eff}}^V = i\chi \left(\hat{a}_L^\dagger \hat{a}_R - \hat{a}_L \hat{a}_R^\dagger \right), \quad (2.79)$$

where

$$\chi = \frac{1}{4}\epsilon\Omega_L^0 \left(\sqrt{\frac{\Omega_R^0}{\Omega_L^0}} + \sqrt{\frac{\Omega_L^0}{\Omega_R^0}} \right) (b - a_0)m_{L,R} = \mathcal{O}(\eta) \quad (2.80)$$

is the velocity parameter of the system. Since $\chi = \mathcal{O}(m_{L,R}) = \mathcal{O}(\eta)$ it follows that $\chi/\xi \ll 1$ in the limiting case of an almost perfectly reflecting mirror. The main contribution to particle creation is therefore induced by the squeezing interaction Hamiltonian, but to include the effects of losses it is necessary to fulfill both squeezing and velocity resonance conditions simultaneously. As the complete effective interaction Hamiltonian one consequently finds with (2.71)

$$\hat{H}_{\text{eff}}^I = i\xi \left[(\hat{a}_L^\dagger)^2 - (\hat{a}_L)^2 \right] + i\chi \left[\hat{a}_L^\dagger \hat{a}_R - \hat{a}_L \hat{a}_R^\dagger \right]. \quad (2.81)$$

2.6.4 Detuned Resonance

In the basic approximation in subsection 2.6.1 – the RWA – so far an exact fulfillment ($\delta = 0$) of the resonance conditions has been assumed. However, in a realistic experiment this will not be the case since the external vibration frequency will in general be "detuned" – it will deviate from the fundamental (or any other) resonance frequency. One can assume one boundary of the cavity to vibrate at the external vibration frequency $\omega' = \omega(1 + \delta)$ parameterized by

$$a(t) = a_0 + \epsilon l_0 \sin[\omega(1 + \delta)t], \quad (2.82)$$

where $\delta \ll 1$ denotes the dimensionless deviation from the exact resonance frequency ω . It remains to be shown if the RWA is capable of describing the effects of detuning. The basic initial assumptions are $\omega T \gg 1$, $\epsilon \ll 1$, and $\delta \ll 1$ with $\epsilon\omega T = \mathcal{O}(1)$ and $\delta\omega T = \mathcal{O}(1)$. Therefore, terms with $\epsilon^I \delta^J (\omega T)^K$ are neglected with the RWA if $I + J > K$ holds. In the case of detuned parametric resonance one finds for the oscillating factors

$$\begin{aligned} \Delta\Omega_\mu^2(t) &= 2\Omega_\mu^0 \frac{\partial\Omega_\mu^0}{\partial a_0} l_0 \epsilon \sin[\omega(1 + \delta)t] + \mathcal{O}(\epsilon^2), \\ M_{\mu\nu}(t) &= m_{\mu\nu} l_0 \omega(1 + \delta) \epsilon \cos[\omega(1 + \delta)t] + \mathcal{O}(\epsilon^2). \end{aligned} \quad (2.83)$$

The generalized integrals of (2.59) can also be written as

$$\begin{aligned}
I_1 &= \frac{i}{2}\Delta + \mathcal{O}\left(\frac{1}{\omega T}\right) = \frac{i}{2}|\Delta|e^{i\varphi} + \mathcal{O}\left(\frac{1}{\omega T}\right), \\
I_1^* &= \frac{-i}{2}|\Delta|e^{-i\varphi} + \mathcal{O}\left(\frac{1}{\omega T}\right), \\
I_2 &= \frac{1}{2}\Delta + \mathcal{O}\left(\frac{1}{\omega T}\right) = \frac{1}{2}|\Delta|e^{i\varphi} + \mathcal{O}\left(\frac{1}{\omega T}\right), \\
I_2^* &= \frac{1}{2}|\Delta|e^{-i\varphi} + \mathcal{O}\left(\frac{1}{\omega T}\right),
\end{aligned} \tag{2.84}$$

where the detuning parameter Δ is given by

$$\Delta = -i\frac{1 - e^{-i\delta\omega T}}{\delta\omega T} = |\Delta|e^{i\varphi}, \quad |\Delta| = \frac{\sqrt{2 - 2\cos(\delta\omega T)}}{|\delta\omega T|}, \tag{2.85}$$

with φ denoting its complex phase. However, the neglect of time-ordering within the RWA is questionable for non-vanishing detuning δ . If one proceeds naively one finds for the example of a rectangular cavity the total effective interaction Hamiltonian

$$\hat{H}_{\text{eff}}^I = i\xi|\Delta|\left[e^{i\varphi}(\hat{a}_L^\dagger)^2 - e^{-i\varphi}(\hat{a}_L)^2\right] + i\chi|\Delta|\left[e^{-i\varphi}\hat{a}_L^\dagger\hat{a}_R - e^{i\varphi}\hat{a}_L\hat{a}_R^\dagger\right]. \tag{2.86}$$

In order to use the simpler expressions obtained earlier it is convenient to take advantage of the invariance of the physical observables under phase transformations of the annihilation and creation operators. By introducing new operators

$$\hat{a}_L \rightarrow \exp(i\varphi/2)\hat{a}_L, \quad \hat{a}_R \rightarrow \exp(3i\varphi/2)\hat{a}_R \tag{2.87}$$

the form of equation (2.81) is completely regained

$$\hat{H}_{\text{eff}}^I = i\xi_\delta\left[(\hat{a}_L^\dagger)^2 - (\hat{a}_L)^2\right] + i\chi_\delta\left[\hat{a}_L^\dagger\hat{a}_R - \hat{a}_L\hat{a}_R^\dagger\right], \tag{2.88}$$

where the squeezing and velocity parameters are modified by the common factor $|\Delta|$

$$\xi_\delta = \xi|\Delta|, \quad \chi_\delta = \chi|\Delta| \tag{2.89}$$

and thus become dependent on the perturbation time T . Consequently, in the RWA the effects of detuning would be taken into account by substituting $\xi \rightarrow \xi_\delta$ and $\chi \rightarrow \chi_\delta$ everywhere in the obtained solutions (integrals over the perturbation time T will not occur). An analogous procedure (with different phase transformations) can also be applied in the case of \oplus coupling.

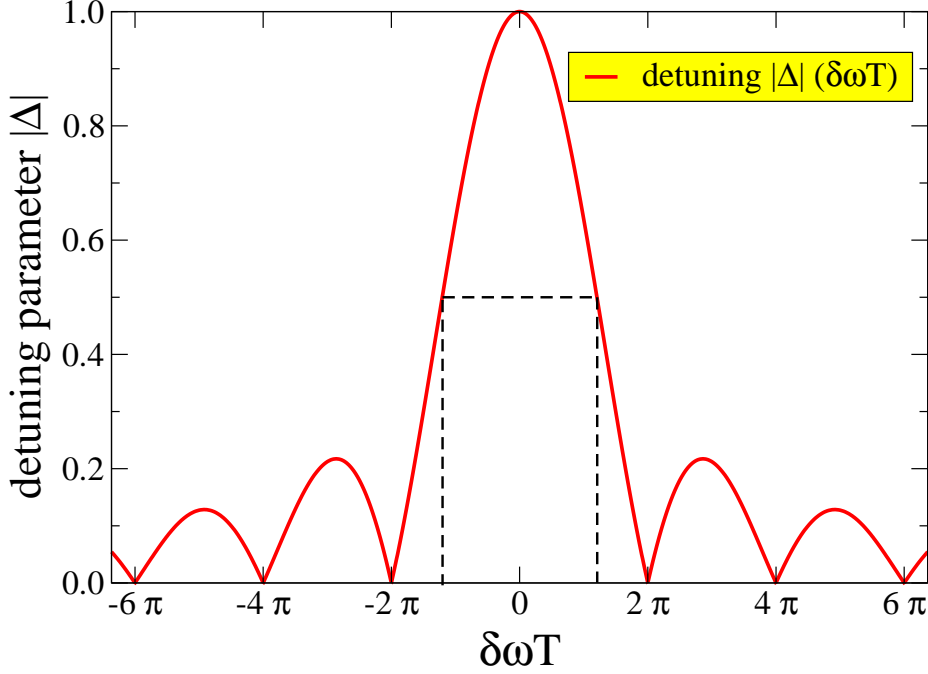


Figure 2.5: The varying detuning parameter $|\Delta|$ is 1 for $\delta = 0$ and vanishes for $\delta\omega T = 2\pi$. In view of $\omega T \gg 1$ this really requires $\delta \ll 1$. The half-width of above curve is 7.582.

The condition on χ and ξ not to vanish – this would completely destroy the dynamical Casimir effect since then the effective interaction Hamiltonians would vanish – leads to an upper bound

$$\omega T |\delta| < 2\pi, \quad (2.90)$$

see also figure 2.5. This constraint shows the RWA does not seem capable of including detuning effects since the upper bound will always be reached at some time. The dependence of the absolute value detuning parameter $|\Delta|$ on the argument $\delta\omega T$ is depicted in figure 2.5. An upper bound for the detuning constant has also been found by other authors, see e.g. [43, 44, 41, 40]. However, in order to find resonant particle creation in these publications the detuning δ had to be bounded by the dimensionless amplitude ϵ , see also section 5.3.

Chapter 3

Response Theory

A closed system in an initial thermal equilibrium can be described by the canonical ensemble where the statistical operator (see e.g. [49, 50, 51]) is given by

$$\hat{\rho}(t=0) = \hat{\rho}_0 = \frac{\exp(-\beta\hat{H}_0)}{\text{Tr}\left\{\exp(-\beta\hat{H}_0)\right\}}, \quad (3.1)$$

with β denoting the initial inverse temperature. The expectation value of an observable $\hat{Y}(t)$ can be obtained via

$$\langle Y(t) \rangle = \text{Tr}\left\{\hat{Y}(t)\hat{\rho}(t)\right\} = \text{Tr}\left\{\hat{\rho}(t)\hat{Y}(t)\right\}. \quad (3.2)$$

3.1 Expectation Values

In the interaction picture the expectation value at time $t = T$ of an observable \hat{Y} reads

$$\begin{aligned} \langle Y(T) \rangle &= \text{Tr}\left\{\hat{Y}\hat{\rho}(T)\right\} = \text{Tr}\left\{\hat{Y}\hat{U}(T,0)\hat{\rho}_0\hat{U}^\dagger(T,0)\right\} \\ &= \text{Tr}\left\{\hat{Y}\hat{\mathcal{T}}_t \exp\left(-i\int_0^T \hat{H}_I(t_1)dt_1\right)\hat{\rho}_0\hat{\mathcal{T}}_t^\dagger \exp\left(+i\int_0^T \hat{H}_I(t_2)dt_2\right)\right\}, \end{aligned} \quad (3.3)$$

where $\hat{\mathcal{T}}_t^\dagger$ denotes the anti-chronological time ordering operator and \hat{U} is the time evolution operator.

For a small interaction Hamiltonian $\hat{H}_I T$ one could expand the time evolution operator yielding a series expansion for $\langle Y(T) \rangle$. However, for the case of parametric resonance (see section 2.6) this procedure is not justified, since the interaction Hamiltonian $\hat{H}_I T$ is not small.

Within the rotating wave approximation in section 2.6.1 an effective time-evolution operator was derived

$$\hat{U}_{\text{eff}}(T, 0) \stackrel{\text{RWA}}{=} \exp \left(-i \hat{H}_{\text{eff}}^I T \right), \quad (3.4)$$

where the effective interaction Hamiltonian (2.81) was given by

$$\hat{H}_{\text{eff}}^I = i\xi \left[(\hat{a}_L^\dagger)^2 - (\hat{a}_L)^2 \right] + i\chi \left[\hat{a}_L^\dagger \hat{a}_R - \hat{a}_L \hat{a}_R^\dagger \right]. \quad (3.5)$$

(Remember, the time-ordering had been neglected within the RWA.) Inserting the effective time-evolution operator one finds for the expectation value of the observable \hat{Y}

$$\langle Y(T) \rangle \stackrel{\text{RWA}}{=} \text{Tr} \left\{ \hat{Y} \exp \left(-i(\hat{H}_{\text{eff}}^S + \hat{H}_{\text{eff}}^V) T \right) \hat{\rho}_0 \exp \left(+i(\hat{H}_{\text{eff}}^S + \hat{H}_{\text{eff}}^V) T \right) \right\}. \quad (3.6)$$

In the case of parametric resonance the effective squeezing interaction Hamiltonian $\hat{H}_{\text{eff}}^S T$ is not small which makes an expansion of the exponentials futile. It is therefore necessary to separate the two Hamiltonians. This can be achieved with the ansatz

$$\exp \left(-i(\hat{H}_{\text{eff}}^S + \hat{H}_{\text{eff}}^V) \tau \right) = \exp \left(-i \hat{H}_{\text{eff}}^S \tau \right) \hat{\sigma}(\tau) \quad (3.7)$$

with $\hat{\sigma}$ being an auxiliary operator. This ansatz also implies the initial condition $\hat{\sigma}(0) = \mathbf{1}$. Differentiating above expression with respect to τ and multiplying with $\exp(+i \hat{H}_{\text{eff}}^S \tau)$ from the left one yields

$$\frac{d\hat{\sigma}(\tau)}{d\tau} = -i \exp(-i \hat{H}_{\text{eff}}^S \tau) \hat{H}_{\text{eff}}^V \exp(+i \hat{H}_{\text{eff}}^S \tau) \hat{\sigma}(\tau) = -i \hat{\mathcal{H}}_{\text{eff}}^V(\tau) \hat{\sigma}(\tau), \quad (3.8)$$

where the (τ -dependent) squeezed effective velocity Hamiltonian has been introduced via

$$\hat{\mathcal{H}}_{\text{eff}}^V(\tau) = \exp \left(+i \hat{H}_{\text{eff}}^S \tau \right) \hat{H}_{\text{eff}}^V \exp \left(-i \hat{H}_{\text{eff}}^S \tau \right). \quad (3.9)$$

Further-on all squeezed operators will be denoted using calligraphy letters. The differential equation for $\hat{\sigma}$ can be solved by formal integration. Iteration of the obtained solution yields the series expansion

$$\begin{aligned} \hat{\sigma}(T) &= \mathbf{1} - i \int_0^T d\tau_1 \hat{\mathcal{H}}_{\text{eff}}^V(\tau_1) \hat{\sigma}(\tau_1) \\ &= \sum_{n=0}^{\infty} (-i)^n \int_0^T d\tau_1 \int_0^{\tau_1} d\tau_2 \dots \int_0^{\tau_{n-1}} d\tau_n \hat{\mathcal{H}}_{\text{eff}}^V(\tau_1) \dots \hat{\mathcal{H}}_{\text{eff}}^V(\tau_n) \\ &= \sum_{n=0}^{\infty} \frac{(-i)^n}{n!} \int_0^T d\tau_1 \int_0^T d\tau_2 \dots \int_0^T d\tau_n \hat{\mathcal{T}}_\tau \left[\hat{\mathcal{H}}_{\text{eff}}^V(\tau_1) \dots \hat{\mathcal{H}}_{\text{eff}}^V(\tau_n) \right] \\ &= \hat{\mathcal{T}}_\tau \left[\exp \left(-i \int_0^T \hat{\mathcal{H}}_{\text{eff}}^V(\tau) d\tau \right) \right]. \end{aligned} \quad (3.10)$$

Though the original time-ordering ($\hat{\mathcal{T}}_t$) had been neglected in the RWA, it has been reintroduced at this point as a parameter ($\hat{\mathcal{T}}_\tau$) ordering. Inserting this solution together with the ansatz (3.7) into the expectation value and using the invariance of the trace under cyclic permutations of its arguments yields

$$\langle Y(T) \rangle \stackrel{\text{RWA}}{=} \text{Tr} \left\{ \hat{\mathcal{Y}}(T) \hat{\mathcal{T}}_\tau \exp \left(-i \int_0^T \hat{\mathcal{H}}_{\text{eff}}^V(\tau_1) d\tau_1 \right) \times \right. \\ \left. \rho_0 \hat{\mathcal{T}}_\tau^\dagger \exp \left(+i \int_0^T \hat{\mathcal{H}}_{\text{eff}}^V(\tau_2) d\tau_2 \right) \right\}. \quad (3.11)$$

Accordingly, also the observables have to be squeezed

$$\hat{\mathcal{Y}}(T) = \exp \left(+i \hat{H}_{\text{eff}}^S T \right) \hat{Y} \exp \left(-i \hat{H}_{\text{eff}}^S T \right), \quad (3.12)$$

but here using the physical perturbation time T . This picture will further-on be denoted with squeezing interaction picture. Note that in this picture the statistical operator at time T relates with the initial statistical operator via

$$\hat{\rho}(T) = \hat{\sigma}(T) \hat{\rho}_0 \hat{\sigma}^\dagger(T). \quad (3.13)$$

As the advantage of these manipulations one can now expand the expectation value $\langle Y(T) \rangle$ into a perturbation series with powers of $\int_0^T \hat{\mathcal{H}}_{\text{eff}}^V(\tau) d\tau = \mathcal{O}(\eta)$. Keeping only terms to second order (see also [39]) one finds

$$\langle Y(T) \rangle = \langle Y^{(0)}(T) \rangle + \langle Y^{(1)}(T) \rangle + \langle Y^{(2)}(T) \rangle + \mathcal{O} \left((\hat{\mathcal{H}}_{\text{eff}}^V)^3 \right), \quad (3.14)$$

where

$$\begin{aligned} \langle Y^{(0)}(T) \rangle &= \text{Tr} \left\{ \hat{\mathcal{Y}}(T) \hat{\rho}_0 \right\}, \\ \langle Y^{(1)}(T) \rangle &= \text{Tr} \left\{ \hat{\mathcal{Y}}(T) \left[\hat{\rho}_0, i \int d\tau_1 \hat{\mathcal{H}}_{\text{eff}}^V(\tau_1) \right] \right\}, \\ \langle Y^{(2)}(T) \rangle &= \text{Tr} \left\{ \hat{\mathcal{Y}}(T) \int d\tau_1 \hat{\mathcal{H}}_{\text{eff}}^V(\tau_1) \hat{\rho}_0 \int d\tau_2 \hat{\mathcal{H}}_{\text{eff}}^V(\tau_2) \right\} \\ &\quad - \frac{1}{2} \text{Tr} \left\{ \hat{\mathcal{Y}}(T) \hat{\mathcal{T}}_\tau \int d\tau_1 \hat{\mathcal{H}}_{\text{eff}}^V(\tau_1) \int d\tau_2 \hat{\mathcal{H}}_{\text{eff}}^V(\tau_2) \hat{\rho}_0 \right\} \\ &\quad - \frac{1}{2} \text{Tr} \left\{ \hat{\mathcal{Y}}(T) \hat{\rho}_0 \hat{\mathcal{T}}_\tau^\dagger \int d\tau_1 \hat{\mathcal{H}}_{\text{eff}}^V(\tau_1) \int d\tau_2 \hat{\mathcal{H}}_{\text{eff}}^V(\tau_2) \right\}. \end{aligned} \quad (3.15)$$

Therefore complete knowledge of the squeezed operators as well as of the commutators will be essential. In above equations the lowest order $\langle Y^{(0)}(T) \rangle$ just represents the result one would

obtain for an ideal cavity ($\eta = 0$), which should enable one to check the results for consistency with other authors. The next term $\langle Y^{(1)}(T) \rangle = \mathcal{O}(\eta)$ accounts for the linear response. Finally the term $\langle Y^{(2)}(T) \rangle = \mathcal{O}(\eta^2)$ consisting of three traces constitutes the quadratic answer. Note that above expansion already implies the immanent failure of the quadratic approximation since at large perturbation times T the perturbation parameter $\int_0^T \hat{\mathcal{H}}_{\text{eff}}^V(t) dt$ will become too large. This problem can only be solved by considering all orders of η in perturbation theory, see also chapter 5.

3.2 The Quadratic Response

The terms in (3.15) are still too complex to perform calculations. Therefore it is advantageous to apply some simplifications to yield a more convenient form.

- Since the statistical operator $\hat{\rho}_0$ involves arbitrarily high powers of creation/annihilation operators it is practical to rewrite the linear response via exploiting the invariance of the trace under cyclic permutations

$$\langle Y^{(1)}(T) \rangle = \text{Tr} \left\{ \left[i \int d\tau_1 \hat{\mathcal{H}}_{\text{eff}}^V(\tau_1), \hat{\mathcal{Y}}(T) \right] \hat{\rho}_0 \right\}, \quad (3.16)$$

such that only a finite number of commutators has to be calculated.

- The quadratic response can also be rewritten to take a more convenient form. Inserting the identity $\hat{\rho}_0 \hat{\mathcal{Y}}(T) = \hat{\mathcal{Y}}(T) \hat{\rho}_0 - [\hat{\mathcal{Y}}(T), \hat{\rho}_0]$ and by making use of the property $\hat{\mathcal{T}}[\hat{A}(t)\hat{B}(t')] + \hat{\mathcal{T}}^\dagger[\hat{A}(t)\hat{B}(t')] = \{\hat{A}(t), \hat{B}(t')\}$ (see also appendix 7.3) one finds

$$\begin{aligned} \langle Y^{(2)}(T) \rangle &= \text{Tr} \left\{ \hat{\mathcal{Y}}(T) \int d\tau_1 \hat{\mathcal{H}}_{\text{eff}}^V(\tau_1) \hat{\rho}_0 \int d\tau_2 \hat{\mathcal{H}}_{\text{eff}}^V(\tau_2) \right\} \\ &\quad - \frac{1}{2} \text{Tr} \left\{ \hat{\mathcal{Y}}(T) \hat{\rho}_0 \left\{ \int d\tau_1 \hat{\mathcal{H}}_{\text{eff}}^V(\tau_1), \int d\tau_2 \hat{\mathcal{H}}_{\text{eff}}^V(\tau_2) \right\} \right\} \\ &\quad + \frac{1}{2} \text{Tr} \left\{ [\hat{\mathcal{Y}}(T), \hat{\rho}_0] \hat{\mathcal{T}} \int d\tau_1 \hat{\mathcal{H}}_{\text{eff}}^V(\tau_1) \int d\tau_2 \hat{\mathcal{H}}_{\text{eff}}^V(\tau_2) \right\} \\ &= \text{Tr} \left\{ \hat{\rho}_0 \int d\tau_1 \hat{\mathcal{H}}_{\text{eff}}^V(\tau_1) \left[\hat{\mathcal{Y}}, \int d\tau_2 \hat{\mathcal{H}}_{\text{eff}}^V(\tau_2) \right] \right\} \\ &\quad + \frac{1}{2} \text{Tr} \left\{ \hat{\rho}_0 \left[\hat{\mathcal{T}} \left(\int d\tau_1 \hat{\mathcal{H}}_{\text{eff}}^V(\tau_1) \int d\tau_2 \hat{\mathcal{H}}_{\text{eff}}^V(\tau_2) \right), \hat{\mathcal{Y}} \right] \right\}. \end{aligned} \quad (3.17)$$

Thus one finds for the complete quadratic response

$$\begin{aligned}
\langle Y(T) \rangle &= \text{Tr} \left\{ \hat{\mathcal{Y}}(T) \hat{\rho}_0 \right\} \\
&+ \text{Tr} \left\{ \left[i \int d\tau_1 \hat{\mathcal{H}}_{\text{eff}}^V(\tau_1), \hat{\mathcal{Y}}(T) \right] \hat{\rho}_0 \right\} \\
&+ \text{Tr} \left\{ \hat{\rho}_0 i \int d\tau_2 \hat{\mathcal{H}}_{\text{eff}}^V(\tau_2) \left[i \int d\tau_1 \hat{\mathcal{H}}_{\text{eff}}^V(\tau_1), \hat{\mathcal{Y}}(T) \right] \right. \\
&+ \left. \frac{1}{2} \hat{\rho}_0 \left[\hat{\mathcal{T}}_\tau \int d\tau_1 \hat{\mathcal{H}}_{\text{eff}}^V(\tau_1) \int d\tau_2 \hat{\mathcal{H}}_{\text{eff}}^V(\tau_2), \hat{\mathcal{Y}}(T) \right] \right\} \\
&+ \mathcal{O} \left((\hat{\mathcal{H}}_{\text{eff}}^V)^3 \right). \tag{3.18}
\end{aligned}$$

This form is now suitable for evaluating the traces since all commutators only concern a finite number of creation and annihilation operators and can therefore easily be calculated.

3.3 Squeezing

In this section the squeezed effective velocity Hamiltonian and the squeezed particle number operator for the resonance modes shall be calculated explicitly. The squeezing operator

$$\hat{S}(\tau) = \exp \left(+i \hat{H}_{\text{eff}}^S \tau \right) = \exp \left(\xi \left[(\hat{a}_L)^2 - (\hat{a}_L^\dagger)^2 \right] \tau \right) \tag{3.19}$$

implies the following transformation rules of the creation and annihilation operators (see e.g. [50, 52])

$$\begin{aligned}
\hat{b}_L(\tau) &= \hat{S}(\tau) \hat{a}_L \hat{S}^\dagger(\tau) = \hat{a}_L \mathcal{C}(\tau) + \hat{a}_L^\dagger \mathcal{S}(\tau), \\
\hat{b}_L^\dagger(\tau) &= \hat{S}(\tau) \hat{a}_L^\dagger \hat{S}^\dagger(\tau) = \hat{a}_L^\dagger \mathcal{C}(\tau) + \hat{a}_L \mathcal{S}(\tau), \tag{3.20}
\end{aligned}$$

with the hyperbolic cosine and sine functions

$$\mathcal{C}(\tau) = \cosh(2\xi\tau), \quad \mathcal{S}(\tau) = \sinh(2\xi\tau). \tag{3.21}$$

Since the effective squeezing Hamiltonian \hat{H}_{eff}^S only contains ladder operators of the fundamental resonance mode L it follows via the commutation relations (2.21) that other modes than L are not affected by the squeezing operator \hat{S} . Applying above transformation rules to the effective velocity Hamiltonian (2.79) derived for the case of \ominus coupling (in subsection 2.6.3) $\hat{H}_{\text{eff}}^V = i\chi(\hat{a}_L^\dagger \hat{a}_R - \hat{a}_L \hat{a}_R^\dagger)$ one finds for its squeezed counterpart

$$\hat{\mathcal{H}}_{\text{eff}}^V(\tau) = \hat{S}(\tau) \hat{H}_{\text{eff}}^V \hat{S}^\dagger(\tau) = i\chi \left[\mathcal{C}(\tau) \left(\hat{a}_L^\dagger \hat{a}_R - \hat{a}_L \hat{a}_R^\dagger \right) + \mathcal{S}(\tau) \left(\hat{a}_L \hat{a}_R - \hat{a}_L^\dagger \hat{a}_R^\dagger \right) \right]. \tag{3.22}$$

When applying the squeezing procedure to the particle number operator one finds again that only the fundamental resonance mode $\hat{N}_L = \hat{a}_L^\dagger \hat{a}_L$ is affected

$$\begin{aligned}\hat{\mathcal{N}}_L(T) &= \hat{S}(T) \hat{N}_L \hat{S}^\dagger(T) = \hat{S}(T) \hat{a}_L^\dagger \hat{S}^\dagger(T) \hat{S}(T) \hat{a}_L \hat{S}^\dagger(T) \\ &= [1 + 2\mathcal{S}^2(T)] \hat{a}_L^\dagger \hat{a}_L + \frac{1}{2}\mathcal{S}(2T) [(\hat{a}_L^\dagger)^2 + (\hat{a}_L)^2] + \mathcal{S}^2(T).\end{aligned}\quad (3.23)$$

3.4 An Example: Particle Creation

For the example of a rectangular cavity as described in section 2.4 the number of created particles due to the dynamical Casimir effect shall be calculated perturbatively. If one was interested in none of the coupling modes (R and L) the calculation would reduce to the initial expectation values since in the linear and quadratic response all commutators would vanish. Therefore the dynamical Casimir effect in the case of parametric resonance produces only particles in the fundamental resonance mode L and in the coupling mode R .

3.4.1 The Fundamental Resonance Mode

Employing the squeezed particle number operator (3.23) it is – with the aid of appendix 7.2 – straightforward to compute the lowest order result

$$\langle N_L^{(0)}(T) \rangle = \text{Tr} \left\{ \hat{\mathcal{N}}_L(T) \hat{\rho}_0 \right\} = (1 + 2\mathcal{S}^2(T)) N_L^0 + \mathcal{S}^2(T), \quad (3.24)$$

where the initial particle number N_L^0 is given by the Bose-Einstein distribution

$$N_L^0 = \text{Tr} \left\{ \hat{a}_L^\dagger \hat{a}_L \hat{\rho}_0 \right\} = \frac{1}{e^{\beta\Omega_L^0} - 1}. \quad (3.25)$$

This is the well-known result that has already been derived in [40, 39] for ideal cavities ($\eta = 0$). The corresponding result with $N_L^0 = 0$ has also been found in [33, 34, 17, 18], where the temperature corrections have not been considered. The calculation of the linear response function requires the commutator of the time-integrated squeezed effective velocity Hamiltonian

$$i \int_0^T \hat{\mathcal{H}}_{\text{eff}}^V(t) dt = \frac{-\chi}{2\xi} \left[(\mathcal{C}(T) - 1) \left(\hat{a}_L \hat{a}_R - \hat{a}_L^\dagger \hat{a}_R^\dagger \right) + \mathcal{S}(T) \left(\hat{a}_L^\dagger \hat{a}_R - \hat{a}_L \hat{a}_R^\dagger \right) \right], \quad (3.26)$$

with the squeezed particle number operator $\hat{\mathcal{N}}_L(T)$

$$\begin{aligned}
\left[i \int_0^T \hat{\mathcal{H}}_{\text{eff}}^V(t) dt, \hat{\mathcal{N}}_L(T) \right] &= \frac{-\chi}{2\xi} \left\{ (\mathcal{C}(T) - 1) (1 + 2\mathcal{S}^2(T)) \left(\hat{a}_L \hat{a}_R + \hat{a}_L^\dagger \hat{a}_R^\dagger \right) \right. \\
&\quad + (\mathcal{C}(T) - 1) \mathcal{S}(2T) \left(\hat{a}_L^\dagger \hat{a}_R + \hat{a}_L \hat{a}_R^\dagger \right) \\
&\quad - \mathcal{S}(T) (1 + 2\mathcal{S}^2(T)) \left(\hat{a}_L^\dagger \hat{a}_R + \hat{a}_L \hat{a}_R^\dagger \right) \\
&\quad \left. - \mathcal{S}(T) \mathcal{S}(2T) \left(\hat{a}_L \hat{a}_R + \hat{a}_L^\dagger \hat{a}_R^\dagger \right) \right\} \\
&= \frac{-\chi}{2\xi} \left\{ F_1(T) \left(\hat{a}_L^\dagger \hat{a}_R + \hat{a}_L \hat{a}_R^\dagger \right) \right. \\
&\quad \left. + F_2(T) \left(\hat{a}_L \hat{a}_R + \hat{a}_L^\dagger \hat{a}_R^\dagger \right) \right\}, \tag{3.27}
\end{aligned}$$

where the auxiliary functions $F_i(T)$ are given by

$$\begin{aligned}
F_1(T) &= [\mathcal{C}(T) - 1] \mathcal{S}(2T) - \mathcal{S}(T) [1 + 2\mathcal{S}^2(T)], \\
F_2(T) &= [\mathcal{C}(T) - 1] [1 + 2\mathcal{S}^2(T)] - \mathcal{S}(T) \mathcal{S}(2T). \tag{3.28}
\end{aligned}$$

Obviously the remaining combinations of creation and annihilation operators are not balanced – see also appendix 7.2 – i.e. the number of creation and annihilation operators of every mode (R and L) is not equal. Hence the linear response vanishes

$$\langle N_L^{(1)}(T) \rangle = \text{Tr} \left\{ \left[i \int_0^T \hat{\mathcal{H}}_{\text{eff}}^V(t) dt, \hat{\mathcal{N}}_L(T) \right] \hat{\rho}_0 \right\} = 0. \tag{3.29}$$

Repeating these calculations for the quadratic response requires some more work. The term without time-ordering in the quadratic response function $\langle Y^{(2)}(T) \rangle = \langle Y_{\hat{\mathcal{T}}}^{(2)} \rangle + \langle Y_{\text{non}}^{(2)} \rangle$ is found to yield

$$\begin{aligned}
\langle Y_{\text{non}}^{(2)} \rangle &= \text{Tr} \left\{ \hat{\rho}_0 i \int d\tau_2 \hat{\mathcal{H}}_{\text{eff}}^V(\tau_2) \left[i \int d\tau_1 \hat{\mathcal{H}}_{\text{eff}}^V(\tau_1), \hat{\mathcal{Y}}(T) \right] \right\} \\
&= \frac{\chi^2}{4\xi^2} \left[[\mathcal{C}(T) - 1] F_1(T) \text{Tr} \left\{ \hat{\rho}_0 \left(\hat{a}_L \hat{a}_R - \hat{a}_L^\dagger \hat{a}_R^\dagger \right) \left(\hat{a}_L^\dagger \hat{a}_R + \hat{a}_L \hat{a}_R^\dagger \right) \right\} \right. \\
&\quad + [\mathcal{C}(T) - 1] F_2(T) \text{Tr} \left\{ \hat{\rho}_0 \left(\hat{a}_L \hat{a}_R - \hat{a}_L^\dagger \hat{a}_R^\dagger \right) \left(\hat{a}_L \hat{a}_R + \hat{a}_L^\dagger \hat{a}_R^\dagger \right) \right\} \\
&\quad + \mathcal{S}(T) F_1(T) \text{Tr} \left\{ \hat{\rho}_0 \left(\hat{a}_L^\dagger \hat{a}_R - \hat{a}_L \hat{a}_R^\dagger \right) \left(\hat{a}_L^\dagger \hat{a}_R + \hat{a}_L \hat{a}_R^\dagger \right) \right\} \\
&\quad \left. + \mathcal{S}(T) F_2(T) \text{Tr} \left\{ \hat{\rho}_0 \left(\hat{a}_L^\dagger \hat{a}_R - \hat{a}_L \hat{a}_R^\dagger \right) \left(\hat{a}_L \hat{a}_R + \hat{a}_L^\dagger \hat{a}_R^\dagger \right) \right\} \right] \\
&= \frac{\chi^2}{4\xi^2} \left\{ [\mathcal{C}(T) - 1] F_2(T) (1 + N_L^0 + N_R^0) + \mathcal{S}(T) F_1(T) (N_L^0 - N_R^0) \right\}. \tag{3.30}
\end{aligned}$$

Considering the term with time-ordering it is convenient to rewrite the expression

$$\begin{aligned}
\langle Y_{\hat{\mathcal{T}}}^{(2)} \rangle &= \frac{1}{2} \text{Tr} \left\{ \hat{\rho}_0 \left[\hat{\mathcal{T}}_{\tau} \int d\tau_1 \hat{\mathcal{H}}_{\text{eff}}^V(\tau_1) \int d\tau_2 \hat{\mathcal{H}}_{\text{eff}}^V(\tau_2), \hat{\mathcal{Y}}(T) \right] \right\} \\
&= \frac{1}{2} \text{Tr} \left\{ \hat{\rho}_0 \int d\tau_1 d\tau_2 \left[\hat{\mathcal{H}}_{\text{eff}}^V(\tau_1) \hat{\mathcal{H}}_{\text{eff}}^V(\tau_2), \hat{\mathcal{Y}}(T) \right] \right\} \\
&\quad + \frac{1}{2} \text{Tr} \left\{ \hat{\rho}_0 \int d\tau_1 d\tau_2 \left[\left[\hat{\mathcal{H}}_{\text{eff}}^V(\tau_2), \hat{\mathcal{H}}_{\text{eff}}^V(\tau_1) \right] \theta(\tau_2 - \tau_1), \hat{\mathcal{Y}}(T) \right] \right\} \\
&= \frac{1}{2} \text{Tr} \left\{ \hat{\rho}_0 \int d\tau_1 d\tau_2 \left[\left[\hat{\mathcal{H}}_{\text{eff}}^V(\tau_2), \hat{\mathcal{H}}_{\text{eff}}^V(\tau_1) \right] \theta(\tau_2 - \tau_1), \hat{\mathcal{Y}}(T) \right] \right\}, \tag{3.31}
\end{aligned}$$

where in the last step it has been used that the commutator of two hermitian operators is anti-hermitian and thus only contributing to the vanishing imaginary parts of the expectation value. (Since other imaginary parts do not arise, the trace over this commutator has to vanish.) It remains to calculate the commutator of the velocity Hamiltonians at different times

$$\begin{aligned}
\left[\hat{\mathcal{H}}_{\text{eff}}^V(\tau_2), \hat{\mathcal{H}}_{\text{eff}}^V(\tau_1) \right] &= \chi^2 [\mathcal{C}(\tau_2) \mathcal{S}(\tau_1) - \mathcal{C}(\tau_1) \mathcal{S}(\tau_2)] \left[\hat{a}_L \hat{a}_R - \hat{a}_L^\dagger \hat{a}_R^\dagger, \hat{a}_L^\dagger \hat{a}_R - \hat{a}_L \hat{a}_R^\dagger \right] \\
&= \chi^2 [\mathcal{C}(\tau_2) \mathcal{S}(\tau_1) - \mathcal{C}(\tau_1) \mathcal{S}(\tau_2)] \times \\
&\quad \left[(\hat{a}_R)^2 - (\hat{a}_L)^2 + (\hat{a}_L^\dagger)^2 - (\hat{a}_R^\dagger)^2 \right]. \tag{3.32}
\end{aligned}$$

Accordingly, the trace with time-ordering is given by

$$\begin{aligned}
\langle Y_{\hat{\mathcal{T}}}^{(2)} \rangle &= \frac{1}{2} \text{Tr} \left\{ \hat{\rho}_0 \left[\hat{\mathcal{T}}_{\tau} \int d\tau_1 \hat{\mathcal{H}}_{\text{eff}}^V(\tau_1) \int d\tau_2 \hat{\mathcal{H}}_{\text{eff}}^V(\tau_2), \hat{\mathcal{Y}}(T) \right] \right\} \\
&= \chi^2 I_{\text{ex}} \text{Tr} \left\{ \hat{\rho}_0 \left[(\hat{a}_R)^2 - (\hat{a}_L)^2 + (\hat{a}_L^\dagger)^2 - (\hat{a}_R^\dagger)^2, \hat{\mathcal{Y}}(T) \right] \right\}, \tag{3.33}
\end{aligned}$$

where the exchange integral I_{ex} is calculated in appendix 7.4. After exploiting the relations between the hyperbolic sine and cosine functions one finally finds as a result for the expectation value of particles in the fundamental resonance mode L

$$\begin{aligned}
\langle N_L(T) \rangle &= \mathcal{S}^2(T) + [1 + 2\mathcal{S}^2(T)] N_L^0 \\
&\quad + \frac{\chi^2}{4\xi^2} [3\mathcal{C}^2(T) - 2\mathcal{C}(T) - 1 - 2\xi T \mathcal{S}(2T)] \\
&\quad + \frac{\chi^2}{4\xi^2} [4\mathcal{C}^2(T) - 2\mathcal{C}(T) - 2 - 4\xi T \mathcal{S}(2T)] N_L^0 \\
&\quad + \frac{\chi^2}{4\xi^2} [2\mathcal{C}^2(T) - 2\mathcal{C}(T)] N_R^0 + \mathcal{O}(\eta^3), \tag{3.34}
\end{aligned}$$

where N_R^0 is the initial particle number of the mode R . The leading terms $T\mathcal{S}(2T)$ in the quadratic answer stem from the time-ordering which is therefore especially important. The

immanent failure of the quadratic approximation is represented by the fact that these leading order terms will cause the particle number to become negative when the duration of the perturbation T becomes too large.

3.4.2 Coupling Modes

Since the effective squeezing Hamiltonian contains only operators of the fundamental resonance mode, the particle number operators of all other modes are not affected by the squeezing procedure. Considering the coupling right dominated mode R one finds for the lowest order

$$\langle N_R^{(0)}(T) \rangle = \text{Tr} \left\{ \hat{\mathcal{N}}_R \hat{\rho}_0 \right\} = \text{Tr} \left\{ \hat{N}_R \hat{\rho}_0 \right\} = N_R^0 = \frac{1}{e^{\beta \Omega_R^0} - 1}. \quad (3.35)$$

In the linear response the commutator of the squeezed effective velocity Hamiltonian with the particle number operator yields unbalanced terms which traces vanishes. Thus also here the linear response is found to vanish

$$\langle N_R^{(1)}(T) \rangle = 0. \quad (3.36)$$

Considering the quadratic response one finds that the trace with time-ordering vanishes since the commutators only yield unbalanced terms. Calculation of the other trace with the commutators finally yields the expectation value of \hat{N}_R

$$\begin{aligned} \langle N_R(T) \rangle &= N_R^0 \\ &+ \frac{\chi^2}{4\xi^2} [2\mathcal{C}^2(T) - 2\mathcal{C}(T) + 1] \\ &+ \frac{\chi^2}{4\xi^2} [2\mathcal{C}^2(T) - 2\mathcal{C}(T)] N_L^0 \\ &+ \frac{\chi^2}{4\xi^2} [-2\mathcal{C}(T) + 2] N_R^0 + \mathcal{O}(\eta^3). \end{aligned} \quad (3.37)$$

For $\eta = 0$ there would not be any created particles in the reservoir due to the dynamical Casimir effect corresponding to a perfect internal mirror.

Remarkably the coefficient of N_L^0 in $\langle N_R(T) \rangle$ equals the coefficient of N_R^0 in $\langle N_L(T) \rangle$. As one will see in chapter 5, this feature is preserved to any order of η in the full response function.

Chapter 4

Master Equation Approach

A fundamental problem in quantum theory is to study the time evolution of states or equivalently the statistical operator. A corresponding differential equation accounting for either the reduced or the complete statistical operator of a system is known as master equation. When considering systems with losses one often defines a complete ideal system consisting of a (generally larger) reservoir and a leaky system. A reduced statistical operator only accounts for either the reservoir or the leaky system and thus obeys a non-unitary time-evolution (changing entropy).

4.1 Introductory Remarks

In the interaction picture the time-evolution of the statistical operator is governed by the von-Neumann (see e.g. [49, 50]) equation

$$\frac{\partial \hat{\rho}(t)}{\partial t} = -i \left[\hat{H}_I(t), \hat{\rho}(t) \right]. \quad (4.1)$$

However, in the present case it is convenient to use yet another picture, where also the time-dependence arising from the effective squeezing interaction Hamiltonian \hat{H}_{eff}^S is carried by the operators. The time evolution of the statistical operator is then only governed by $\hat{\mathcal{H}}_{\text{eff}}^V$. According to (3.13) the statistical operator in this picture is given by

$$\begin{aligned} \hat{\rho}(T) &= \hat{\sigma}(T) \hat{\rho}_0 \hat{\sigma}^\dagger(T) \\ &= \hat{\mathcal{T}}_\tau \left[\exp \left(-i \int_0^T \hat{\mathcal{H}}_{\text{eff}}^V(\tau) d\tau \right) \right] \hat{\rho}_0 \hat{\mathcal{T}}_\tau^\dagger \left[\exp \left(+i \int_0^T \hat{\mathcal{H}}_{\text{eff}}^V(\tau) d\tau \right) \right]. \end{aligned} \quad (4.2)$$

Hence one finds via differentiation that the time evolution of the statistical operator in this modified interaction picture is governed by a modified von-Neumann equation

$$\frac{\partial \hat{\rho}(t)}{\partial t} = -i \left[\hat{\mathcal{H}}_{\text{eff}}^V(t), \hat{\rho}(t) \right] = -i \hat{\mathcal{L}}(t) \hat{\rho}(t), \quad (4.3)$$

where above equation also serves as a definition for the action of the Liouvillian super operator $\hat{\mathcal{L}}(t)$ on the statistical operator $\hat{\rho}_0$ (see also [49, 50]). When describing systems with losses one is only interested in the part of the statistical operator accounting for the leaky system. Accordingly one can define a reduced statistical operator (see also e.g. [52]) accounting only for the system with losses via averaging over the degrees of freedom of the reservoir

$$\hat{\rho}_L(t) = \text{Tr}_R \{ \hat{\rho}(t) \}. \quad (4.4)$$

In above definition Tr_R means that the trace only concerns the modes of the reservoir cavity

$$\text{Tr}_R \{ \hat{A} \} = \sum_{n_1^R, n_2^R, \dots = 0}^{\infty} \langle n_1^R, n_2^R, \dots | \hat{A} | n_1^R, n_2^R, \dots \rangle, \quad (4.5)$$

where n_i^R is the particle occupation number of the i^{th} mode of the reservoir. Introducing the time-independent projection super operator $\hat{\mathfrak{P}} = \hat{\mathfrak{P}}^2$ (cf. [50]) via its action on an arbitrary operator $\hat{A}(t)$

$$\hat{\mathfrak{P}} \hat{A}(t) = \hat{\rho}_R(0) \text{Tr}_R \{ \hat{A}(t) \} \quad (4.6)$$

it is obvious that it projects the complete statistical operator

$$\hat{\mathfrak{P}} \hat{\rho}(t) = \hat{\rho}_R(0) \hat{\rho}_L(t) \quad (4.7)$$

onto the reduced effective statistical operator $\hat{\rho}_L(t)$ of the leaky system.

4.2 The Zwanzig Master Equation

Multiplying the von Neumann equation (4.3) with $\hat{\mathfrak{P}}$ and $(1 - \hat{\mathfrak{P}})$ respectively one obtains two equations of which the latter can be used to eliminate the term $(1 - \hat{\mathfrak{P}}) \hat{\rho}(t)$ in the first one. With the reduced time evolution super operator

$$\hat{\mathfrak{U}}(t, t') = \exp \left(-i(1 - \hat{\mathfrak{P}}) \int_{t'}^t \hat{\mathcal{L}}(t'') dt'' \right) \quad (4.8)$$

one obtains Zwanzig's generalized master equation [50]

$$\begin{aligned} \hat{\mathfrak{P}} \frac{\partial \hat{\rho}(t)}{\partial t} = & -i \hat{\mathfrak{P}} \hat{\mathfrak{L}}(t) \hat{\mathfrak{P}} \hat{\rho}(t) - i \hat{\mathfrak{P}} \hat{\mathfrak{L}}(t) \hat{\mathfrak{U}}(t, 0) (1 - \hat{\mathfrak{P}}) \hat{\rho}(0) \\ & - \hat{\mathfrak{P}} \hat{\mathfrak{L}}(t) \int_0^t \hat{\mathfrak{U}}(t, t') (1 - \hat{\mathfrak{P}}) \hat{\mathfrak{L}}(t') \hat{\mathfrak{P}} \hat{\rho}(t') dt'. \end{aligned} \quad (4.9)$$

This equation holds to all orders in perturbation theory (η) but its application in practice is not easy. Assuming the complete system to be in an initial thermal equilibrium state yields considerable simplifications [50].

1. Since $\hat{\mathcal{H}}_{\text{eff}}^V$ from section 3.3 contains only odd and $\hat{\rho}_R(0)$ only even powers of the creation and annihilation operators for the mode R it follows with appendix 7.2 that

$$\text{Tr}_R \left\{ \hat{\mathcal{H}}_{\text{eff}}^V \hat{\rho}_R(0) \right\} = 0. \quad (4.10)$$

In the Zwanzig master equation this means equivalently

$$\hat{\mathfrak{P}} \hat{\mathfrak{L}}(t) \hat{\mathfrak{P}} \hat{\rho}(t) = 0. \quad (4.11)$$

2. The (initial) statistical operator of the thermal equilibrium factorizes

$$\hat{\rho}_0 = \hat{\rho}(0) = \hat{\rho}_L(0) \otimes \hat{\rho}_R(0), \quad (4.12)$$

hence one finds (with $\text{Tr}_R\{\hat{\rho}_R\} = 1$)

$$(1 - \hat{\mathfrak{P}}) \hat{\rho}(0) = 0. \quad (4.13)$$

These assumptions yield a simplified Zwanzig master equation

$$\frac{\partial \hat{\mathfrak{P}} \hat{\rho}(t)}{\partial t} = - \hat{\mathfrak{P}} \hat{\mathfrak{L}}(t) \int_0^t \hat{\mathfrak{U}}(t, t') \hat{\mathfrak{L}}(t') \hat{\mathfrak{P}} \hat{\rho}(t') dt'. \quad (4.14)$$

This exact master equation accounts for $\hat{\mathfrak{P}} \hat{\rho}(t)$ and thus for the statistical operator of the leaky system $\hat{\rho}_L(t)$. It is still exact but too difficult to solve which makes it necessary to apply some approximations in practice.

4.3 Approximations

If the coupling between the system and the reservoir is sufficiently weak to allow a perturbative treatment one can apply several approximations. For the special case of a rectangular cavity as proposed in section 2.4 the expansion parameter $\eta \ll 1$ accounting for the transmittance of the internal mirror was introduced. With the assumption of left-dominated modes coupling to right-dominated modes in subsection 2.6.3 the effective velocity interaction Hamiltonian was found to be small $\hat{H}_{\text{eff}}^V = \mathcal{O}(\eta)$. Since it contains the ladder operators of right- and left-dominated modes, respectively, it represents the coupling between system and reservoir and therefore fulfills the aforementioned requirement. To obtain a reassessment of the response theory approach of chapter 3 only those approximations which keep the level of accuracy at $\mathcal{O}(\eta^2)$ are appropriate.

4.3.1 Born Approximation

The squeezed effective velocity Hamiltonian $\hat{\mathcal{H}}_{\text{eff}}^V$ is of $\mathcal{O}(\eta)$ which also implies $\hat{\mathcal{L}} = \mathcal{O}(\eta)$. Accordingly, the approximation $\hat{\mathcal{U}}(t, t') = \mathbf{1} + \mathcal{O}(\eta)$ (also known as *Born approximation* [52, 50]) leads to the neglect of terms that are of $\mathcal{O}(\eta^3)$ in the Zwanzig master equation. Therefore one finds via the Born approximation

$$\frac{\partial \hat{\mathfrak{P}} \hat{\rho}(t)}{\partial t} = -\hat{\mathfrak{P}} \hat{\mathcal{L}}(t) \int_0^t \hat{\mathcal{L}}(t') \hat{\mathfrak{P}} \hat{\rho}(t') dt' + \mathcal{O}(\eta^3) \quad (4.15)$$

an approximate master equation accounting for the reduced statistical operator. Eliminating the projection super operator $\hat{\mathfrak{P}}$ in favor of the effective statistical operator $\hat{\rho}_L(t)$ via $\hat{\mathfrak{P}} \hat{\rho}(t) = \hat{\rho}_R(0) \hat{\rho}_L(t)$ yields

$$\frac{\partial \hat{\rho}_L(t)}{\partial t} = -\text{Tr}_R \left\{ \hat{\mathcal{L}}(t) \int_0^t \hat{\mathcal{L}}(t') \hat{\rho}_R(0) \hat{\rho}_L(t') dt' \right\} + \mathcal{O}(\eta^3) . \quad (4.16)$$

This Born master equation is retarded, i.e. the calculation of a solution is complicated by the occurrence of $\hat{\rho}_L(t')$ on the right hand side. Accordingly, yet another approximation is advantageous.

4.3.2 Markov Approximation

Since according to equation (4.3) the Liouvillian operator $\hat{\mathcal{L}} = \mathcal{O}(\eta)$ is comparably small, one finds via formally integrating (4.16) that the substitution $\hat{\rho}_L(t') \rightarrow \hat{\rho}_L(t)$ on the right hand side

corresponds to an approximation neglecting terms of $\mathcal{O}(\eta^4)$ in the reduced density operator $\hat{\rho}_L(t)$. This does not change the level of accuracy $[\mathcal{O}(\eta^2)]$ at this point and is therefore certainly justified. The corresponding approximation is also known as *short memory approximation* [50, 51, 52] and yields

$$\frac{\partial \hat{\rho}_L(t)}{\partial t} = -\text{Tr}_R \left\{ \int_0^t \hat{\mathcal{L}}(t) \hat{\mathcal{L}}(t') \hat{\rho}_R(0) \hat{\rho}_L(t) dt' \right\} + \mathcal{O}(\eta^3) . \quad (4.17)$$

Using the definition of the Liouvillian operator $\hat{\mathcal{L}}$ in equation (4.3) one can equivalently write

$$\begin{aligned} \frac{\partial \hat{\rho}_L(t)}{\partial t} = & +\text{Tr}_R \left\{ \hat{\mathcal{H}}_{\text{eff}}^V(t) \hat{\rho}_R(0) \hat{\rho}_L(t) \int_0^t \hat{\mathcal{H}}_{\text{eff}}^V(t') dt' \right\} \\ & -\text{Tr}_R \left\{ \hat{\mathcal{H}}_{\text{eff}}^V(t) \int_0^t \hat{\mathcal{H}}_{\text{eff}}^V(t') dt' \hat{\rho}_R(0) \hat{\rho}_L(t) \right\} + \text{h.c.} + \mathcal{O}(\eta^3) , \end{aligned} \quad (4.18)$$

where h.c. stands for the hermitian conjugate operators. Performing the traces over the reservoir yields a master equation accounting for the leaky system, which does not contain any operators of the reservoir.

4.3.3 Approximate Master Equation

The calculation of the traces involves terms of the form

$$\begin{aligned} \text{Tr}_R \left\{ \left[\hat{a}_L^\dagger \hat{a}_R - \hat{a}_L \hat{a}_R^\dagger \right] \hat{\rho}_R(0) \hat{\rho}_L(t) \left[\hat{a}_L \hat{a}_R - \hat{a}_L^\dagger \hat{a}_R^\dagger \right] \right\} &= \hat{a}_L^\dagger \hat{\rho}_L(t) \hat{a}_L \text{Tr}_R \{ \hat{a}_R \hat{\rho}_R(0) \hat{a}_R \} \\ &\quad - \hat{a}_L^\dagger \hat{\rho}_L(t) \hat{a}_L^\dagger \text{Tr}_R \left\{ \hat{a}_R \hat{\rho}_R(0) \hat{a}_R^\dagger \right\} \\ &\quad - \hat{a}_L \hat{\rho}_L(t) \hat{a}_L \text{Tr}_R \left\{ \hat{a}_R^\dagger \hat{\rho}_R(0) \hat{a}_R \right\} \\ &\quad + \hat{a}_L \hat{\rho}_L(t) \hat{a}_L^\dagger \text{Tr}_R \left\{ \hat{a}_R^\dagger \hat{\rho}_R(0) \hat{a}_R^\dagger \right\} \\ &= -\hat{a}_L^\dagger \hat{\rho}_L(t) \hat{a}_L^\dagger N_R^0 \\ &\quad - \hat{a}_L \hat{\rho}_L(t) \hat{a}_L (1 + N_R^0) . \end{aligned} \quad (4.19)$$

Note that Tr_R is invariant only under cyclic permutations of operators accounting for the reservoir. Operators accounting for the left cavity are not affected by the trace. Finally, one

yields as a master equation

$$\begin{aligned}
\frac{\partial \hat{\rho}_L(t)}{\partial t} = & g_1(t) \left[2\hat{a}_L^\dagger \hat{\rho}_L(t) \hat{a}_L - \hat{a}_L \hat{a}_L^\dagger \hat{\rho}_L(t) - \hat{\rho}_L(t) \hat{a}_L \hat{a}_L^\dagger \right] \\
& + g_2(t) \left[2\hat{a}_L \hat{\rho}_L(t) \hat{a}_L^\dagger - \hat{a}_L^\dagger \hat{a}_L \hat{\rho}_L(t) - \hat{\rho}_L(t) \hat{a}_L^\dagger \hat{a}_L \right] \\
& + g_3(t) \left[\hat{a}_L^\dagger \hat{\rho}_L(t) \hat{a}_L^\dagger + \hat{a}_L \hat{\rho}_L(t) \hat{a}_L \right] \\
& - g_4(t) \left[(\hat{a}_L^\dagger)^2 \hat{\rho}_L(t) + \hat{\rho}_L(t) (\hat{a}_L)^2 \right] \\
& - g_5(t) \left[(\hat{a}_L)^2 \hat{\rho}_L(t) + \hat{\rho}_L(t) (\hat{a}_L^\dagger)^2 \right] + \mathcal{O}(\eta^3)
\end{aligned} \tag{4.20}$$

where the functions $g_i(t)$ are given by

$$\begin{aligned}
g_1(t) &= \frac{\chi^2}{2\xi} \mathcal{S}(t) \{ \mathcal{C}(t)(2N_R^0 + 1) - N_R^0 - 1 \} , \\
g_2(t) &= \frac{\chi^2}{2\xi} \mathcal{S}(t) \{ \mathcal{C}(t)(2N_R^0 + 1) - N_R^0 \} , \\
g_3(t) &= \frac{\chi^2}{2\xi} \{ \mathcal{C}^2(t) + \mathcal{S}^2(t) - \mathcal{C}(t) \} (2N_R^0 + 1) , \\
g_4(t) &= \frac{\chi^2}{2\xi} \{ [\mathcal{C}^2(t) + \mathcal{S}^2(t) - \mathcal{C}(t)] N_R^0 + \mathcal{C}^2(t) - \mathcal{C}(t) \} , \\
g_5(t) &= \frac{\chi^2}{2\xi} \{ [\mathcal{C}^2(t) + \mathcal{S}^2(t) - \mathcal{C}(t)] N_R^0 + \mathcal{S}^2(t) \} .
\end{aligned} \tag{4.21}$$

Above differential equation is quite different from the one used in [43, 44] which was not derived starting from first principles. The effective statistical operator $\hat{\rho}_L(t)$ whose time dependence is governed by above equation obeys a non-unitary time-evolution (see also [49, 39]), which in general leads to a changing entropy $S_L(t) = -\text{Tr}_L \{ \hat{\rho}_L(t) \ln \hat{\rho}_L(t) \}$. By inspection of the right hand side of (4.20) one can easily verify that the time evolution preserves the hermiticity and the trace of $\hat{\rho}_L$. A more persuasive indication for the correctness of the master equation can be found by taking the limit of no squeezing, i.e. $\xi \rightarrow 0$. With

$$\begin{aligned}
\lim_{\xi \rightarrow 0} g_1(t) &= \chi^2 t N_R^0 , & \lim_{\xi \rightarrow 0} g_2(t) &= \chi^2 t (N_R^0 + 1) , \\
\lim_{\xi \rightarrow 0} g_{i=3,4,5}(t) &= 0
\end{aligned} \tag{4.22}$$

one arrives at a simplified master equation

$$\begin{aligned}
\frac{\partial \hat{\rho}_L}{\partial t} &\stackrel{\xi \rightarrow 0}{=} \gamma_D \frac{N_R^0}{2} \left[2\hat{a}_L^\dagger \hat{\rho}_L \hat{a}_L - \hat{a}_L \hat{a}_L^\dagger \hat{\rho}_L - \hat{\rho}_L \hat{a}_L \hat{a}_L^\dagger \right] \\
&+ \gamma_D \frac{N_R^0 + 1}{2} \left[2\hat{a}_L \hat{\rho}_L \hat{a}_L^\dagger - \hat{a}_L^\dagger \hat{a}_L \hat{\rho}_L - \hat{\rho}_L \hat{a}_L^\dagger \hat{a}_L \right] ,
\end{aligned} \tag{4.23}$$

where the damping coefficient γ_D is given by $\gamma_D = 2\chi^2 t$. Apart from the time-dependence of the damping coefficient above equation is exactly the well-known master equation for a harmonic oscillator coupled to a thermal bath, see e.g. [52]. This time-dependence of γ_D is a remnant of the dynamic master equation describing the time-dependent system in the limit $\xi \rightarrow 0$.

4.4 Solution Of The Master Equation

The simplified master equation (4.20) is a linear operator equation. However, the occurrence of $\hat{\rho}_L(t)$ on the right hand side complicates the calculation of a solution for the effective statistical operator. Since the functions $g_i(t)$ are of $\mathcal{O}(\chi^2) = \mathcal{O}(\eta^2)$ the level of accuracy is maintained by applying the additional approximation $\hat{\rho}_L(t) \approx \hat{\rho}_L(0)$ on the right hand side, which can be interpreted as an additional Markov approximation. (Thereby terms of $\mathcal{O}(\eta^4)$ were neglected.) Consequently, an effective density operator is finally found via integration of the master equation (4.20)

$$\begin{aligned}
\hat{\rho}_L(T) = & \hat{\rho}_L(0) \\
& + G_1(T) \left[2\hat{a}_L^\dagger \hat{\rho}_L(0) \hat{a}_L - \hat{a}_L \hat{a}_L^\dagger \hat{\rho}_L(0) - \hat{\rho}_L(0) \hat{a}_L \hat{a}_L^\dagger \right] \\
& + G_2(T) \left[2\hat{a}_L \hat{\rho}_L(0) \hat{a}_L^\dagger - \hat{a}_L^\dagger \hat{a}_L \hat{\rho}_L(0) - \hat{\rho}_L(0) \hat{a}_L^\dagger \hat{a}_L \right] \\
& + G_3(T) \left[\hat{a}_L^\dagger \hat{\rho}_L(0) \hat{a}_L^\dagger + \hat{a}_L \hat{\rho}_L(0) \hat{a}_L \right] \\
& - G_4(T) \left[(\hat{a}_L^\dagger)^2 \hat{\rho}_L(0) + \hat{\rho}_L(0) (\hat{a}_L)^2 \right] \\
& - G_5(T) \left[(\hat{a}_L)^2 \hat{\rho}_L(0) + \hat{\rho}_L(0) (\hat{a}_L^\dagger)^2 \right] + \mathcal{O}(\eta^3) .
\end{aligned} \tag{4.24}$$

The time-integrated coefficient functions $G_i(T) = \int_0^T g_i(t) dt$ are given by

$$\begin{aligned}
G_1(T) &= \frac{\chi^2}{4\xi^2} \left\{ [\mathcal{C}^2(T) - \mathcal{C}(T)] N_R^0 + \frac{1}{2} \mathcal{C}^2(T) - \mathcal{C}(T) + \frac{1}{2} \right\} , \\
G_2(T) &= \frac{\chi^2}{4\xi^2} \left\{ [\mathcal{C}^2(T) - \mathcal{C}(T)] N_R^0 + \frac{1}{2} \mathcal{C}^2(T) - \frac{1}{2} \right\} , \\
G_3(T) &= \frac{\chi^2}{4\xi^2} \{ [2\mathcal{C}(T)\mathcal{S}(T) - 2\mathcal{S}(T)] N_R^0 + \mathcal{C}(T)\mathcal{S}(T) - \mathcal{S}(T) \} , \\
G_4(T) &= \frac{\chi^2}{4\xi^2} \left\{ [\mathcal{C}(T)\mathcal{S}(T) - \mathcal{S}(T)] N_R^0 + \frac{1}{2} \mathcal{C}(T)\mathcal{S}(T) - \mathcal{S}(T) + \xi T \right\} , \\
G_5(T) &= \frac{\chi^2}{4\xi^2} \left\{ [\mathcal{C}(T)\mathcal{S}(T) - \mathcal{S}(T)] N_R^0 + \frac{1}{2} \mathcal{C}(T)\mathcal{S}(T) - \xi T \right\} .
\end{aligned} \tag{4.25}$$

With this statistical operator for the leaky system one can now calculate the number of created particles in all modes accounting for the left cavity (the system with losses).

4.5 An Example: Particle Creation

Obviously, all other modes than the fundamental resonance mode L do not show a quadratic response since their creation and annihilation operators commute with those of the resonance mode. Note that in the used squeezing interaction picture one will have to use the squeezed particle number operator $\hat{\mathcal{N}}_L(T)$. Therefore one finds for the lowest order

$$\langle N_L^{(0)}(T) \rangle = \mathcal{S}^2(T) + [1 + 2\mathcal{S}^2(T)] N_L^0. \quad (4.26)$$

This result is in complete agreement with subsection 3.4.1 and therefore also consistent with the conclusions found in other publications. According to (4.25) the functions $G_i(T)$ are all of $\mathcal{O}(\eta^2)$ which automatically leads to the vanishing of the linear response

$$\langle N_L^{(1)}(T) \rangle = 0. \quad (4.27)$$

The quadratic response can be brought into the form

$$\begin{aligned} \langle N_L^{(2)}(T) \rangle &= \mathcal{S}^2(T) G_1(T) \text{Tr} \left\{ 2\hat{a}_L^\dagger \hat{\rho}_L(0) \hat{a}_L - \hat{a}_L \hat{a}_L^\dagger \hat{\rho}_L(0) - \hat{\rho}_L(0) \hat{a}_L \hat{a}_L^\dagger \right\} \\ &\quad + \mathcal{S}^2(T) G_2(T) \text{Tr} \left\{ 2\hat{a}_L \hat{\rho}_L(0) \hat{a}_L^\dagger - \hat{a}_L^\dagger \hat{a}_L \hat{\rho}_L(0) - \hat{\rho}_L(0) \hat{a}_L^\dagger \hat{a}_L \right\} \\ &\quad + [1 + 2\mathcal{S}^2(T)] G_1(T) \text{Tr} \left\{ \hat{a}_L^\dagger \hat{a}_L \left[2\hat{a}_L^\dagger \hat{\rho}_L(0) \hat{a}_L - \hat{a}_L \hat{a}_L^\dagger \hat{\rho}_L(0) - \hat{\rho}_L(0) \hat{a}_L \hat{a}_L^\dagger \right] \right\} \\ &\quad + [1 + 2\mathcal{S}^2(T)] G_2(T) \text{Tr} \left\{ \hat{a}_L^\dagger \hat{a}_L \left[2\hat{a}_L \hat{\rho}_L(0) \hat{a}_L^\dagger - \hat{a}_L^\dagger \hat{a}_L \hat{\rho}_L(0) - \hat{\rho}_L(0) \hat{a}_L^\dagger \hat{a}_L \right] \right\} \\ &\quad + \frac{1}{2} \mathcal{S}(2T) G_3(T) \text{Tr} \left\{ \left[(\hat{a}_L^\dagger)^2 + (\hat{a}_L)^2 \right] \left[\hat{a}_L^\dagger \hat{\rho}_L(0) \hat{a}_L^\dagger + \hat{a}_L \hat{\rho}_L(0) \hat{a}_L \right] \right\} \\ &\quad - \frac{1}{2} \mathcal{S}(2T) G_4(T) \text{Tr} \left\{ \left[(\hat{a}_L^\dagger)^2 + (\hat{a}_L)^2 \right] \left[(\hat{a}_L^\dagger)^2 \hat{\rho}_L(0) + \hat{\rho}_L(0) (\hat{a}_L)^2 \right] \right\} \\ &\quad - \frac{1}{2} \mathcal{S}(2T) G_5(T) \text{Tr} \left\{ \left[(\hat{a}_L^\dagger)^2 + (\hat{a}_L)^2 \right] \left[(\hat{a}_L)^2 \hat{\rho}_L(0) + \hat{\rho}_L(0) (\hat{a}_L^\dagger)^2 \right] \right\} \\ &= (1 + 2\mathcal{S}^2(T)) G_1(T) [2N_L^0 + 2] + (1 + 2\mathcal{S}^2(T)) G_2(T) [-2N_L^0] \\ &\quad + \frac{1}{2} \mathcal{S}(2T) G_3(T) [2N_L^0 + 2 \text{Tr} \{ (\hat{a}_L^\dagger \hat{a}_L)^2 \hat{\rho}_0 \}] \\ &\quad - \frac{1}{2} \mathcal{S}(2T) G_4(T) [6N_L^0 + 4 + 2 \text{Tr} \{ (\hat{a}_L^\dagger \hat{a}_L)^2 \hat{\rho}_0 \}] \\ &\quad - \frac{1}{2} \mathcal{S}(2T) G_5(T) [-2N_L^0 + 2 \text{Tr} \{ (\hat{a}_L^\dagger \hat{a}_L)^2 \hat{\rho}_0 \}]. \end{aligned} \quad (4.28)$$

At a first glance the occurrence of terms with $\text{Tr} \left\{ (\hat{a}_L^\dagger \hat{a}_L)^2 \hat{\rho}_0 \right\}$ seems to be in contradiction with the results obtained via the response theory approach in subsection 3.4.1 but due to the relation

$$G_3(T) - G_4(T) - G_5(T) = 0 \quad (4.29)$$

following from (4.25) these contributions cancel. The terms linear in T in $G_{4/5}(T)$ lead to the terms proportional to $\xi T \mathcal{S}(2T)$ in the expectation value $\langle N_L(T) \rangle$. Finally, one finds complete agreement with the quadratic response of Section 3.4.1, i.e.

$$\begin{aligned} \langle N_L(T) \rangle &= \mathcal{S}^2(T) + [1 + 2\mathcal{S}^2(T)] N_L^0 \\ &\quad + \frac{\chi^2}{4\xi^2} [3\mathcal{C}^2(T) - 2\mathcal{C}(T) - 1 - 2\xi T \mathcal{S}(2T)] \\ &\quad + \frac{\chi^2}{4\xi^2} [4\mathcal{C}^2(T) - 2\mathcal{C}(T) - 2 - 4\xi T \mathcal{S}(2T)] N_L^0 \\ &\quad + \frac{\chi^2}{4\xi^2} [2\mathcal{C}^2(T) - 2\mathcal{C}(T)] N_R^0 + \mathcal{O}(\eta^3) . \end{aligned} \quad (4.30)$$

For the derivation of particle creation effects of right-dominated modes one would have to derive an effective statistical operator for the reservoir. In this case another projection super operator $\hat{\mathfrak{P}}'$ would have to be defined such that it would project onto the corresponding right-dominated modes

$$\hat{\mathfrak{P}}' \hat{\rho}(t) = \hat{\rho}_L(0) \text{Tr}_L \{ \hat{\rho}(t) \} . \quad (4.31)$$

The general procedure however, would be the same as for left-dominated modes.

Chapter 5

A Non-Perturbative Approach

In the previous chapters it turned out that the particle occupation number of the resonance mode L would become negative at some time T . This unphysical result poses a contradiction with the positive definiteness of the particle number operator and roots in the immanent failure of perturbation theory at large perturbation times T . Note that the expansion had not been done in the squeezed effective velocity Hamiltonian $\hat{\mathcal{H}}_{\text{eff}}^V$ but rather in $\int_0^T \hat{\mathcal{H}}_{\text{eff}}^V dt$ which can always grow very large even if $\hat{\mathcal{H}}_{\text{eff}}^V$ is a small quantity. This problem is therefore only solved by including all orders of η .

5.1 General Procedure

The most general form for a quadratic and possibly time-dependent Hamiltonian containing the creation and annihilation operators of K modes is given by

$$\hat{H} = i \sum_{i,j=1}^K \left[\hat{a}_i C_{ij} \hat{a}_j - \hat{a}_i^\dagger C_{ij}^* \hat{a}_j^\dagger \right] + i \sum_{i,j=1}^K \hat{a}_i^\dagger D_{ij} \hat{a}_j, \quad (5.1)$$

where the factor i has been separated for convenience. The matrix elements $C_{ij} \in \mathbb{C}$ and $D_{ij} \in \mathbb{C}$ are complex-valued and can depend on time. Due to the commutation relations (2.21) and the hermiticity of \hat{H} the matrices have to obey

$$C_{ij} = C_{ji}, \quad D_{ij} = -D_{ji}^*, \quad (5.2)$$

which means that the squeezing matrix \underline{C} is symmetric and the hopping matrix \underline{D} is anti-hermitian. Suppose the time-dependence of an arbitrary operator \hat{A} is given by

$$\hat{A}(T) = \exp(i\hat{H}T) \hat{A}(0) \exp(-i\hat{H}T). \quad (5.3)$$

Since $\hat{A}(T)$ can be expressed in ladder operators one finds with the unitarity of $\exp(i\hat{H}T)$ that their time-dependence is also governed by

$$\hat{a}(T) = \exp(i\hat{H}T)\hat{a}(0)\exp(-i\hat{H}T), \quad (5.4)$$

with \hat{H} being possibly T -dependent. This possible time-dependence makes the introduction of an auxiliary parameter ϑ while keeping the time T fixed necessary

$$\hat{a}(\vartheta) = \exp(i\hat{H}T\vartheta)\hat{a}(\vartheta=0)\exp(-i\hat{H}T\vartheta). \quad (5.5)$$

Above expression can be evaluated via introducing the $2K$ dimensional column vector

$$\underline{\hat{x}}(\vartheta) = \begin{pmatrix} \hat{a}_1(\vartheta) \\ \vdots \\ \hat{a}_K(\vartheta) \\ \hat{a}_1^\dagger(\vartheta) \\ \vdots \\ \hat{a}_K^\dagger(\vartheta) \end{pmatrix} = \exp(i\hat{H}T\vartheta)\underline{\hat{x}}(0)\exp(-i\hat{H}T\vartheta). \quad (5.6)$$

To obtain the vector $\underline{\hat{x}}(\vartheta)$ at time T one is therefore interested its value at $\vartheta = 1$. Differentiation with respect to ϑ yields

$$\frac{d\underline{\hat{x}}(\vartheta)}{d\vartheta} = iT \left[\hat{H}, \underline{\hat{x}}(\vartheta) \right] = T \exp(i\hat{H}T\vartheta) \left[i\hat{H}, \underline{\hat{x}}(0) \right] \exp(-i\hat{H}T\vartheta), \quad (5.7)$$

where $\underline{\hat{x}}(0)$ just contains the initial creation and annihilation operators whose commutator with the Hamiltonian can easily be calculated. Two cases need to be distinguished

- $1 \leq l \leq K$ In this case one finds

$$\left[i\hat{H}, \hat{x}_l(0) \right] = \left[i\hat{H}, \hat{a}_l \right] = \sum_{j=1}^K \left[D_{lj}\hat{a}_j - 2C_{lj}^*\hat{a}_j^\dagger \right] = \sum_{j=1}^{2K} A_{lj}\hat{x}_j(0), \quad (5.8)$$

where A_{lj} stands for the corresponding coefficient matrix.

- $K+1 \leq l \leq 2K$ For such values of l one obtains

$$\begin{aligned} \left[i\hat{H}, \hat{x}_l(0) \right] &= \left[i\hat{H}, \hat{a}_l^\dagger \right] = \left(\left[i\hat{H}, \hat{a}_{l-K} \right] \right)^\dagger \\ &= \sum_{j=1}^K \left[D_{l-K,j}^*\hat{a}_j^\dagger - 2C_{l-K,j}\hat{a}_j \right] = \sum_{j=1}^{2K} A_{lj}\hat{x}_j(0). \end{aligned} \quad (5.9)$$

Accordingly, the matrix elements of the coefficient matrix \underline{A} are given by

$$A_{lj} = \begin{cases} D_{lj} & \text{if } 1 \leq j \leq K \text{ and } 1 \leq l \leq K \\ -2C_{l,j-K}^* & \text{if } K+1 \leq j \leq 2K \text{ and } 1 \leq l \leq K \\ -2C_{l-K,j} & \text{if } 1 \leq j \leq K \text{ and } K+1 \leq l \leq 2K \\ D_{l-K,j-K}^* & \text{if } K+1 \leq j \leq 2K \text{ and } K+1 \leq l \leq 2K \end{cases}, \quad (5.10)$$

or, equivalently

$$\underline{A} = \begin{pmatrix} \underline{D} & -2\underline{C}^* \\ -2\underline{C} & \underline{D}^* \end{pmatrix}. \quad (5.11)$$

Here the fact has been used that \hat{H} is only quadratic: The commutation relations (2.21) lead to a linear combination of creation and annihilation operators that can always be written as a (possibly time-dependent) matrix \underline{A} acting on $\hat{x}(\vartheta)$. The time evolution of $\hat{x}(\vartheta)$ is therefore governed by the differential equation

$$\frac{d\hat{x}(\vartheta)}{d\vartheta} = T \exp(i\hat{H}T\vartheta) \underline{A} \hat{x}(0) \exp(-i\hat{H}T\vartheta) = \underline{A} T \hat{x}(\vartheta). \quad (5.12)$$

The matrix \underline{A} can be diagonalized if $\underline{C}\underline{D} = \underline{D}^*\underline{C}$ holds. In any case, the complete solution of the aforementioned differential equation can be obtained via

$$\hat{x}(\vartheta) = \exp(\underline{A}T\vartheta) \hat{x}(0), \quad (5.13)$$

and hence

$$\hat{x}(T) = \hat{x}(\vartheta = 1) = \exp(\underline{A}T) \hat{x}(0) = \underline{U}(T) \hat{x}(0), \quad (5.14)$$

which reduces the problem to find the exponential matrix of \underline{A} , i.e. the time evolution matrix

$$\underline{U}(T, 0) = \exp(\underline{A}T), \quad (5.15)$$

that can always be calculated, regardless on the particular form of \underline{A} .

5.2 Generalized Expectation Values

For the calculation of particle number expectation values the following generalized expectation value is helpful. An expectation value of an arbitrary product of creation and annihilation operators at time T can be evaluated via

$$\begin{aligned} \langle x_i(T) x_j(T) \rangle &= \text{Tr} \{ \hat{x}_i(T) \hat{x}_j(T) \hat{\rho}_0 \} \\ &= \sum_{m,n=1}^{2K} U_{im}(T) U_{jn}(T) \text{Tr} \{ \hat{x}_m(0) \hat{x}_n(0) \hat{\rho}_0 \}, \end{aligned} \quad (5.16)$$

where the initial trace (see also appendix 7.2) is found to yield

$$\text{Tr} \{ \hat{x}_m(0) \hat{x}_n(0) \hat{\rho}_0 \} = \delta_{m,n-K} (1 + N_m^0) + \delta_{m,n+K} N_n^0. \quad (5.17)$$

Accordingly, one finds for the quadratic expectation value

$$\begin{aligned} \langle x_i(T) x_j(T) \rangle &= \sum_{n=1}^{2K} [U_{i,n+K}(T) N_n^0 + U_{i,n-K}(T) (1 + N_{n-K}^0)] U_{jn}(T) \\ &= \sum_{n=K+1}^{2K} U_{i,n-K}(T) U_{jn}(T) (1 + N_{n-K}^0) + \sum_{n=1}^K U_{i,n+K}(T) U_{jn}(T) N_n^0 \\ &= \sum_{n=1}^K \{ U_{in}(T) U_{j,n+K}(T) \\ &\quad + [U_{in}(T) U_{j,n+K}(T) + U_{i,n+K}(T) U_{jn}(T)] N_n^0 \}. \end{aligned} \quad (5.18)$$

Therefore any quadratic expectation value can always be reduced to the initial particle occupation numbers. If one considers the expectation values of particle number operators, the first term in above sum accounts for the vacuum contributions, whereas the other terms include the temperature effects.

5.3 An Example: Particle Creation

Having simplified the Hamiltonian describing the complete system via applying the RWA in subsection 2.6.1 the effective interaction Hamiltonian was found to be

$$\hat{H}_{\text{eff}}^I = \hat{H}_{\text{eff}}^S + \hat{H}_{\text{eff}}^V = i\xi \left[(\hat{a}_L^\dagger)^2 - (\hat{a}_L)^2 \right] + i\chi \left[\hat{a}_L^\dagger \hat{a}_R - \hat{a}_L \hat{a}_R^\dagger \right]. \quad (5.19)$$

This expression occurs in the time evolution operator in the interaction picture, i.e. to calculate the expectation value of an observable \hat{Y} one has to evaluate

$$\langle Y(T) \rangle = \text{Tr} \left\{ \hat{Y} e^{-i\hat{H}_{\text{eff}}^I T} \hat{\rho}_0 e^{+i\hat{H}_{\text{eff}}^I T} \right\} = \text{Tr} \left\{ e^{+i\hat{H}_{\text{eff}}^I T} \hat{Y} e^{-i\hat{H}_{\text{eff}}^I T} \hat{\rho}_0 \right\}. \quad (5.20)$$

Since \hat{Y} can be expressed by ladder operators one just has to evaluate the time-dependence of the creation and annihilation operators $\hat{a}_\sigma(T) = e^{+i\hat{H}_{\text{eff}}^I T} \hat{a}_\sigma e^{-i\hat{H}_{\text{eff}}^I T}$. The effective interaction Hamiltonian (2.81) involves only $K = 2$ different modes, the vector $\underline{\hat{x}}(\vartheta)$ will therefore be four-dimensional

$$\underline{\hat{x}}(\vartheta) = \begin{pmatrix} \hat{a}_L(\vartheta) \\ \hat{a}_R(\vartheta) \\ \hat{a}_L^\dagger(\vartheta) \\ \hat{a}_R^\dagger(\vartheta) \end{pmatrix} = \begin{pmatrix} \hat{x}_1(\vartheta) \\ \hat{x}_2(\vartheta) \\ \hat{x}_3(\vartheta) \\ \hat{x}_4(\vartheta) \end{pmatrix}. \quad (5.21)$$

Accordingly, one can identify the diagonal real squeezing matrix

$$\underline{C} = \begin{pmatrix} -\xi & 0 \\ 0 & 0 \end{pmatrix} \quad (5.22)$$

resulting from the effective squeezing Hamiltonian and the antisymmetric real hopping matrix

$$\underline{D} = \begin{pmatrix} 0 & \chi \\ -\chi & 0 \end{pmatrix}, \quad (5.23)$$

which results from the effective velocity Hamiltonian in the case of \ominus coupling. Equivalently, the coefficient matrix is given by

$$\underline{A} = \begin{pmatrix} 0 & \chi & 2\xi & 0 \\ -\chi & 0 & 0 & 0 \\ 2\xi & 0 & 0 & \chi \\ 0 & 0 & -\chi & 0 \end{pmatrix}. \quad (5.24)$$

This matrix can easily be diagonalized, for the eigenvalues of \underline{A} one finds

$$\begin{aligned} \lambda_1 &= \xi + \sqrt{\xi^2 - \chi^2}, \\ \lambda_2 &= \xi - \sqrt{\xi^2 - \chi^2}, \\ \lambda_3 &= -\xi + \sqrt{\xi^2 - \chi^2}, \\ \lambda_4 &= -\xi - \sqrt{\xi^2 - \chi^2}. \end{aligned} \quad (5.25)$$

Note that in the coupling assumed in subsection 2.6.3 $\chi = \mathcal{O}(m_{L,R}) = \mathcal{O}(\eta)$, i.e. that $\chi^2 < \xi^2$ holds. Therefore the eigenvalues λ_i are real. The matrix $\underline{U}(T) = \exp(\underline{A}T)$ can be calculated using some computer algebra system and is given in appendix 7.5. Since one wants to calculate the expectation values of particle number operators the following two generalized expectation values are of special interest

$$\begin{aligned} \langle N_L(T) \rangle = \langle \hat{x}_3 \hat{x}_1 \rangle &= (U_{13}U_{31} + U_{14}U_{32}) \\ &\quad + (U_{13}U_{31} + U_{11}U_{33})N_L^0 \\ &\quad + (U_{12}U_{34} + U_{14}U_{32})N_R^0, \\ \langle N_R(T) \rangle = \langle \hat{x}_4 \hat{x}_2 \rangle &= (U_{23}U_{41} + U_{24}U_{42}) \\ &\quad + (U_{23}U_{41} + U_{21}U_{43})N_L^0 \\ &\quad + (U_{24}U_{42} + U_{22}U_{44})N_R^0. \end{aligned} \quad (5.26)$$

The first lines in above equations therefore denote the vacuum contribution to the particle creation, whereas the rest is induced by temperature corrections. Accordingly, one finds for the particle creation in the fundamental resonance mode L

$$\begin{aligned}
\langle N_L(T) \rangle = & \frac{1}{4(\xi^2 - \chi^2)} \left\{ \xi \cosh \left[2T \left(\xi + \sqrt{\xi^2 - \chi^2} \right) \right] \left[\xi + \sqrt{\xi^2 - \chi^2} \right] \right. \\
& + \xi \cosh \left[2T \left(\xi - \sqrt{\xi^2 - \chi^2} \right) \right] \left[\xi - \sqrt{\xi^2 - \chi^2} \right] \\
& \left. - 2\chi^2 \cosh [2T\xi] - 2(\xi^2 - \chi^2) \right\} \\
& + \frac{N_L^0}{2(\xi^2 - \chi^2)} \left\{ \xi \cosh \left[2T \left(\xi + \sqrt{\xi^2 - \chi^2} \right) \right] \left[\xi + \sqrt{\xi^2 - \chi^2} \right] \right. \\
& + \xi \cosh \left[2T \left(\xi - \sqrt{\xi^2 - \chi^2} \right) \right] \left[\xi - \sqrt{\xi^2 - \chi^2} \right] \\
& \left. - \chi^2 \cosh [2T\xi] \left[\cosh \left(2T\sqrt{\xi^2 - \chi^2} \right) + 1 \right] \right\} \\
& + \frac{N_R^0}{2(\xi^2 - \chi^2)} \left\{ \chi^2 \cosh [2T\xi] \left[\cosh \left(2T\sqrt{\xi^2 - \chi^2} \right) - 1 \right] \right\}. \tag{5.27}
\end{aligned}$$

The number of created particles due to the dynamical Casimir effect is therefore growing exponentially with the perturbation time T . Depending on the initial particle content of the cavity (which is equivalent with the initial temperature) the temperature effects will enhance the dynamical Casimir effect. Inserting the corresponding matrix elements for the coupling right-dominated mode R one finds for its expectation value

$$\begin{aligned}
\langle N_R(T) \rangle = & \frac{1}{4(\xi^2 - \chi^2)} \left\{ \xi \cosh \left[2T \left(\xi + \sqrt{\xi^2 - \chi^2} \right) \right] \left[\xi - \sqrt{\xi^2 - \chi^2} \right] \right. \\
& + \xi \cosh \left[2T \left(\xi - \sqrt{\xi^2 - \chi^2} \right) \right] \left[\xi + \sqrt{\xi^2 - \chi^2} \right] \\
& \left. - 2\chi^2 \cosh [2T\xi] - 2(\xi^2 - \chi^2) \right\} \\
& + \frac{N_L^0}{2(\xi^2 - \chi^2)} \left\{ \chi^2 \cosh [2T\xi] \left[\cosh \left(2T\sqrt{\xi^2 - \chi^2} \right) - 1 \right] \right\} \\
& + \frac{N_R^0}{2(\xi^2 - \chi^2)} \left\{ \xi \cosh \left[2T \left(\xi + \sqrt{\xi^2 - \chi^2} \right) \right] \left[\xi - \sqrt{\xi^2 - \chi^2} \right] \right. \\
& + \xi \cosh \left[2T \left(\xi - \sqrt{\xi^2 - \chi^2} \right) \right] \left[\xi + \sqrt{\xi^2 - \chi^2} \right] \\
& \left. - \chi^2 \cosh [2T\xi] \left[\cosh \left(2T\sqrt{\xi^2 - \chi^2} \right) + 1 \right] \right\}. \tag{5.28}
\end{aligned}$$

Accordingly, also outside the leaky cavity particles are produced due to the dynamical Casimir effect. The remarkable agreement of coefficients of N_R^0 in $\langle N_L \rangle$ and of N_L^0 in $\langle N_R \rangle$ as had already been noticed in the quadratic answer is preserved for all orders in η . Therefore these terms seem to fit the classical picture of particle transportation through a permeable membrane where the particle flux is proportional to the number of particles on the other side. The other terms therefore seem to resemble pure quantum effects.

Considering the effects of detuning it is visible that – following the naive approach of subsection 2.6.4 – the effect of substituting $\xi \rightarrow |\Delta| \xi$ and $\chi \rightarrow |\Delta| \chi$ in the expectation values is the introduction of an effective time scale

$$T_{\text{eff}} = |\Delta| T = \frac{\sqrt{2 - 2 \cos(\delta \omega T)}}{|\delta| \omega} = T \left[1 - \frac{(\delta \Omega_L^0 T)^2}{6} + \mathcal{O}((\delta \Omega_L^0 T)^4) \right]. \quad (5.29)$$

Since (5.27) and (5.28) are monotonously increasing functions of T_{eff} , the effect of particle creation would be largest when T_{eff} reaches its maximum at

$$\begin{aligned} \frac{\partial T_{\text{eff}}}{\partial T}(T_{\text{max}}) &\stackrel{\text{RWA}}{=} 0, \\ |\delta| \omega T_{\text{max}} &\stackrel{\text{RWA}}{=} 2 |\delta| \Omega_L^0 T_{\text{max}} = \pi, \end{aligned} \quad (5.30)$$

see also figure 6.1. Such a maximum is unphysical and inconsistent with the results obtained in the literature [40, 41, 43, 44] where an exponential growth is found as long as $\delta < \epsilon/2$. This might indicate that the neglect of time-ordering within the RWA is not applicable in the case of a non-vanishing detuning. In addition, so far a constant detuning δ has been assumed. This assumption is justified only in the beginning, when the back-reaction of the field is still small, but in general the detuning will depend on the back-reaction and therefore also on the perturbation time T . The experimentalist will therefore always find a maximum number of created particles. In the RWA the particle number can in any case be expressed by exponentials $\langle N(T) \rangle \propto \exp(\lambda_i |\Delta| T)$ which suggests that parametric excitation can only occur if the arguments of the exponentials become large, i.e. $\lambda_i |\Delta| T > 1$. Neglecting the velocity effect ($\chi = 0$) the only positive eigenvalue is given by $\lambda_1 = 2\xi$. Accordingly, the corresponding exponent

$$2\xi |\Delta| T = \frac{1}{4} \left(\frac{\Omega_L^{x0}}{\Omega_L^0} \right)^2 \frac{\epsilon}{|\delta|} \sqrt{2 - 2 \cos(2\delta \Omega_L^0 T)} \quad (5.31)$$

is found to be bounded by

$$0 \leq 2\xi |\Delta| T \leq \frac{1}{2} \frac{\epsilon}{|\delta|} \left(\frac{\Omega_L^{x0}}{\Omega_L^0} \right)^2. \quad (5.32)$$

The upper boundary should exceed 1 in order to gain larger values in the exponent, i.e. the effect of particle production will only be considerable if

$$|\delta| < \frac{1}{2} \left(\frac{\Omega_L^{x0}}{\Omega_L^0} \right)^2 \epsilon \quad (5.33)$$

holds. This upper bound for the detuning is similar to the results in [40, 41, 43, 44]. However, here the criterion is not strict – due to the neglect of time-ordering in the case of a non-vanishing detuning and in addition one would always find a maximum number of created particles.

5.4 Comparison With Known Results

Consistency of the results obtained via the non-perturbative approach with the perturbatively obtained earlier results can be checked by expansion around $\chi = 0$ up to second order. However, even for larger values of η with moderate perturbation times T the quadratic approximation is a very good one. The figures 5.1 and 5.2 shall illustrate the quality of the approximation.

Note that at least the quadratic answer is necessary to treat particle creation effects outside the leaky cavity. In figures 5.1 and 5.2 the effects of temperature have already been included. At room temperature these effects enhance the pure vacuum effect by several orders of magnitude (see also [38, 39, 40]).

To compare these results with those obtained by other authors one does not only have to look at the lowest order results, but can also consider a different scenario. It has been predicted in [40] that in an ideal cavity the number of produced particles will exhibit oscillations in the case of strong inter-mode coupling. This case can easily be reproduced if one considers a case outside the initial intentions where χ assumes large values, in particular $\chi \geq \xi$. In view of the arising imaginary eigenvalues in (5.25) it is obvious that the particle numbers in (5.27) and (5.28) will exhibit oscillations. It can be checked explicitly that the imaginary parts of the particle number cancel as they have to (the particle number is a physical observable). This scenario is unrealistic if one considers the coupling between left- and right-dominated modes as was done in subsection 2.6.3, since χ is then relatively small. However, in the case of strong inter-mode coupling of left-dominated modes (in analogy to [40]), i.e. if R stood for another left-dominated mode, χ may very well become large enough to cause oscillations, see also figure 5.3. Remarkably the phase of the two modes is exactly half the period: When $\langle N_L(T) \rangle$ is at its maximum, then $\langle N_R(T) \rangle$ is at its minimum and vice versa. This fits nicely with the picture of mode hopping mediated by the inter-mode coupling χ . One even observes a decrease of the particle number in the L -mode for small times. When defining an effective temperature (see

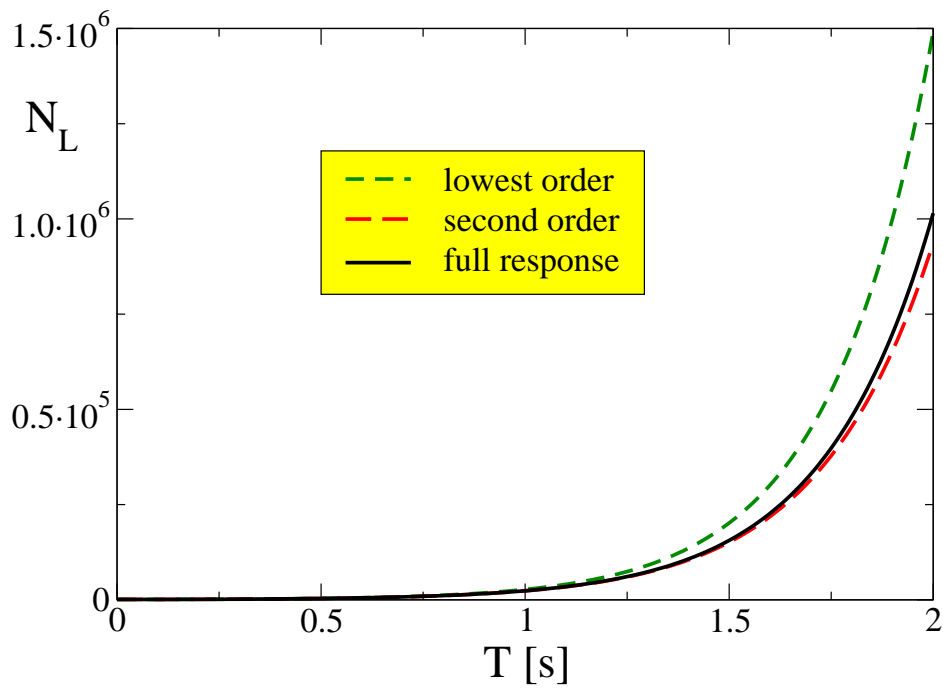


Figure 5.1: Particle creation in the fundamental resonance mode N_L for $N_L^0 = 1000$, $N_R^0 = 100$, $\xi = 1$ Hz, and $\chi = 0.5$ Hz. An exponential growth is found in all cases. The lowest order result corresponds to the assumption of an ideal cavity, whereas higher orders resemble the corrections due to leakage.

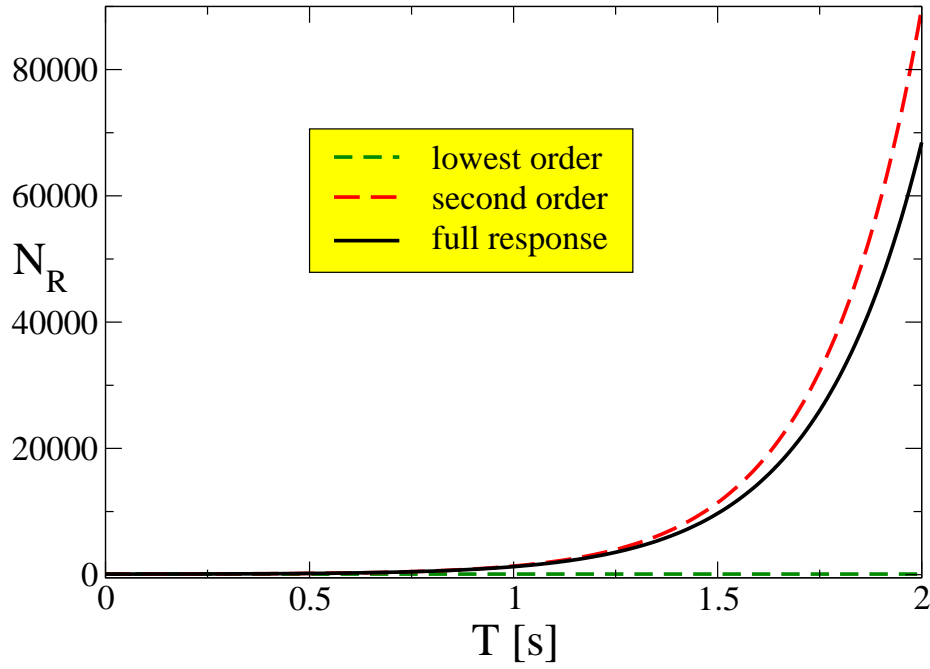


Figure 5.2: Particle creation in the right-dominated coupling resonance mode N_R for $N_L^0 = 1000$, $N_R^0 = 100$, $\xi = 1$ Hz, and $\chi = 0.5$ Hz. The lowest order result (ideal cavity) just corresponds to a constant initial particle number. The particle production in the reservoir due to the NSCE is a much smaller effect compared with figure 5.1.

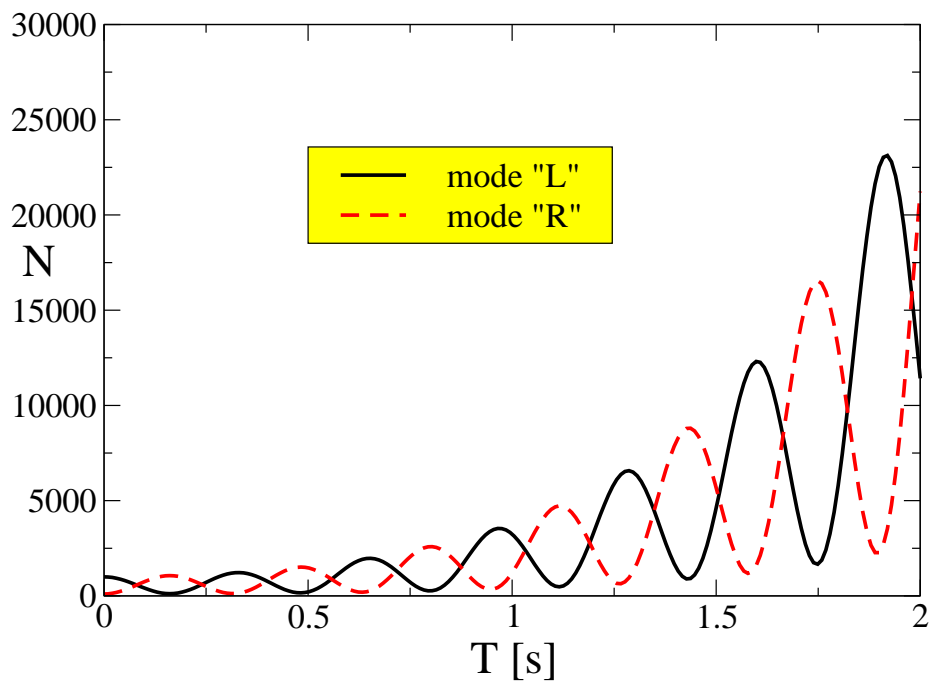


Figure 5.3: Another scenario. The particle numbers in the resonance modes N_L and N_R show oscillations for $N_L^0 = 1000$, $N_R^0 = 100$, $\xi = 1$ Hz and $\chi = 11$ Hz. This scenario is possible if χ exceeds ξ , i.e. in the case of strong inter-mode coupling of equally-dominated modes.

e.g. [39]) this would correspond to an effective cooling of the L -mode. An extreme case of the \ominus coupling scenario would be the limit of no diagonal squeezing, i.e. $\xi \rightarrow 0$. In this case one would (within the RWA) just obtain oscillations of the particle numbers with the total particle number being constant $\langle N_L(T) \rangle + \langle N_R(T) \rangle = N_L^0 + N_R^0$. Therefore this case can not be used to induce resonant particle production with comparably low external vibration frequencies.

5.5 Multi-Mode Squeezing

In Section 2.6.1 a special case of coupling had been assumed. Since the scenario of \oplus coupling leads to a non-diagonal multi-mode squeezing velocity Hamiltonian, also the consequences arising from this combination would be of interest. In this case the squeezing matrix \underline{C} does also contain non-diagonal elements. Assuming the effective interaction Hamiltonian to be given by

$$\hat{H}_{\text{eff}}^I = i\xi \left[(\hat{a}_L^\dagger)^2 - (\hat{a}_L)^2 \right] + i\chi_\oplus \left[\hat{a}_L^\dagger \hat{a}_R^\dagger - \hat{a}_L \hat{a}_R \right], \quad (5.34)$$

one finds that the hopping matrix \underline{D} vanishes, since no hopping operators are involved. The coefficient matrix \underline{A} consequently reads

$$\underline{A} = \begin{pmatrix} 0 & 0 & 2\xi & \chi_\oplus \\ 0 & 0 & \chi_\oplus & 0 \\ 2\xi & \chi_\oplus & 0 & 0 \\ \chi_\oplus & 0 & 0 & 0 \end{pmatrix}. \quad (5.35)$$

The solutions one finds for the full response function of the resonance modes are slightly modified. The expectation value of the fundamental resonance mode L determines as

$$\begin{aligned}
\langle N_L(T) \rangle = & \frac{1}{4(\xi^2 + \chi_\oplus^2)} \left\{ \xi \cosh \left[2T \left(\xi + \sqrt{\xi^2 + \chi_\oplus^2} \right) \right] \left[\xi + \sqrt{\xi^2 + \chi_\oplus^2} \right] \right. \\
& + \xi \cosh \left[2T \left(\xi - \sqrt{\xi^2 + \chi_\oplus^2} \right) \right] \left[\xi - \sqrt{\xi^2 + \chi_\oplus^2} \right] \\
& \left. + 2\chi_\oplus^2 \cosh [2T\xi] \cosh \left(2T\sqrt{\xi^2 + \chi_\oplus^2} \right) - 2(\xi^2 + \chi_\oplus^2) \right\} \\
& + \frac{N_L^0}{2(\xi^2 + \chi_\oplus^2)} \left\{ \xi \cosh \left[2T \left(\xi + \sqrt{\xi^2 + \chi_\oplus^2} \right) \right] \left[\xi + \sqrt{\xi^2 + \chi_\oplus^2} \right] \right. \\
& + \xi \cosh \left[2T \left(\xi - \sqrt{\xi^2 + \chi_\oplus^2} \right) \right] \left[\xi - \sqrt{\xi^2 + \chi_\oplus^2} \right] \\
& \left. + \chi_\oplus^2 \cosh [2T\xi] \left[\cosh \left(2T\sqrt{\xi^2 + \chi_\oplus^2} \right) + 1 \right] \right\} \\
& + \frac{N_R^0}{2(\xi^2 + \chi_\oplus^2)} \left\{ \chi_\oplus^2 \cosh [2T\xi] \left[\cosh \left(2T\sqrt{\xi^2 + \chi_\oplus^2} \right) - 1 \right] \right\}. \tag{5.36}
\end{aligned}$$

In contrast to equation (5.27) the limit of no diagonal squeezing, i.e. $\xi \rightarrow 0$ does still induce an exponential growth of the particle number. Any resonant creation of particles therefore requires a non-vanishing squeezing matrix \underline{C} , see also [39, 38]. Accordingly, the \oplus coupling configuration can be employed for particle creation without fulfilling the single-mode squeezing

resonance condition $\omega = 2\Omega_\mu^0$. For the corresponding coupling mode R one finds as a result

$$\begin{aligned}
\langle N_R(T) \rangle = & \frac{1}{4(\xi^2 + \chi_\oplus^2)} \left\{ \xi \cosh \left[2T \left(\xi + \sqrt{\xi^2 + \chi_\oplus^2} \right) \right] \left[\xi - \sqrt{\xi^2 + \chi_\oplus^2} \right] \right. \\
& + \xi \cosh \left[2T \left(\xi - \sqrt{\xi^2 + \chi_\oplus^2} \right) \right] \left[\xi + \sqrt{\xi^2 + \chi_\oplus^2} \right] \\
& \left. + 2\chi_\oplus^2 \cosh [2T\xi] \cosh \left(2T\sqrt{\xi^2 + \chi_\oplus^2} \right) - 2(\xi^2 + \chi_\oplus^2) \right\} \\
& + \frac{N_L^0}{2(\xi^2 + \chi_\oplus^2)} \left\{ \chi_\oplus^2 \cosh [2T\xi] \left[\cosh \left(2T\sqrt{\xi^2 + \chi_\oplus^2} \right) - 1 \right] \right\} \\
& + \frac{N_R^0}{2(\xi^2 + \chi_\oplus^2)} \left\{ \xi \cosh \left[2T \left(\xi + \sqrt{\xi^2 + \chi_\oplus^2} \right) \right] \left[\xi - \sqrt{\xi^2 + \chi_\oplus^2} \right] \right. \\
& + \xi \cosh \left[2T \left(\xi - \sqrt{\xi^2 + \chi_\oplus^2} \right) \right] \left[\xi + \sqrt{\xi^2 + \chi_\oplus^2} \right] \\
& \left. + \chi_\oplus^2 \cosh [2T\xi] \left[\cosh \left(2T\sqrt{\xi^2 + \chi_\oplus^2} \right) + 1 \right] \right\} . \tag{5.37}
\end{aligned}$$

Again one finds an agreement of the coefficients of N_R^0 in $\langle N_L(T) \rangle$ and of N_L^0 in $\langle N_R(T) \rangle$ but since the effective interaction Hamiltonian does not contain hopping operators this must be credited with multi-mode correlation effects.

Chapter 6

Discussion

The aim of this thesis was to find an application for the canonical approach to vibrating cavities with losses. It could be demonstrated explicitly that this is possible – provided the complete system including the reservoir is solved. The canonical approach has proven to be applicable also for this kind of system. Within the RWA the employed methods (response theory, master equation ansatz, and a non-perturbative approach) were found to lead to consistent results. For the example of a rectangular cavity in the case of parametric resonance the particle number has been demonstrated to exhibit an exponential growth if the effective interaction Hamiltonian contains squeezing generators. However, it turned out that the RWA does not seem capable of including the effects of detuning.

Comparing the three basic procedures it must be mentioned that the response theory approach and the master equation ansatz do require about the same effort. However, these methods only hold to quadratic order in $\int_0^T \hat{\mathcal{H}}_{\text{eff}}^V(t) dt$ which leads to the restriction that the obtained results are only valid within a certain time limit. The non-perturbative approach presented in chapter 5 is not subject to this restriction and is therefore favorable. The required effort is comparably low, since the necessary calculations can be performed using computer algebra systems. However, considering the possibility of more complicated mode couplings the computing time could become quite large. In special cases it might therefore be advantageous to employ the response theory approach.

6.1 Estimates

In view of a possible experimental observation of quantum radiation it is perhaps helpful to gain an impression of the relevant parameters.

A leaky cavity with a typical size of $l_0 = b - a_0 = 1$ cm would have a fundamental resonance frequency of $\Omega_L^0 \approx 150$ GHz. Accordingly the external vibration frequency would have to be around $\omega \approx 300$ GHz. Note that one can always adjust the size of the cavity to lower these values. The corresponding coupling right dominated mode must have a frequency of about $\Omega_R^0 = 3\Omega_L^0 \approx 450$ GHz. Currently a cavity quality factor of $Q \approx 10^8$ and a dimensionless vibration amplitude $\epsilon \approx 10^{-8}$ are within the range of experimental possibilities, see also [43, 44, 40] and references therein. At room temperature $1/\beta \approx 300$ K one finds for the initial particle content $N_L^0 \approx 240$ in the leaky cavity and $N_R^0 \approx 80$ in the reservoir (independent of its size). For the calculation of the velocity parameter χ a reasonable value for the ideality of the internal mirror is needed – strictly speaking the perturbation parameter η . This can be achieved via the quality factor Q of a resonator as defined in [53]

$$Q = 2\pi \frac{\text{Energy in Cavity}}{\text{Energy loss per period}}. \quad (6.1)$$

For the model system in section 2.4 a classical estimate yields

$$Q = \frac{2\pi}{|\mathcal{T}|^2} = 2\pi \left(1 + \left(\frac{\gamma}{\Omega_L^x} \right)^2 \right) = \mathcal{O} \left(\frac{1}{\eta^2} \right), \quad (6.2)$$

where \mathcal{T} denotes the transmission amplitude through the internal dispersive mirror. Accordingly the corresponding perturbation parameter $\eta = \Omega_\mu^{x0}/\gamma$ fulfills $\eta = \mathcal{O}(10^{-4})$.

Using these values the squeezing parameter of subsection 2.6.1 determines as $\xi \approx 150$ Hz and a reasonable value for the velocity parameter can be given by $\chi \approx 2$ mHz. Since $\chi^2 \ll \xi^2$ the quadratic response completely suffices for moderate duration of the vibration.

With these parameters the exponential particle production in the fundamental resonance mode (in the left cavity) is calculated in figure 6.1. The dynamical Casimir effect would therefore be enhanced significantly [of about $\mathcal{O}(10^2)$] at room temperature, see also figure 6.1. This is in agreement with other results, see e.g. [38, 39, 40]. In a possible experiment one would consequently have to match the resonance conditions within the range of detuning (here assumed to be $\delta 2\Omega_L^0 \approx 200$ Hz) for only some milliseconds to yield measurable results. However, the assumption of a constant detuning is unphysical, since the detuning will depend on the back-reaction of the created field on the moving mirror in an experiment. Finding a maximum number of created particles at a constant detuning – see also figure 6.1 – might indicate that the neglect of time-ordering is not applicable in the case of non-vanishing detuning. A heated cavity might then even be advantageous – provided the cavity is still nearly ideal at its characteristic thermal wavelength. Generally the external frequency will have to coincide with

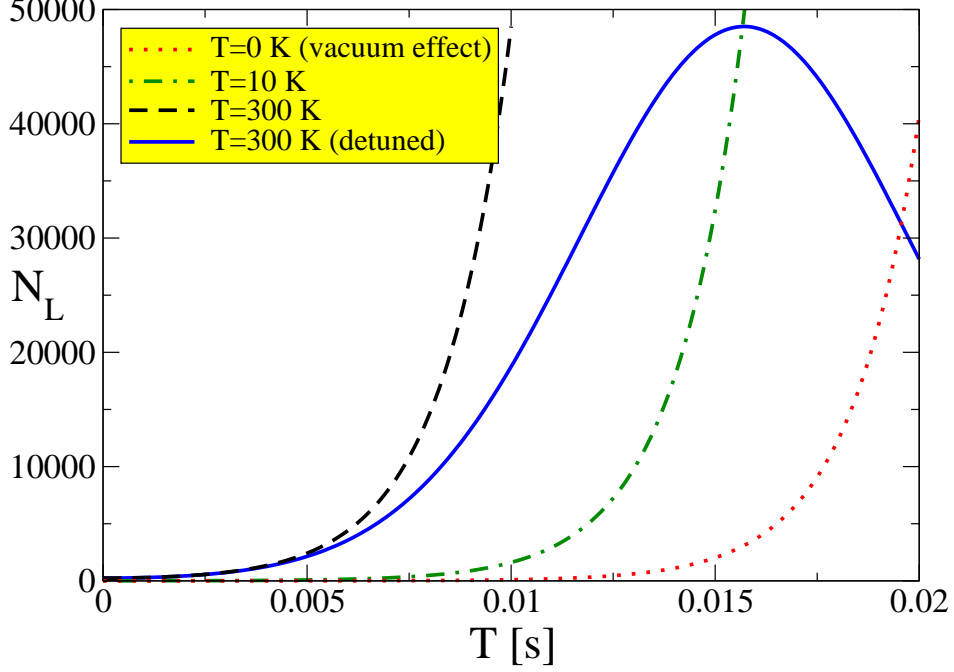


Figure 6.1: Comparison of the particle production rates in the fundamental resonance mode $\langle N_L(T) \rangle$. Temperature effects do dominate the pure vacuum effect already at very low temperatures. At room temperature (300 K) one finds the initial occupation numbers $N_L^0 = 240$ and $N_R^0 = 80$. The curves were calculated using $\xi = 150$ Hz for the squeezing parameter and $\chi = 2$ mHz for the velocity parameter. The external vibration frequency would have to be $\omega = 300$ GHz. In this case the (unphysical) assumption of a constant detuning of $\delta\omega = 200$ Hz would already induce considerable deviations. The maximum is then reached at $T_{\max} = \pi/(200 \text{ Hz}) \approx 0.015$ s and indicates that one has left the region where the neglect of time-ordering in the RWA is applicable. However, initially the two room-temperature curves are in agreement. Finite temperature effects enhance the pure vacuum effect by several orders of magnitude.

the resonance frequency within the range of for several oscillations, which typically implies an initial detuning of $|\delta| < \epsilon/2$ [43, 44, 40].

Note that the shift of the eigenfrequencies of the cavity induced by the finite transmittance of the internal mirror – as given in equation (2.44) – of order $\eta = \mathcal{O}(10^{-4}) \gg |\delta|$ needs to be considered since it constitutes a comparably large effect.

An experimental verification of the dynamical Casimir effect with the configuration of a rectangular cavity seems to be a challenging problem but within the reach of the current experimental apparatus.

6.2 Conclusions

In order to produce measurable effects the cavity would have to vibrate for only some milliseconds, see also figure 6.1. But even after only one millisecond ($\approx 10^8$ periods) a classical estimate (6.2) based on a cavity quality factor of $Q = 10^8$ (or equivalently $\eta = 10^{-4}$) would result in drastic energy losses. However, as has been shown in the present thesis, the calculations based on a quantum treatment of the dynamical Casimir effect show that the effects of losses are almost negligible compared to the rate of particle creation in the resonance case. The calculations in this thesis are based on the simplifying assumption that the surrounding cavity – including both the reservoir and the leaky cavity – is an ideal system. The error made by this presumption is of $\mathcal{O}(Q^{-1})$ (with Q being the quality factor of the surrounding cavity) and therefore certainly negligible. In addition any back-reactions of the created field on the mirror were neglected. This will certainly lead to a varying and therefore time-dependent detuning $\delta(T)$. Therefore, if the perturbation time T becomes too large, back-reaction effects need to be considered, since the detuning will eventually exceed its critical value [43, 44, 41, 40] $\delta \geq \epsilon/2$ above which resonant particle creation is impossible.

In some cases cavities with quality factors as large as $Q = 10^8$ may not be available or one will not be satisfied with the error of a surrounding cavity. In such situations however, an experimental verification of the dynamical Casimir effect could be facilitated by a configuration where the vibrating cavity is enclosed by a slightly larger one (or even a series) as is demonstrated in figure 6.2. This would increase the ideality (or Q -factor) of the complete system and therefore minimize the error made by the assumption of a surrounding ideal cavity. For some cavity configurations it will be possible to resonantly create particles via multi-mode squeezing (\oplus coupling, see subsection 2.6.3) induced by the effective velocity Hamiltonian. However, for a complete understanding of the spectrum of the produced particles the complete eigenfrequency

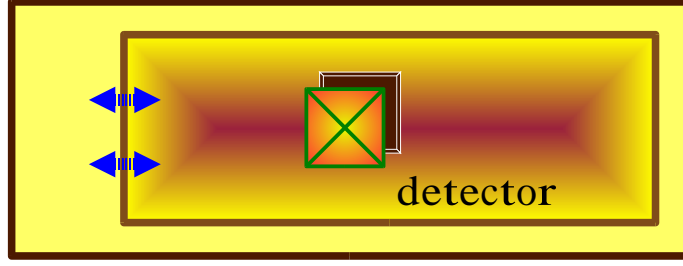


Figure 6.2: Sketch of a vibrating cavity enclosed by a larger one. This configuration may facilitate the experimental verification of the dynamical Casimir effect inside the smaller cavity.

spectrum of the involved modes must be known. In this case particles would be produced due to the velocity term.

6.3 Outlook

In this thesis the trajectory of the mirror has been assumed to be prescribed, i.e. the mirror has not been treated as a dynamical variable. This simplification is justified, if the quantum effects of the field are comparably small with the mirror's inertia. But just in the case of parametric resonance these quantum effects accumulate in time and at some point constitute a large effect, see the particle number in figure 6.1. To predict the long-time-behavior of the system, the back-reaction of the field (i.e. the created particles) will have to be examined, see e.g. [45, 46]. This can also be achieved by a Hamiltonian formulation [28].

For the experimental observation of quantum radiation it will be necessary to place some kind of detecting device (represented by a two-level atom, an ionized gas, etc.) in the cavity. This will have considerable consequences (see e.g. [33, 34, 55]), since the presence of a detector will also influence the field.

A further step towards a realistic experiment will be to consider the electromagnetic field instead of massless scalars. In this case several new difficulties arise:

1. The boundary conditions on the field cannot just simply be described by Dirichlet (or Neumann) conditions. Especially for moving walls their form will be more complicated due to Ampere's law (mixing of the electric (\mathbf{E}) and magnetic (\mathbf{B}) fields). This would complicate the time-dependence of the eigenfrequencies and eigenfunctions but these can still be obtained, since the corresponding differential equation is linear.

2. As the electromagnetic field is a gauge field, one has to eliminate the unphysical degrees of freedom in order to quantize it. Again, for dynamic external conditions this requires special care, see e.g. [54].
3. The different polarizations of photons need to be taken into account. This is of special interest concerning the fulfillment of the resonance conditions, since these modes will in general be degenerated which will increase the number of involved frequencies.

The interaction Hamiltonian is determined by the eigenfrequencies and eigenfunctions of the cavity. For several stationary geometries (rectangular, cylindrical, spherical) these are well-known and can be divided into transversal electric (TE) and transversal magnetic (TM) modes, see e.g. [53]. In order to consider losses which will influence the effective velocity Hamiltonian it will be necessary to find an appropriate model for a dispersive mirror. This can be achieved by using an arbitrarily thin dielectric model slab with an infinite permittivity: $\varepsilon(x) = 1 + \alpha \delta(x)$, see also [48]. As was shown there, this leads to a similar eigenmode equation. Accordingly, it can be expected that the formalism presented in this thesis also holds for photons and that in a corresponding experiment photons would be detected.

Chapter 7

Appendix

7.1 Eigenfunctions

The insertion of the eigenfrequencies into the ansatz (2.37) leads to the normalized eigenfunctions $f_\mu(x)$. These split up into two classes of solutions. In the case of left-dominated modes one finds for their x -dependence

$$f_{n_x, \text{left}}^x(x) = \begin{cases} \sqrt{\frac{2}{b-a}} \left\{ \sin \left(n_x \pi \frac{x-a}{b-a} \right) - \eta_{n_x, l} \left[\frac{1}{2} \cos \left(n_x \pi \frac{x-a}{b-a} \right) \frac{x-a}{b-a} \right. \right. \\ \left. \left. + \frac{1}{4n_x \pi} \sin \left(n_x \pi \frac{x-a}{b-a} \right) \right] \right\} + \mathcal{O}(\eta_{n_x, l}^2) & \text{if } a < x < b \\ \frac{\sqrt{\frac{2}{b-a}} (-1)^{n_x+1}}{2 \sin \left(n_x \pi \frac{c-b}{b-a} \right)} \sin \left(n_x \pi \frac{c-x}{b-a} \right) \eta_{n_x, l} + \mathcal{O}(\eta_{n_x, l}^2) & \text{if } b < x < c \end{cases}, \quad (7.1)$$

whereas for right-dominated modes the eigenfunctions determine according to

$$f_{n_x, \text{right}}^x(x) = \begin{cases} \frac{\sqrt{\frac{2}{c-b}} (-1)^{n_x+1}}{2 \sin \left(n_x \pi \frac{b-a}{c-b} \right)} \sin \left(n_x \pi \frac{x-a}{c-b} \right) \eta_{n_x, r} + \mathcal{O}(\eta_{n_x, l}^2) & \text{if } a < x < b \\ \sqrt{\frac{2}{c-b}} \left\{ \sin \left(n_x \pi \frac{c-x}{c-b} \right) - \eta_{n_x, r} \left[\frac{1}{2} \cos \left(n_x \pi \frac{c-x}{c-b} \right) \frac{c-x}{c-b} \right. \right. \\ \left. \left. + \frac{1}{4n_x \pi} \sin \left(n_x \pi \frac{c-x}{c-b} \right) \right] \right\} + \mathcal{O}(\eta_{n_x, r}^2) & \text{if } b < x < c \end{cases}. \quad (7.2)$$

Accordingly, the corresponding coupling factor between a left- and a right-dominated mode is of $\mathcal{O}(\eta)$.

7.2 Traces Of Ladder Operators

Some rules shall be provided here to enable a convenient calculation of traces involving a diagonal statistical operator $\hat{\rho}_0$ with combinations of initial creation and annihilation operators. The unperturbed Hamiltonian \hat{H}_0 is diagonal, i.e.

$$\hat{H}_0 = \sum_{\mu} \Omega_{\mu}^0 \left(\hat{a}_{\mu}^{\dagger} \hat{a}_{\mu} + \frac{1}{2} \right). \quad (7.3)$$

With the definition of the initial statistical operator

$$\hat{\rho}_0 = \frac{\exp \left(-\beta \hat{H}_0 \right)}{\text{Tr} \left\{ \exp \left(-\beta \hat{H}_0 \right) \right\}} \quad (7.4)$$

it follows that its series expansion will contain arbitrary powers of $\hat{N}_{\mu} = \hat{a}_{\mu}^{\dagger} \hat{a}_{\mu}$. The trace can be performed in the Fock-space, where

$$\begin{aligned} \hat{a}_i^{\dagger} |n\rangle &= \sqrt{n+1} |n+1\rangle \\ \hat{a}_i |n\rangle &= \sqrt{n} |n-1\rangle \end{aligned} \quad (7.5)$$

holds. Since the states are orthonormal

$$\langle n|m \rangle = \delta_{nm}, \quad (7.6)$$

it is obvious that the only non-vanishing traces may arise from terms where the creation and annihilation operators – contained in the operator \hat{A} – do not create orthogonal states

$$\text{Tr} \left\{ \hat{A} \right\} = \sum_{n_1, n_2, \dots = 0}^{\infty} \langle n_1, n_2, \dots | \hat{A} | n_1, n_2, \dots \rangle, \quad (7.7)$$

where n_i denotes the particle occupation number of the i^{th} mode. As a consequence, only the "balanced" traces where the number of creation operators of a particular mode equals the number of annihilation operators of that mode yield non-vanishing results. Together with the commutation relations (2.21) these traces can be reduced to the initial expectation values of creation and annihilation operators. For some relevant basic types of traces these calculations shall be done here.

- All "unbalanced" traces where the number of creation operators of a certain mode does not equal the number of corresponding annihilation operators must vanish. This also implies the vanishing of traces with an odd total number of ladder operators.

- The statistical operator is normalized

$$\text{Tr} \{ \hat{\rho}_0 \} = 1. \quad (7.8)$$

- The initial expectation value N_μ^0 is defined as

$$\text{Tr} \{ \hat{a}_\mu^\dagger \hat{a}_\nu \hat{\rho}_0 \} = \delta_{\mu\nu} N_\mu^0 = \frac{\delta_{\mu\nu}}{e^{\beta \Omega_\mu^0} - 1}, \quad (7.9)$$

if $\hat{\rho}_0$ describes a thermal equilibrium state.

- Via the commutation relations this also implies

$$\text{Tr} \{ \hat{a}_\mu \hat{a}_\nu^\dagger \hat{\rho}_0 \} = \delta_{\mu\nu} (1 + N_\mu^0). \quad (7.10)$$

- Some higher order traces are of special importance

$$\begin{aligned} \text{Tr} \{ [\hat{a}_\mu^\dagger \hat{a}_\mu \hat{a}_\nu \hat{a}_\nu^\dagger - \hat{a}_\mu \hat{a}_\mu^\dagger \hat{a}_\nu^\dagger \hat{a}_\nu] \hat{\rho}_0 \} &= N_\mu^0 - N_\nu^0, \\ \text{Tr} \{ [\hat{a}_\mu \hat{a}_\mu^\dagger \hat{a}_\nu \hat{a}_\nu^\dagger - \hat{a}_\mu^\dagger \hat{a}_\mu \hat{a}_\nu^\dagger \hat{a}_\nu] \hat{\rho}_0 \} &= 1 + N_\mu^0 + N_\nu^0. \end{aligned} \quad (7.11)$$

7.3 Properties Of Time Ordering

The following relation of time- and anti-time ordering is often useful

$$\hat{\mathcal{T}}_t [\hat{A}_1(t_1) \hat{A}_2(t_2)] + \hat{\mathcal{T}}_t^\dagger [\hat{A}_1(t_1) \hat{A}_2(t_2)] = \{ \hat{A}_1(t_1), \hat{A}_2(t_2) \} \quad (7.12)$$

to eliminate anti-time ordering in the time-evolution operator. The time-ordered product of two operators can also be rewritten as

$$\begin{aligned} \hat{\mathcal{T}}_t [\hat{A}_1(t_1) \hat{A}_2(t_2)] &= \hat{A}_1(t_1) \hat{A}_2(t_2) + \hat{A}_2(t_2) \hat{A}_1(t_1) \Theta(t_2 - t_1) + \hat{A}_1(t_1) \hat{A}_2(t_2) [\Theta(t_1 - t_2) - 1] \\ &= \hat{A}_1(t_1) \hat{A}_2(t_2) + [\hat{A}_2(t_2), \hat{A}_1(t_1)] \Theta(t_2 - t_1), \end{aligned} \quad (7.13)$$

where the relation $\Theta(x) - 1 = -\Theta(-x)$ has been used. Note that the commutator of two hermitian operators is anti-hermitian. Above identity can be generalized to arbitrary time-ordered products. The time-ordered product of n operators is given by

$$\begin{aligned} \hat{\mathcal{T}} [\hat{A}_1(t_1) \dots \hat{A}_n(t_n)] &= \sum_{P \in S_n} \hat{A}_{P(1)}(t_{P(1)}) \dots \hat{A}_{P(n)}(t_{P(n)}) \times \\ &\quad \Theta(t_{P(1)} - t_{P(2)}) \dots \Theta(t_{P(n-1)} - t_{P(n)}), \end{aligned} \quad (7.14)$$

where S_n denotes the permutation group of the numbers $\{1, 2, 3, \dots, n\}$. Obviously every permutation $P \in S_n$ of the operators has to occur and the Heaviside functions regulate when the particular permutation has to be employed. Separating the identity permutation P_e yields

$$\begin{aligned} \hat{\mathcal{T}} \left[\hat{A}_1(t_1) \dots \hat{A}_n(t_n) \right] &= \hat{A}_1(t_1) \dots \hat{A}_n(t_n) \Theta(t_1 - t_2) \dots \Theta(t_{n-1} - t_n) \\ &+ \sum_{P \in S_n \setminus P_e} \hat{A}_{P(1)}(t_{P(1)}) \dots \hat{A}_{P(n)}(t_{P(n)}) \times \\ &\quad \Theta(t_{P(1)} - t_{P(2)}) \dots \Theta(t_{P(n-1)} - t_{P(n)}), \end{aligned} \quad (7.15)$$

where the first term already has the expected structure. Any given permutation $P \in S_n$ can be rewritten using the following scheme. Supposing $P(l) = 1$ for a certain permutation and omitting the time-dependencies one finds

$$\begin{aligned} \hat{A}_{P(1)} \dots \hat{A}_{P(n)} &= \hat{A}_1 \hat{A}_{P(2)} \dots \hat{A}_{P(l-1)} \hat{A}_{P(l+1)} \dots \hat{A}_{P(n)} \\ &- \left[\hat{A}_1, \hat{A}_{P(1)} \right] \hat{A}_{P(2)} \dots \hat{A}_{P(l-1)} \hat{A}_{P(l+1)} \dots \hat{A}_{P(n)} \\ &- \dots \\ &- \hat{A}_{P(1)} \dots \hat{A}_{P(l-2)} \left[\hat{A}_1, \hat{A}_{P(l-1)} \right] \hat{A}_{P(l+1)} \dots \hat{A}_{P(n)} \\ &= \hat{A}_1 \dots \hat{A}_n \\ &- (\text{All necessary terms with commutators}), \end{aligned} \quad (7.16)$$

where in the last step the scheme has been carried on with $P(m) = 2, P(n) = 3, \dots$. Accordingly, any permutation $P \in S_n$ can be rewritten as

$$\begin{aligned} \hat{A}_{P(1)} \dots \hat{A}_{P(n)} &= \hat{A}_1 \dots \hat{A}_n \\ &- \sum_{\text{sets}\{k,l\}} \delta(P, \{k, l\}) \hat{A}_{P(1)} \dots \left[\hat{A}_{P(k)}, \hat{A}_{P(l)} \right] \dots \hat{A}_{P(n)}, \end{aligned} \quad (7.17)$$

where $\delta(P, \{k, l\})$ projects onto the relevant terms in the sum to yield an identity

$$\delta(P, \{k, l\}) = \begin{cases} 1 & \text{if } \{k, l\} \text{ does occur in (7.16)} \\ 0 & \text{otherwise} \end{cases}. \quad (7.18)$$

Together with the relation

$$\sum_{P \in S_n} \Theta(t_{P(1)} - t_{P(2)}) \dots \Theta(t_{P(n-1)} - t_{P(n)}) = 1 \quad (7.19)$$

it follows that the time-ordered product of n operators can be written as

$$\begin{aligned}
\hat{\mathcal{T}} \left[\hat{A}_1(t_1) \dots \hat{A}_n(t_n) \right] &= \hat{A}_1(t_1) \dots \hat{A}_n(t_n) \\
&- \sum_{P \in S_n \setminus P_e} \Theta(t_{P(1)} - t_{P(2)}) \dots \Theta(t_{P(n-1)} - t_{P(n)}) \times \\
&\sum_{\text{sets}\{k,l\}} \delta(P, \{k, l\}) \hat{A}_{P(1)}(t_{P(1)}) \dots \times \\
&\left[\hat{A}_{P(l)}(t_{P(l)}) , \hat{A}_{P(k)}(t_{P(k)}) \right] \dots \hat{A}_{P(n)}(t_{P(n)}) .
\end{aligned} \tag{7.20}$$

7.4 Integrals

Some integrals used in this thesis are listed here. The time-integration of the squeezed effective velocity Hamiltonian requires integrals of the hyperbolic sine and cosine functions

$$\int_0^T \mathcal{C}(t) dt = \frac{1}{2\xi} \mathcal{S}(T) , \quad \int_0^T \mathcal{S}(t) dt = \frac{1}{2\xi} [\mathcal{C}(T) - 1] . \tag{7.21}$$

The time-ordering in the quadratic response can be reduced to integrals of the form

$$\begin{aligned}
I_{\text{ex}} &= \int_0^T dt_1 \int_0^T dt_2 \Theta(t_2 - t_1) [\mathcal{S}(t_1) \mathcal{C}(t_2) - \mathcal{S}(t_2) \mathcal{C}(t_1)] \\
&= \frac{1}{4\xi^2} [2\xi T - \mathcal{S}(T)] .
\end{aligned} \tag{7.22}$$

7.5 Time Evolution Matrix

For reasons of completeness the full time evolution matrix $\underline{U}(T, 0) = \exp(\underline{A}T)$ with \underline{A} being the coefficient matrix (5.24) shall be given here explicitly.

$$\begin{aligned}
\underline{U}(T, 0) = & \begin{bmatrix} \frac{1}{4} \frac{T^2 \chi^2 (\%9 - \%8 + \%7 - \%6 + \%5 + \%4 + \%3 + \%2)}{(T\xi + \%1) \sqrt{-T^2(-\xi^2 + \chi^2)} (T\xi - \%1)}, -\frac{1}{4} \%10, \\ -\frac{1}{4} \frac{T^2 \chi^2 (\%3 + \%2 - \%4 - \%5 + \%9 - \%8 + \%6 - \%7)}{(T\xi + \%1) \sqrt{-T^2(-\xi^2 + \chi^2)} (T\xi - \%1)}, \frac{1}{4} \%11 \end{bmatrix} \\
& \begin{bmatrix} \frac{1}{4} \%10, -\frac{1}{4} \frac{T^2 \chi^2 (\%9 - \%8 + \%7 - \%6 - \%5 - \%4 - \%3 - \%2)}{(T\xi + \%1) \sqrt{-T^2(-\xi^2 + \chi^2)} (T\xi - \%1)}, -\frac{1}{4} \%11, \\ \frac{1}{4} \frac{T^2 \chi^2 (\%9 - \%3 - \%8 - \%2 + \%4 + \%6 - \%7 + \%5)}{(T\xi + \%1) \sqrt{-T^2(-\xi^2 + \chi^2)} (T\xi - \%1)} \end{bmatrix} \\
& \begin{bmatrix} -\frac{1}{4} \frac{T^2 \chi^2 (\%3 + \%2 - \%4 - \%5 + \%9 - \%8 + \%6 - \%7)}{(T\xi + \%1) \sqrt{-T^2(-\xi^2 + \chi^2)} (T\xi - \%1)}, \frac{1}{4} \%11, \\ \frac{1}{4} \frac{T^2 \chi^2 (\%9 - \%8 + \%7 - \%6 + \%5 + \%4 + \%3 + \%2)}{(T\xi + \%1) \sqrt{-T^2(-\xi^2 + \chi^2)} (T\xi - \%1)}, -\frac{1}{4} \%10 \end{bmatrix} \\
& \begin{bmatrix} -\frac{1}{4} \%11, \frac{1}{4} \frac{T^2 \chi^2 (\%9 - \%3 - \%8 - \%2 + \%4 + \%6 - \%7 + \%5)}{(T\xi + \%1) \sqrt{-T^2(-\xi^2 + \chi^2)} (T\xi - \%1)}, \frac{1}{4} \%10, \\ -\frac{1}{4} \frac{T^2 \chi^2 (\%9 - \%8 + \%7 - \%6 - \%5 - \%4 - \%3 - \%2)}{(T\xi + \%1) \sqrt{-T^2(-\xi^2 + \chi^2)} (T\xi - \%1)} \end{bmatrix}, \tag{7.23}
\end{aligned}$$

where the shorthand notations $\%1 \dots \%11$ are given by

$$\begin{aligned}
\%1 &= \sqrt{-T^2(-\xi^2 + \chi^2)}, \\
\%2 &= e^{(-T\xi + \%1)} \sqrt{-T^2(-\xi^2 + \chi^2)}, \\
\%3 &= e^{(-T\xi - \%1)} \sqrt{-T^2(-\xi^2 + \chi^2)}, \\
\%4 &= e^{(T\xi - \%1)} \sqrt{-T^2(-\xi^2 + \chi^2)}, \\
\%5 &= e^{(T\xi + \%1)} \sqrt{-T^2(-\xi^2 + \chi^2)}, \\
\%6 &= e^{(T\xi - \%1)} T\xi, \\
\%7 &= e^{(T\xi + \%1)} T\xi, \\
\%8 &= e^{(-T\xi + \%1)} T\xi, \\
\%9 &= e^{(-T\xi - \%1)} T\xi,
\end{aligned}$$

$$\begin{aligned}
\%10 &= \frac{\chi \left(e^{(-T\xi - \%1)} - e^{(-T\xi + \%1)} + e^{(T\xi - \%1)} - e^{(T\xi + \%1)} \right) T}{\sqrt{-T^2 (-\xi^2 + \chi^2)}}, \\
\%11 &= \frac{\chi \left(-e^{(T\xi - \%1)} + e^{(T\xi + \%1)} + e^{(-T\xi - \%1)} - e^{(-T\xi + \%1)} \right) T}{\sqrt{-T^2 (-\xi^2 + \chi^2)}}.
\end{aligned} \tag{7.24}$$

As was anticipated, the arguments in the exponentials are linear combinations of the eigenvalues (5.25).

7.6 Employed Symbols

symbol explanation

$\hat{a}_\mu^\dagger, \hat{a}_\mu$	creation/annihilation operators for the mode μ
$a(t)$	parameter for the moving boundary
\hat{A}	an operator
\underline{A}	$2K \times 2K$ dimensional coefficient matrix
b	position of the dispersive mirror
c	position of the ideal reservoir boundary
$\mathcal{C}(t)$	hyperbolic cosine function $\cosh(2\xi t)$
\underline{C}	$K \times K$ dimensional squeezing matrix
\mathbb{C}	the complex numbers
d	thickness of the dielectric slab
\underline{D}	$K \times K$ dimensional hopping matrix
$f_\mu(\mathbf{r}; t)$	suitable set of eigenfunctions to diagonalize \hat{H}_0
$G(t)$	the domain characterizing the cavity
$g_{\mu\nu}$	metric
H	Hamilton function
\hat{H}	Hamiltonian
K	number of modes in the quadratic Hamiltonian
L	Lagrange function
\mathcal{L}	Lagrange density
\hat{L}	Lagrangian
$\hat{\mathcal{L}}(t)$	Liouville super operator
l_0	characteristic length of the cavity
L_μ	coefficient of the left part of the mode f_μ
$M_{\mu\nu}(t)$	inter-mode coupling matrix
\hat{N}_μ	particle number operator for the mode μ
N_L^0	initial particle occupation number of the mode L
N_R^0	initial particle occupation number of the mode R
$P(i)$	permutation $\in S_n$
P_μ	canonical conjugated momentum
R_μ	coefficient of the right part of the mode f_μ
$\hat{\mathfrak{P}}$	projection super operator

symbol	explanation
Q_μ	generalized coordinate
Q	quality factor of a resonator
\mathcal{R}	reflection amplitude
$\mathcal{S}(t)$	hyperbolic sine function $\sinh(2\xi t)$
$\hat{S}(\tau)$	squeezing operator $\exp\left(i\hat{H}_{\text{eff}}^S\tau\right)$
S_n	permutation group of the numbers $\{1, 2, \dots, n\}$
\mathcal{T}	transmission amplitude
T	duration of a disturbance
T_{eff}	effective time $ \Delta T$
\hat{T}_t	ordering operator with respect to the variable t
$\hat{U}(t_2, t_1)$	time evolution operator
$\hat{\mathcal{U}}(t_2, t_1)$	reduced time evolution super operator
$\underline{U}(T)$	$2K \times 2K$ dimensional time evolution matrix
$V(\mathbf{r}; t)$	external potential
$\hat{x}(\vartheta)$	$2K$ dimensional column vector of ladder operators
\hat{Y}	an observable
Δy	cavity length in y -direction
Δz	cavity length in z -direction
α	parameter for the model of $\varepsilon(x)$
β	initial inverse temperature
γ	coupling strength of the potential
$\Delta\Omega_\mu^2(t)$	deviation of the eigenfrequencies $\Omega_\mu^2(t) - (\Omega_\mu^0)^2$
δ_{ij}	discrete Kronecker symbol
$\delta(x)$	Dirac's delta distribution
Δ	detuning parameter $ \Delta e^{i\varphi}$
δ	dimensionless deviation from the exact resonance
$\varepsilon(\mathbf{r}; t)$	relative permittivity
ε_s	relative permittivity of the dielectric slab
ϵ	dimensionless vibration amplitude
η_μ	perturbation parameter Ω_μ^{x0}/γ
η	fundamental perturbation parameter Ω_{1l}^{x0}

symbol	explanation
$\Theta(x)$	Heaviside step function
ϑ	auxiliary parameter
λ_i	eigenvalues of the coefficient matrix \underline{A}
ξ	squeezing parameter
ξ_δ	detuned squeezing parameter $ \Delta \xi$
$\hat{\rho}$	statistical operator
$\hat{\sigma}$	time evolution operator in the squeezing interaction picture
$\Phi(\mathbf{r}, t)$	massless scalar field
φ	complex phase of the detuning parameter Δ
χ	velocity parameter
χ_δ	detuned velocity parameter $ \Delta \chi$
χ_\oplus	velocity parameter for the \oplus -coupling scenario
$\Omega_\mu(t)$	perturbed eigenfrequency
Ω_μ^0	unperturbed eigenfrequency
$\Delta\Omega_\mu^2(t)$	frequency deviation $\Omega_\mu^2(t) - (\Omega_\mu^0)^2$
ω	external vibration frequency
∇^2	Laplace's differential operator
∂_μ	differentiation with respect to x^μ
$\mathbf{1}$	identity operator

Chapter 8

Acknowledgements

I would like to express my special gratitude to my supervisor Prof. Dr. G. Soff for offering and advising this fascinating research-subject.

Dr. R. Schützhold deserves a special thanks for his supervision and support. Without his extreme knowledge, his guidance, and his critical corrections this work could not have proceeded this far.

Furthermore I am indebted to Priv.-Doz. Dr. G. Plunien for his helpful comments and discussions that have enriched this work by many interesting details.

I am also indebted to A. Knauf for her critical correction readings.

All co-workers at the work group "Hadronen und Kerne" under the leadership of Prof. Dr. G. Soff shall be thanked for the plentiful advice and comments.

I would like to thank my family for supporting and encouraging me during my studies in Dresden.

Bibliography

- [1] H. B. Casimir, *On The Attraction Between Two Perfectly Conducting Plates*, Kon. Ned. Akad. Wetensch. Proc. **51**, 793 (1948).
- [2] S. K. Lamoreaux, *Demonstration of the Casimir force in the 0.6 to 6 micrometers range*, Phys. Rev. Lett. **78**, 5 (1997).
- [3] U. Mohideen and A. Roy, *Precision measurement of the Casimir force from 0.1 to 0.9 μm* , Phys. Rev. Lett. **81**, 4549 (1998).
- [4] M. Bordag, *Quantum Field Theory Under the Influence of External Conditions*, (Teubner, Stuttgart, 1996); M. Bordag, *The Casimir Effect 50 Years Later*, (World Scientific, Singapore, 1999).
- [5] M. Bordag, B. Geyer, G. L. Klimchitskaya and V. M. Mostepanenko, *Casimir force at both nonzero temperature and finite conductivity*, Phys. Rev. Lett. **85**, 503 (2000).
- [6] R. Golestanian and M. Kardar, *The mechanical response of vacuum*, Phys. Rev. Lett. **78**, 3421 (1997).
- [7] M. T. Jaekel and S. Reynaud, *Motional Casimir force*, J. Phys. I (France) **2**, 149 (1992).
- [8] M. Jaekel and S. Reynaud, *Inertia of Casimir energy*, J. Phys. I **3**, 1093 (1993).
- [9] M. Jaekel and S. Reynaud, *Quantum fluctuations of mass for a mirror in vacuum*, Phys. Lett. A **180**, 9 (1993).
- [10] M. Jaekel and S. Reynaud, *Friction and inertia for a mirror in a thermal field*, Phys. Lett. A **172**, 319 (1993).
- [11] M. Jaekel and S. Reynaud, *Quantum fluctuations of position of a mirror in vacuum*, J. Phys. I (France) **3**, 1 (1993).

- [12] J. Schwinger, *Casimir Energy for Dielectrics*, Proc. Natl. Acad. Sci. USA **89**, 4091 (1992); *Casimir Energy for Dielectrics: Spherical Geometry*, ibid. **89**, 11118 (1992); *Casimir Light: A Glimpse*, ibid. **90**, 958 (1993); *Casimir Light: The Source*, ibid. **90**, 2105 (1993); *Casimir Light: Photon Pairs*, ibid. **90**, 4505 (1993); *Casimir Light: Pieces of the Action*, ibid. **90**, 7285 (1993); *Casimir Light: Field Pressure*, ibid. **91**, 6473 (1994).
- [13] G. T. Moore, *Quantum Theory of the Electromagnetic Field in a Variable-Length One-Dimensional Cavity*, J. Math. Phys. **11**, 2679 (1970).
- [14] S. A. Fulling and P. C. W. Davies, *Radiation from Moving Mirrors in Two Dimensional Space-Time: Conformal Anomaly*, Proc. R. Soc. Lond. A **348**, 393 (1976).
- [15] C. K. Law, *Resonance Response of the Quantum Vacuum to an Oscillating Boundary*, Phys. Rev. Lett. **73**, 1931 (1994).
- [16] M. Castagnino and R. Ferraro, *The Radiation From Moving Mirrors: The Creation And Absorption Of Particles*, Annals Phys. **154**, 1 (1984).
- [17] V. V. Dodonov, A. A. Klimov, and D. E. Nikonov, *Quantum phenomena in resonators with moving walls*, J. Math. Phys. **34**, 2742 (1993).
- [18] V. V. Dodonov, A. B. Klimov, and A. E. Nikonov, *Quantum phenomena in nonstationary media*, Phys. Rev. A **47**, 4422 (1993).
- [19] O. Méplan and C. Cignoux, *Exponential Growth of the Energy of a Wave in a 1D Vibrating Cavity: Application to the Quantum Vacuum*, Phys. Rev. Lett. **76**, 408 (1996).
- [20] M. Jaekel and S. Reynaud, *Vacuum fluctuations, accelerated motion and conformal frames*, Quant. Semiclass. Opt. **7**, 499 (1995).
- [21] A. Lambrecht, M. Jaekel, and S. Reynaud, *Motion Induced Radiation from a Vibrating Cavity*, Phys. Rev. Lett. **77**, 615 (1996).
- [22] A. Lambrecht, M. T. Jaekel, and S. Reynaud, *Frequency up-converted radiation from a cavity moving in vacuum*, Eur. Phys. J. D **3**, 95 (1998).
- [23] M. Jaekel and S. Reynaud, *Causality, stability and passivity for a mirror in vacuum*, Phys. Lett. A **167**, 227 (1992).

- [24] L. H. Ford and A. Vilenkin, *Quantum Radiation By Moving Mirrors*, Phys. Rev. D **25**, 2569 (1982).
- [25] K. Ujihara, *Quantum theory of a one-dimensional optical cavity with output coupling. Field Quantization*, Phys. Rev. A **12**, 148 (1975).
- [26] J. Gea-Banachloche, Ning Lu, L. M. Pedrotti, S. Prasad, M. O. Scully, and K. Wodkiewicz, *Treatment of the spectrum of squeezing based on the modes of the universe. I. Theory and a physical picture*, Phys. Rev. A **41**, 369 (1990).
- [27] R. J. Glauber and M. Lewenstein, *Quantum Optics Of Dielectric Media*, Phys. Rev. A **43**, 467 (1991).
- [28] C. K. Law, *Effective Hamiltonian for the radiation in a cavity with a moving mirror and a time-varying dielectric medium*, Phys. Rev. A **49**, 433 (1994).
- [29] M. Razavy and J. Terning, *Quantum Radiation In A One-Dimensional Cavity With Moving Boundaries*, Phys. Rev. D **31**, 307 (1985).
- [30] Ying Wu, M. -C. Chu, and P. T. Leung, *Dynamics of the quantized radiation field in a cavity vibrating at the fundamental frequency*, Phys. Rev. A **59**, 3032 (1999).
- [31] V. B. Braginsky and F. Ya. Khalili, *Friction and fluctuations produced by the quantum ground state*, Phys. Lett. A **161**, 197 (1991).
- [32] J. Ji, H. Jung, J. Park, and K. Soh, *Production of photons by the parametric resonance in the dynamical Casimir effect*, Phys. Rev. A **56**, 4440 (1997).
- [33] V. V. Dodonov and A. B. Klimov, *Generation and detection of photons in a cavity with a resonantly oscillating boundary*, Phys. Rev. A **53**, 2664 (1996).
- [34] V. V. Dodonov, *Photon creation and excitation of a detector in a cavity with a resonantly vibrating wall*, Phys. Lett. A **207**, 126 (1995).
- [35] P. A. M. Neto and L. A. S. Machado, *Quantum radiation generated by a moving mirror in free space*, Phys. Rev. A **54**, 3420 (1996).
- [36] M. R. Setare and A. A. Saharian, *Particle creation by moving spherical shell in the dynamical Casimir effect*, Mod. Phys. Lett. A **16**, 927 (2001); *Particle creation in an oscillating spherical cavity*, *ibid.* **16**, 1269 (2001).

- [37] E. Sassaroli, Y. N. Srivastava, and A. Widom, *Photon production by the dynamical Casimir effect*, Phys. Rev. A **50**, 1027 (1994).
- [38] R. Schützhold, G. Plunien, and G. Soff, *Trembling cavities in the canonical approach*, Phys. Rev. A **57**, 2311 (1998).
- [39] G. Plunien, R. Schützhold, and G. Soff, *Dynamical Casimir effect at finite temperature*, Phys. Rev. Lett. **84**, 1882 (2000); R. Schützhold, G. Plunien, and G. Soff, *Quantum radiation at finite temperature*, [quant-ph/0105118], to appear in Phys. Rev. A (2001).
- [40] M. Crocce, D. A. R. Dalvit, and F. D. Mazzitelli, *Resonant photon creation in a three dimensional oscillating cavity*, Phys. Rev. A **64**, 013808 (2001).
- [41] V. V. Dodonov, *Resonance Photon Generation in a Vibrating Cavity*, J. Phys. A **31**, 9835 (1998).
- [42] V. V. Dodonov, *Squeezing and photon distribution in a vibrating cavity*, J. Phys. A **32**, 6711 (1999).
- [43] V. V. Dodonov, *Dynamical Casimir effect in a nondegenerate cavity with losses and de-tuning*, Phys. Rev. A **58**, 4147 (1998).
- [44] V. V. Dodonov, *Generation of photons in a lossy and detuned cavity with an oscillating boundary*, Phys. Lett. A **244**, 517 (1998).
- [45] G. Barton and A. Calogeracos, *On the Quantum Electrodynamics of a dispersive mirror. I. Mass shifts, radiation, and radiative reaction*, Annals Phys. **238**, 227 (1995); A. Calogeracos, and G. Barton, *On the Quantum Electrodynamics of a dispersive mirror. II. The boundary condition and the applied force via Dirac's theory of constraints*, Annals Phys. **238**, 268 (1995).
- [46] G. M. Salamone and G. Barton, *Quantum radiative reaction on a dispersive mirror in one dimension*, Phys. Rev. A **51**, 3506 (1995).
- [47] C. K. Law, *Interaction between a moving mirror and radiation pressure: A Hamiltonian formulation*, Phys. Rev. A **51**, 2537 (1995).
- [48] R. Lang, M. O. Scully, and W. E. Lamb Jr., *Why is the Laser Line So Narrow? A Theory of Single-Quasimode Laser Operation*, Phys. Rev. A **7**, 1788 (1973).

- [49] E. Fick and G. Sauermann, *Quantenstatistik Dynamischer Prozesse*, (Harri Deutsch, Frankfurt/Main, 1983); *The Quantum Statistics of Dynamic Processes*, (Springer, Berlin, 1983).
- [50] L. Mandel and E. Wolf, *Optical Coherence and Quantum Optics*, (Cambridge University Press, Cambridge, 1995).
- [51] K. Bartschat, *Density Matrices in Atomic, Molecular & Optical Physics Handbook*, edited by G. W. F. Drake, (AIP Press, Woodbury, New York, 1996).
- [52] M. Freyberger, K. Vogel, W. Schleich, and R. F. O'Connell, *Quantized Field Effects in Atomic, Molecular & Optical Physics Handbook*, edited by G. W. F. Drake, (AIP Press, Woodbury, New York, 1996).
- [53] J. D. Jackson, *Classical Electrodynamics*, (Wiley, New York, 1999).
- [54] R. Schützhold, G. Plunien, and G. Soff, *Quantum radiation in external background fields*, Phys. Rev. A **58**, 1783 (1998).
- [55] C. K. Law, T. W. Chen, and P. T. Leung, *Jaynes-Cummings model in leaky cavities: An exact pure-state approach*, Phys. Rev. A **61**, 023808-1 (2000).
- [56] G. Schaller, R. Schützhold, G. Plunien, and G. Soff, *Dynamical Casimir Effect in a Designed Leaky Cavity*, [quant-ph/0203068], to appear in Phys. Lett. A.
- [57] G. Schaller, R. Schützhold, G. Plunien, and G. Soff, *Dynamical Casimir Effect in a Leaky Cavity at Finite Temperature*, [quant-ph/0203139], submitted to Phys. Rev. A.

Declaration

Hereby I declare that I have composed this thesis without illegitimate help of third parties in the scope of support at the Institute for Theoretical Physics and that I have marked all sources as such.

Gernot Schaller

Erklärung

Hiermit erkläre ich, dass ich diese Arbeit im Rahmen der Betreuung am Institut für Theoretische Physik ohne unzulässige Hilfe Dritter verfasst und alle Quellen als solche gekennzeichnet habe.

Gernot Schaller